

**INVESTIGATING THE ROLE OF PROTEIN TYROSINE PHOSPHATASE ALPHA IN
FOCAL ADHESION DYNAMICS AND CELL MIGRATION**

by

Cassandra Dawson

B.Sc., The University of Western Ontario, 2014

A THESIS SUBMITTED IN PARTIAL FULFILLMENT OF
THE REQUIREMENTS FOR THE DEGREE OF

MASTER OF SCIENCE

in

THE FACULTY OF GRADUATE AND POSTDOCTORAL STUDIES
(Experimental Medicine)

THE UNIVERSITY OF BRITISH COLUMBIA

(Vancouver)

June 2017

© Cassandra Dawson, 2017

Abstract

Cell migration is an important phenomenon in many physiological and pathological processes such as wound healing, embryogenesis, and cancer cell metastasis. Integrins bind components of the extracellular matrix and initiate a cascade of intracellular signaling changes that regulate focal adhesion dynamics and reorganization of the actin cytoskeleton. Focal adhesions are multiprotein complexes that are continuously assembled, remodeled, and disassembled to enable cell migration.

Protein tyrosine phosphatase alpha (PTP α) is a receptor-like transmembrane protein that is involved in integrin signaling. In response to integrin stimulation, PTP α mediates Src activation through dephosphorylation of the inhibitory phosphosite of Src. This leads to formation of the Src-FAK complex which in turn phosphorylates PTP α at the Tyr789 site. PTP α -Tyr789 phosphorylation has been demonstrated to be an important event in coordinating focal adhesion formation, cytoskeletal rearrangement, and cell migration. Mouse embryonic fibroblasts (MEFs) lacking PTP α expression or expressing an unphosphorylatable mutant (Y789F) PTP α exhibit impaired focal adhesion formation and cell migration. In this study, I investigated the focal adhesion dynamics and cell migration capabilities of newly generated lines of wild-type and PTP α -deficient MEFs. Although these newly generated cells did not fully recapitulate the previously reported PTP α -dependent focal adhesion dynamics and cell migration defects, I observed that cells lacking PTP α expression exhibited defects in cell polarity and directionality, mechanisms that coordinate migration. My findings suggest that alterations to key

signaling components or pathways in these cells may be responsible for coordinating focal adhesion dynamics and cell migration irrespective of PTP α expression.

Lay Summary

The ability of cells to move is critical to many physiological processes, such as wound healing and response to inflammation. Cell migration is also intimately linked to the development and progression of human diseases, notably the spread of cancer cells to form new tumors at other sites in the body. Interactions between a cell and its environment regulate cell movement, and involve physical linkages between external molecules and receptors on the cell surface that initiate changes inside the cell. An important change is the formation of large molecular complexes called focal adhesions that produce signals to coordinate cell shape and movement. In this study I investigated the role of PTP α , a cell surface protein that promotes cell movement, focal adhesion formation (shape, lifetime) and migration (directionality, cell orientation). Understanding the molecules and processes that control cell migration could lead to treatments to inhibit abnormal migration in diseases such cancer.

Preface

The research presented in this thesis dissertation was conducted in Dr. Catherine J. Pallen's laboratory at BC Children's Hospital Research Institute. Under Dr. Pallen's supervision, I have participated in the identification and design of this research project, in addition to conducting all experiments, data collection and analysis of the findings. All research has been carried out in accordance with UBC Biological Safety Training Course, certificate number 2015-jQqKr.

The mice were bred, maintained, and sacrificed by Dr. Jing Wang. Genotype confirmation of the mouse embryos by PCR was performed by Dr. Jing Wang. I performed the dissection, harvest and culture of mouse embryonic fibroblasts with the help of Dr. Hoa Le.

Animal care was conducted according to the guidelines of the University of British Columbia and the Canadian Council on Animal Care. Approval was obtained from the University of British Columbia Animal Care Committee, certificate number A14-0020.

Table of Contents

Abstract.....	ii
Lay Summary	iv
Preface.....	v
Table of Contents	vi
List of Tables	x
List of Figures.....	xi
List of Abbreviations	xiii
Acknowledgements	xvii
Dedication	xviii
Chapter 1: Introduction	1
1.1 Cell migration	1
1.1.1 Physiological and pathological processes requiring migration.....	1
1.2 Cell signaling and coordination of movement	2
1.2.1 Integrin signaling	2
1.2.2 Focal adhesion formation.....	3
1.2.3 Focal adhesion coordination of the actin cytoskeleton	5
1.2.4 Focal adhesion disassembly and turnover in cell movement	7
1.2.5 Key players in focal adhesion signaling – FAK, Src, paxillin, vinculin, Cas.....	9
1.3 Protein tyrosine phosphatases	15
1.3.1 Protein tyrosine phosphatase alpha.....	17

1.3.2	PTP α in receptor-mediated activation of Src family kinases and signaling	18
1.3.3	PTP α in integrin signaling	19
1.3.3.1	Catalytic signaling role of PTP α	20
1.3.3.2	Non-catalytic signaling role of PTP α	20
1.3.3.3	PTP α recruits focal adhesion proteins	21
1.3.4	PTP α and migration	22
1.4	Rationale and hypothesis	24
Chapter 2: Materials and Methods		30
2.1	Cell lines and cell culture	30
2.1.1	Spontaneous immortalization of MEFs	31
2.1.2	Depletion of PTP α from WT2 MEFs and MDA-MB-231 cells	32
2.2	Antibodies and immunological detection reagents	33
2.2.1	Primary antibodies	33
2.2.2	Secondary antibodies	33
2.3	Fibronectin stimulation of cells	33
2.3.1	Cell culture and stimulation	33
2.3.2	Cell stimulation for imaging	34
2.4	TIRF microscopy	35
2.5	Cell lysis and immunoblotting	35
2.6	Wound healing assay	36
2.7	Transwell assay	37

2.7.1	Transwell assay for MEFs	37
2.7.2	Transwell assay for MDA-MB-231 cells.....	38
2.8	Directionality assay.....	39
2.9	MTOC polarization assay	39
2.10	Statistical analysis	40

Chapter 3: The Role of PTP α and PTP α -Y789 Phosphorylation in Integrin-Stimulated

Focal Adhesion Formation, Morphology, and Turnover41

3.1	Rationale	41
3.2	Wild-type (WT) and PTP α knockout (KO) MEF cell lines	42
3.3	Focal adhesion formation in established WT and PTP α KO MEF cell lines	43
3.4	Focal adhesion formation in newly generated WT and PTP α KO MEF cell lines	44
3.5	Focal adhesion dynamics in established and newly generated WT and PTP α KO MEFs	45
3.6	Role of PTP α -pTyr789 in focal adhesion morphology and turnover in MEFs	47
3.7	Investigation of the molecular responses of newly generated MEFs to integrin stimulation.....	49
3.8	Discussion	51

Chapter 4: The Role of PTP α and PTP α -Y789 Phosphorylation in Migration Ability,

Directionality, and Cell Polarity61

4.1	Rationale	61
-----	-----------------	----

4.2	The role of PTP α in wound healing.....	62
4.3	The role of PTP α -pTyr789 in wound healing	63
4.4	Investigating the role of PTP α in Transwell migration	64
4.5	The role of PTP α and PTP α -pTyr789 in directional cell movement	65
4.6	The role of PTP α in cell polarization at the wound edge	66
4.7	Discussion.....	68
Chapter 5: General Discussion		79
5.1	PTP α in integrin-mediated focal adhesion dynamics and SFK phosphorylation	79
5.2	PTP α -dependence in migration ability, directionality, and cell polarity	81
5.3	Potential reasons for discrepancy in results	82
5.3.1	Spontaneous immortalization of MEFs	83
5.3.2	Dissection and culture of primary MEFs	87
5.3.3	Epithelial to mesenchymal transition.....	88
5.3.4	MDA-MB-231 cell migration.....	90
5.3.5	CRISPR/Cas off-target effects.....	91
5.4	Retrospective experimental directions	92
5.5	Conclusion	94
Chapter 6: Bibliography.....		96

List of Tables

Table 4.1 Focal adhesion characteristics and cell migration properties of MEFs	78
--	----

List of Figures

Figure 1.1 The focal adhesion complex	25
Figure 1.2 The focal adhesion cycle	26
Figure 1.3. Overview of the protein tyrosine phosphatase (PTP) superfamily.....	27
Figure 1.4. The two roles of PTP α in integrin signaling	28
Figure 1.5 Key integrin-mediated adhesion proteins in focal adhesion signaling	29
Figure 3.1 PTP α expression and morphology of WT and PTP α KO cell lines	55
Figure 3.2 PTP α regulates focal adhesion morphology in integrin-stimulated MEFs	56
Figure 3.3 PTP α plays a role in focal adhesion formation and dynamics in integrin-stimulated MEFs.....	57
Figure 3.4 Focal adhesion morphology is affected by the absence of PTP α -Tyr789 in integrin-stimulated MEFs	58
Figure 3.5 Focal adhesion dynamics are affected by the absence of PTP α -Tyr789 in integrin-stimulated MEFs	59
Figure 3.6 Early integrin-stimulated signaling events in WT and PTP α KO MEFs.....	60
Figure 4.1 Wound healing abilities of WT and PTP α KO MEFs.....	71
Figure 4.2 Wound healing ability of PTP α -depleted MEFs	72
Figure 4.3 Wound healing ability of PTP α -depleted MDA-MB-231 Cells	73
Figure 4.4 Wound healing ability of mutant MEFs expressing PTP α -Y789F	74

Figure 4.5: Migration ability of PTP α KO MEFs and PTP α -depleted MDA-MB-231 Cells 75

Figure 4.6 Directionality and migration efficiency are unaffected by the absence of PTP α or
mutation of PTP α -Tyr789 in MEFs..... 76

Figure 4.7 Microtubule organizing centers (MTOCs) improperly orient in PTP α -depleted MEFs
at the wound edge 77

List of Abbreviations

Abl	Abelson murine leukemia oncogene
Arp2	actin-related protein 2
Arp3	actin-related protein 3
Asp	aspartic acid
BCAR3	breast cancer anti-estrogen resistance 3
BCR-ABL	breakpoint cluster region-Abelson murine leukemia fusion protein
BSA	bovine serum albumin
Cas	Crk-associated substrate
CCH	Cas family C-terminal homology domain
CH2	Cdc25 homology domain
CNS	central nervous system
DMEM	Dulbecco's modified Eagle medium
DSP	dual specific protein phosphatases
ECM	extracellular matrix
EDTA	ethylenediaminetetraacetic acid
eGFP	enhanced green fluorescent protein
ERK2	extracellular signal-regulated kinase 2
EyA	eyes absent
FA	focal adhesion
FAK	focal adhesion kinase
FAT	focal adhesion targeting

FBS	fetal bovine serum
FC	focal complex
FERM	protein 4.1, ezrin, radixin, moesin domain
FN	fibronectin
GAP	GTPase activating protein
GEF	guanine nucleotide exchange factor
Grb2	growth factor receptor-bound protein 2
HG	highly glycosylated
HRP	horseradish peroxidase
Ig	immunoglobulin
IGF-1	insulin growth factor-1
IL-1 β	interleukin-1 beta
KO	knockout
LD	leucine-rich domain
LIM	Lin-1, Isl-1, Mec-3
LIM2	Lin-1, Isl-1, Mec-3 protein 2
LIM3	Lin-1, Isl-1, Mec-3 protein 3
LMPTP	low molecular weight protein tyrosine phosphatase
MAPK	mitogen-activated protein kinase
MEF	mouse embryonic fibroblast
MKP	MAPK phosphatase
MLC	myosin II regulatory light chain
NA	nascent adhesion

Nck	non-catalytic region of tyrosine kinase adaptor protein
NGS	normal goat serum
NMDA	N-methyl-D-aspartate
NP-40	Nonidet P-40
P/S	penicillin/streptomycin
PBS	phosphate-buffered saline
PCR	polymerase chain reaction
PFA	paraformaldehyde
Phe	phenylalanine
PI3K	phosphoinositide 3-kinase
PLL	Poly-L-Lysine
PMSF	phenylmethylsulfonyl fluoride
PR	proline-rich
PTK	protein tyrosine kinase
PTP	protein tyrosine phosphatase
PTP α	protein tyrosine phosphatase alpha
PVDF	polyvinylidene difluoride
Rac1	Ras-related C3 botulinum toxin substrate 1
RIPA	radioimmunoprecipitation assay
ROCK	Rho-associated kinase
RPTP	receptor-like protein tyrosine phosphatase
SDS	sodium dodecyl sulfate
SDS-PAGE	sodium dodecyl sulfate polyacrylamide gel electrophoresis

SF	serum-free
SFK	Src family kinase
SH2	Src homology 2
SH3	Src homology 3
SH4	Src homology 4
siRNA	small interfering ribonucleic acid
STI	soybean trypsin inhibitor
SV40	Simian Virus-40 large tumor-antigen
TIRF	total internal reflection fluorescence
Tyr	tyrosine
WASP	Wiskott-Aldrich syndrome protein
WT	wild-type

Acknowledgements

I would like to extend my sincere thanks to my supervisor, Dr. Catherine Pallen, for taking a chance on me and seeing me through the many difficulties I have faced throughout this project. Your attention to detail and ambition are traits that I admire and hope to project in my future.

I am greatly appreciative for my supportive committee members Dr. James Lim and Dr. Laura Sly who have always provided invaluable feedback and encouragement throughout my research project. I would also like to thank Dr. James Lim for allowing me to access the TIRF microscope and all of his tireless support with training and troubleshooting, as well as data acquisition, processing and interpretation.

To my incredible lab members, I would like to extend my warmest thanks, for always listening, and providing feedback or suggestions whenever possible. Thank you for keeping me laughing and creating a supportive and fun lab environment.

To my parents and brother, who have somehow managed to provide immense support and comfort from across the country, thank you for all that you do for me.

Lastly, to my Vancouver family: Drew, Dom, Rachel, Ally G, Ally Mac, Luke, and Kate, thank you for your undying support, for making me laugh on the toughest days, and always giving me the encouragement I needed to keep going.

Dedication

To my family, for believing in me when I fail to do so. Thank you for always supporting my aspirations, no matter how far away they take me. Anything is possible with you in my corner.

Chapter 1: Introduction

1.1 Cell migration

Cell migration is a fundamental process for the development and maintenance of the body. Cells receive signals from their external environment that trigger intracellular events that direct a cell to relocate to where it is needed. Many physiological processes require cell movement, while many pathological processes manifest from defective or abnormal cell movement. Therefore, cell migration is an important phenomenon to understand.

1.1.1 Physiological and pathological processes requiring migration

Cell migration is critical to many physiological processes including embryonic development, wound healing, and immune response (Michaelis, 2014). During gastrulation in the developing embryo, sheets of cells migrate to give rise to the three germ layers of the embryo which later differentiate into the specialized cells that comprise and define tissues and organs (Michaelis, 2014). Epithelial cell migration is critical to wound healing and renewal of the skin (Ridley et al., 2003). Leukocytes from the circulation migrate to areas of inflammation to destroy foreign microorganisms, initiate immune responses, and clear the tissue of debris (Ridley et al., 2003).

Cell migration is a critical component of the body's ability to maintain homeostasis. However, this process requires precise regulation as many diseases occur when cell migration is defective or aberrant. Defective cell migration in embryogenesis can manifest in abnormalities in the brain, lungs, and heart. Impaired cell migration in epithelial cells and leukocytes may lead to issues involving delayed wound healing and chronic inflammation. Any system that requires cell

migration is vulnerable to impairments in this process. In contrast, a cell that acquires the ability to migrate can be just as problematic. Tumor metastasis is a process in which cancer cells can break away from the primary tumor and migrate to a distant location in the body, and is responsible for most cancer-related fatalities (Yamaguchi et al., 2005). The drastic implications of aberrant cell migration demonstrate the importance of elucidating the exact molecular mechanisms involved in migration, with the potential to exploit them to develop targeted therapies to treat diseases.

1.2 Cell signaling and coordination of movement

1.2.1 Integrin signaling

Integrins are cell surface receptor proteins that are fundamental to a cell's ability to detect and respond to its extracellular environment. Integrins provide structural and functional linkages from the extracellular matrix (ECM) to the intracellular cytoskeleton. Their heterodimer structure comprises two non-covalently linked α and β subunits. There are 18 α and 8 β subunits that associate in 24 unique combinations to provide ligand specificity and non-redundant functions in mammals (Hynes, 2002). Their distinct functions have been elucidated using knockout mouse models of α and β subunits. Understanding the specific structure and function of integrins has been immensely advantageous as they are implicated in many human diseases such as cancer, inflammation, and autoimmune disorders (Hynes, 2002). To date, 3 of the 24 known integrins are being therapeutically targeted using monoclonal antibodies, peptides, and small molecules for treatment of thrombosis prevention, multiple sclerosis, and Crohn's disease (Ley et al., 2016). Despite the specificity of integrins, many can recognize multiple ligands and in turn, one ligand may bind to more than one integrin (Humphries, 1990; Ruoslahti and Pierschbacher, 1987).

Integrins are categorized into four groups according to which types of ligands they interact with.

1) RGD-binding integrins recognize ligands that contain an RGD tripeptide motif, such as fibronectin (FN); 2) LDV-binding integrins recognize the LDV acidic motif, this motif is also present in FN; 3) A-domain β 1 integrins wherein the subunit contains an A-domain which provides specificity for binding laminin and collagen; and 4) non- α A-domain containing laminin-binding integrins (Humphries et al., 2006).

The complexity of integrins and their interactions with various ligands allows precise communication of conditions of the dynamic extracellular environment to the intracellular environment, and *vice versa*. This bidirectional integrin signaling is referred to as “inside-out” and “outside-in” signaling. Inside-out signaling refers to changes to integrin cytoplasmic domains that translate to adjustments in the extracellular domain affinity for ligand binding, in order to promote or discourage cell-ECM or cell-cell adhesions (Ginsberg et al., 1992). On the other hand, outside-in signaling involves extracellular integrin ligation which triggers intracellular signaling and integrin clustering (Kim et al., 2004). The “outside-in” pathway is characteristic of migrating cells, as integrin engagement initiates a cascade of intracellular changes that leads to the formation of focal adhesions that link the ECM to the cytoskeleton, directing cell movement (Zaidel-Bar et al., 2004).

1.2.2 Focal adhesion formation

Focal adhesions are transient, multiprotein complexes that coordinate cell shape and movement. Structurally, they mediate the linkage between integrins and the actin cytoskeleton through contact with the actin stress fibers. Functionally, they facilitate a complex network of protein-protein interactions that lead to changes in cell shape to coordinate movement.

Focal adhesions form in a hierarchical manner at the leading edge of the migrating cell. Nascent adhesions form at the leading edge of the membrane protrusion known as the lamellipodium. These nascent adhesions can quickly turn over (in ~60 s) or mature to larger (~1µm diameter), “dot-like” focal complexes that can exist for several min (Parsons et al., 2010). Focal complexes arise when nascent adhesions continue to grow and recruit early adhesion proteins starting with talin and paxillin, and later including vinculin, α -actinin, and focal adhesion kinase (FAK) (Zaidel-Bar et al., 2004). As the lamellipodium advances, focal complexes are continuously assembled and disassembled. However, when the lamellipodium stops protruding or retracts, these focal complexes are replaced with more robust, definitive focal adhesions (Zaidel-Bar et al., 2004). Focal adhesions are large (2 µm wide, 3-10 µm long in fibroblasts), elongated adhesions, that are linked to large actin stress fibers (Zimmerman et al., 2004). These integrin-mediated focal adhesions contain at least 232 proteins that give rise to the “integrin adhesome” (Winograd-Katz et al., 2014), however, proteomic studies have further elucidated between 600-900 focal adhesion-enriched proteins (Fig.1.1A) (Humphries et al., 2009; Kuo et al., 2011; Schiller et al., 2011). These molecules form a multitude of interactions in order to: a) act as a scaffold to support the structural attachment of the ECM-bound cell to the actin cytoskeleton, or b) provide a regulatory function by initiating signaling pathways which allow the cell to respond to the conditions of the external environment by regulating cell shape and dynamics (Winograd-Katz et al., 2014). The scaffolding molecules within focal adhesions include adhesion receptors, adapters, cytoskeletal and actin binding proteins; while the regulatory molecules include kinases, phosphatases, GTPases and their regulatory GAP and GEF proteins, as well as ubiquitin ligases and proteases (Zaidel-Bar and Geiger, 2010; Zaidel-Bar et al., 2007).

1.2.3 Focal adhesion coordination of the actin cytoskeleton

Interaction between focal adhesions and the actin cytoskeleton is required for maturation and turnover of adhesions to promote cell migration. Adhesion formation at the leading edge of the cell is closely linked to lamellipodial and filipodial protrusions (Parsons et al., 2010). These protrusions are driven by the polymerization of actin filaments that are organized into two areas of the leading edge: the lamellipodium and the lamellum (Fig. 1.2A) (Ponti et al., 2004). The lamellipodium is the broad protrusion of the leading edge that comprises actin organized in dendritic branches located just beneath the cell membrane in the cytosol (Pollard and Borisy, 2003). Actin polymerization in the lamellipodium is driven by the Arp2/3 complex. The Arp 2/3 complex is regulated by Cdc42 and Rac, which are Rho GTPases that regulate WASP family proteins. These WASP family proteins activate Arp2 and Arp3, which act as a complex to bind actin filaments and induce polymerization in a branched or dendritic organization (Nicholson-Dykstra et al., 2005; Pollard and Borisy, 2003). In the lamellipodium, actin filaments rapidly shuffle from the cell edge toward the center of the cell, driven by the resistance of the membrane as actin is polymerized at the leading edge; in a process termed retrograde flow. In the lamellum, retrograde flow is much slower, and actin filaments are organized into thicker actin bundles that run parallel to one another, towards the direction of the leading edge (Parsons et al., 2010). There is a transition zone in the area between the lamellum and lamellipodium which is the site of depolymerization of dendritic actin and reorganization of actin into bundles (Fig. 1.2A) (Hotulainen and Lappalainen, 2006; Rottner et al., 1999; Shemesh et al., 2009).

As actin polymerization and depolymerization are closely linked to focal adhesion formation and disassembly, it is unclear which of these processes precedes the other (Parsons et al., 2010). There are two models that propose the order in which focal adhesion nucleation and

elongation occurs. The first model proposes that adhesions form in response to integrin ligation, which in turn promotes integrin clustering and assembly of adhesion complexes. These focal adhesions comprise important adhesion proteins that mediate direct or indirect linkage of integrins to dendritic actin filaments such as talin, vinculin, and α -actinin. The second model suggests that assembly of adhesions is initiated by polymerization of dendritic actin and that adhesion proteins such as vinculin and FAK bind directly to the Arp2/3 complexes before the nucleation of the adhesion. Furthermore, this interaction could promote formation of integrin-clustering complexes preceding the engagement of the extracellular domain of integrins to the ECM (Parsons et al., 2010). Although these models propose two distinct pathways of adhesion nucleation in the migrating cell, it is unlikely that they are mutually exclusive, but rather that they function simultaneously to allow the rapid nucleation of adhesions.

In the protruding edge of the migrating cell, specifically in the leading edge of the lamellipodium, nascent adhesions are formed at a similar rate to the protrusion rate (Choi et al., 2008). These nascent adhesions help to stabilize and further promote the protruding lamellipodium (Kuo, 2013). The adhesions either mature into focal adhesion complexes at the leading edge of the lamellipodium where actin is being polymerized, or disassemble as the trailing edge of the lamellipodium, a site of actin depolymerization, moves past them (Vicente-Manzanares et al., 2009). The nascent adhesions contain Rac1 regulatory proteins, including activators, effectors, and downstream targets, which induce dendritic actin polymerization necessary for continual membrane protrusion (Kuo, 2013). Nascent adhesions mature as actin filaments cross-link with α -actinin creating a physical template for elongation of the adhesion to occur, producing focal complexes (Kuo, 2013; Vicente-Manzanares et al., 2009). Further maturation of these complexes to focal adhesions requires bundling of these actin filaments,

creating stress fibers that provide a stronger linkage from the integrin to the cytoskeleton (Fig. 1.2A) (Kuo, 2013; Vicente-Manzanares et al., 2009). In addition to α -actinin, other early adhesion proteins aid in the linkage of actin to the focal adhesion. For instance, talin is a mediator in the linkage of integrins to actin and is required for adhesion stability and disassembly. Vinculin can bind directly to actin, as well as to the actin cross-linker α -actinin (Fig. 1.B) (Vicente-Manzanares et al., 2009). These focal adhesion proteins strengthen the linkage between integrins and actin filaments.

The formation of focal adhesions requires compositional reorganization of key regulatory proteins. These regulatory proteins contribute to the strength of the adhesion through their enzymatic activity (Kuo, 2013). The small GTPase RhoA drives focal adhesion maturity through activating myosin II, thereby increasing contractility in the adhesions. RhoA activation of Rho-associated kinase (ROCK) inhibits myosin light chain phosphatase to promote phosphorylation of the myosin II regulatory light chain (MLC) (Leung et al., 1996; Maekawa et al., 1999). This action generates contractility within the actin filaments and contributes cellular tension that is instrumental to focal adhesion maturity (Helfman et al., 1999). Continued activation of myosin II maintains these contractile forces thereby intensifying cellular tension, which results in the contraction of the actin stress fibers towards the adhesion site and results in translocation of the cell body (Kuo, 2013).

1.2.4 Focal adhesion disassembly and turnover in cell movement

Directional cell migration requires a dynamic cycle of focal adhesion formation at the leading edge of a cell, translocation of the cell body toward the new adhesions, coupled with disassembly of focal adhesions and retraction of the tail at the rear of the cell (Fig. 1.2B). The

simultaneous assembly and turnover of adhesions is essential for continuous movement to occur. Focal adhesion kinase (FAK) and Src kinase regulate turnover in protrusions. FAK-deficient fibroblasts show a reduction in migration likely due to the increased number of large adhesions at the cell periphery that results in defective turnover (Ilic et al., 1995; Sieg et al., 2000; Webb et al., 2004). The autophosphorylation of FAK at Tyr397 and the subsequent activity of the kinase are important for FAK-mediated turnover (Hamadi et al., 2005; Webb et al., 2004). FAK inhibition of Rho activity has also been indicated to promote turnover of focal adhesions (Ren et al., 2000). Src catalytic activity and membrane association is also implicated in adhesion turnover and dissociation from FAK in cell motility (Fincham and Frame, 1998).

Focal adhesion disassembly is also associated with the retraction of the leading edge, as the protrusion extends and retracts during migration (Parsons et al., 2010). Another site of focal adhesion disassembly is at the retraction and detachment of the trailing edge of the migrating cell (Huttenlocher and Horwitz, 2011). Focal adhesion disassembly at sites of retraction is often associated with what appears to be the “sliding” of adhesions. This sliding movement of the adhesions is due to the centripetal movement of the cell edge and subsequent displacement of adhesion structures. The mechanisms behind adhesion sliding are not properly understood, however it is believed to be a Rho GTPase/ myosin II-dependent treadmilling, as the outer edge of the adhesion appears to disassemble while the central edge assembles (Ballestrem et al., 2001; Digman et al., 2008). Thus, the exchange of individual adhesion components results in a translocation of the adhesion. Occasionally, the integrins remain attached to the matrix behind the migrating cell, indicating the capability of the migrating cell to sever integrins from the cytoplasmic adhesion components during detachment (Palecek et al., 1998).

Adhesion disassembly in regions of cell retraction has also been linked to the Ca^{2+} -activated protease calpain. Calpains mediate cleavage of various adhesion proteins; such as FAK, talin, and paxillin (Carragher et al., 1999; Franco and Huttenlocher, 2005). Downregulation or inhibition of calpain leads to large adhesion complexes, inhibited cell detachment, and decreased cell speed in migration (Franco and Huttenlocher, 2005; Palecek et al., 1998).

1.2.5 Key players in focal adhesion signaling – FAK, Src, paxillin, vinculin, Cas

Integrin-mediated focal adhesions form at the plasma membrane of the cell and provide physical and molecular connections between the cell and its environment. Focal adhesions act as signaling hubs to interpret biochemical and physical cues from the external environment to elicit multiple cellular responses; from differentiation and death, to reorganization of the actin cytoskeleton and cell movement. Focal adhesions involve many scaffolding and signaling molecules that contribute to their biochemical complexity, which permits their diverse functions (Case et al., 2015). There are a few key focal adhesion molecules that are at the forefront of adhesion signaling – FAK, Src, paxillin, vinculin, and Cas, and these will be discussed in greater detail.

Focal Adhesion Kinase (FAK): FAK is a 125 kDa non-receptor tyrosine kinase that is ubiquitously expressed and highly conserved (Ilic et al., 1995; Mitra et al., 2005). The kinase is comprised of three domains: an N-terminal FERM domain, a central kinase domain, and a C-terminal focal adhesion targeting (FAT) domain, in addition to containing a proline-rich (PR1 and PR2) region (Mitra et al., 2005). In the absence of integrin ligation, FAK is inactive due to an auto-inhibitory interaction between the FERM and kinase domains, that undergoes a

conformational change upon integrin stimulation to mediate FAK activation (Lietha et al., 2007). FAK is a key mediator of integrin signaling which localizes to focal adhesions indirectly through association of the FAT domain with key focal adhesion proteins, paxillin and talin (Mitra et al., 2005).

Integrin stimulation promotes many signaling events, among the earliest being the autophosphorylation of FAK at Tyr397 (Sieg et al., 2000; Toutant et al., 2002). This phosphorylation event creates a high-affinity binding site for Src homology 2 (SH2)-containing Src family kinases (SFKs), which generates a Src-FAK complex (Schlaepfer et al., 2004). Src binding to FAK enhances Src kinase activity (Schlaepfer et al., 2004) and initiates phosphorylation of FAK in the activation loop at Tyr576/577, permitting its maximal activation (Ruest et al., 2000). The activated Src-FAK complex has many downstream targets that regulate various pathways involved in cell cycle progression, proliferation, focal adhesion dynamics, and cell migration (Mitra and Schlaepfer, 2006).

FAK is both a signaling kinase and a scaffolding protein, which enables it to modulate numerous intracellular signaling pathways that effect remodeling of the cytoskeleton, turnover of focal adhesions, and ultimately cell migration (Mitra et al., 2005). One important target of the Src-FAK complex is p130 Crk-associated substrate (Cas), which promotes Rac-dependent cell-motility upon interaction (Hanks et al., 2003; Mitra and Schlaepfer, 2006). In fact, FAK differentially activates and inhibits Rho GTPases to modulate cell movement (Parsons et al., 2010; Ridley et al., 2003; Wu et al., 2004b; Zhai et al., 2003). FAK interacts with Grb2 to activate Ras and the ERK2/MAPK pathway (Mitra et al., 2005) to regulate focal adhesion turnover, cell proliferation and survival (Hanks et al., 2003; Mitra et al., 2005; Webb et al., 2004). FAK knockout cells show reduced cell motility and have increased numbers of focal

adhesions that are larger and defective in turnover (Ilic et al., 1995; Sieg et al., 1999). Therefore, FAK is an integral part of signal transduction pathways that allow external cues from the ECM to be transmitted intracellularly, and in turn, convey internal responses back to the ECM.

Src: Src is a 60 kDa non-receptor tyrosine kinase. It is the prototype member of the SFKs, a family of nine members, most notably Src, Fyn, and Yes (Playford and Schaller, 2004). Src and other SFKs are involved in cell proliferation, differentiation, motility, and survival (Thomas and Brugge, 1997). Structurally from the N- to C-terminus, Src contains an N-terminal myristoyl group, three Src-homology domains (SH4, SH3, and SH2), a protein tyrosine kinase domain, and a C-terminal regulatory tail (Roskoski, 2005). Src modulates many downstream effectors including several integrin signaling proteins (paxillin, vinculin, talin, Cas and cortactin) and FAK (Brown and Cooper, 1996).

Src localizes to focal adhesions through the myristoylation site in the N-terminus and the constitutive association of the SH3 domain with the cytoplasmic tail of $\beta 3$ integrins (Arias-Salgado et al., 2005; de Virgilio et al., 2004). Src contains an inhibitory phosphorylation site at Tyr527 in the C-terminal tail, that forms an intramolecular interaction with the SH2 domain upon phosphorylation (pTyr527), resulting in an inactive conformation (Roskoski, 2004; Zheng et al., 2000). Integrin activation and subsequent clustering promotes the dephosphorylation of the inhibitory site, which is catalyzed by the protein tyrosine phosphatases PTP α and PTP1B (den Hertog et al., 1993; Liang et al., 2005; Pallen, 2003; Zheng et al., 1992). PTP α -deficient cells demonstrate a reduction in activity of Src and Fyn coupled with increased Src-pTyr527 (Ponniah et al., 1999; Su et al., 1999). Additional mechanisms of Src activation include

autophosphorylation of Tyr416 in the activation loop of Src and displacement of the regulatory intramolecular interactions involving the SH2 and SH3 domains (Thomas and Brugge, 1997).

The formation of the Src-FAK complex at focal adhesions regulates the phosphorylation of two key adhesion molecules, paxillin and Cas (Bellis et al., 1995; Cary et al., 1998; Schaller and Parsons, 1995). Cas and paxillin are important for the recruitment of additional molecules to adhesions to modulate the organization of the cytoskeleton. Small molecule-mediated inhibition of SFKs results in defective focal adhesion turnover (Webb et al., 2004) and fibroblasts derived from mice deficient in Src, Yes, and Fyn (SYF cells) exhibit reduced spread and motility (Klinghoffer et al., 1999).

Paxillin: Paxillin is a 68 kDa scaffolding protein that functions to facilitate cell signaling, through direct and indirect association with other structural or regulatory proteins at focal adhesions (Deakin and Turner, 2008). Paxillin is one of the earliest focal adhesion proteins detected in adhesions at the leading edge of the cell (Digman et al., 2008) and is phosphorylated following cell adhesion to the ECM (Burrige et al., 1992). Paxillin is therefore a defining component, and a promoter of, the developing adhesion (Deakin and Turner, 2008).

The N-terminal half of paxillin controls the majority of the protein's signaling activity and contains five leucine and aspartate-rich LD motifs (LD1-LD5) (Tumbarello et al., 2002). The LD motifs are necessary for cytoskeletal coordination and cell migration due to their direct association with adhesion proteins such as FAK, vinculin, actopaxin, and PYK2 (FAK-family member), as well as their indirect association with molecules such as Cas, Src, Grb2 and talin (Turner, 2000). The LD4 motif plays an important role in controlling Rho GTPase signaling and focal adhesion turnover (Turner et al., 1999; West et al., 2001; Zhao et al., 2000). A proline-rich

region in the N-terminus of paxillin creates a docking site which Src can bind through its SH3 domain (Weng et al., 1993). The C-terminal half comprises four tandem LIM domains, two of which (LIM2 and LIM3) are critical for localization of paxillin to focal adhesions (Brown et al., 1996; Brown et al., 1998). Two key paxillin phosphosites in the N-terminus at Tyr31 and Tyr118 are phosphorylated by the Src-FAK complex (Bellis et al., 1995; Burridge et al., 1992; Schaller and Parsons, 1995; Turner, 2000) and are important in mediating focal adhesion dynamics and rearrangement of the actin cytoskeleton (Richardson et al., 1997).

Vinculin: Vinculin is a 117 kDa adaptor protein that is a key regulator of focal adhesions (Carisey and Ballestrem, 2011; Humphries et al., 2007). Its structure consists of an N-terminal head, a proline-rich hinge region, and a C-terminal tail domain (Eimer et al., 1993; Winkler et al., 1996). Activation of vinculin is mediated by auto-inhibitory intramolecular binding between the head and tail domains (Johnson and Craig, 1994; Johnson and Craig, 1995), which undergo a conformational change upon simultaneous interaction with several binding partners when localized to focal adhesions (Chen et al., 2005; Chen et al., 2006a). Talin and α -actinin bind to the head; Arp2/3 to the neck; and actin and paxillin bind to the tail domains (Humphries et al., 2007).

Vinculin has numerous direct binding partners at focal adhesions that regulate maturation, stability and strength of adhesions, ECM mechanosensing, and dynamics of the actin cytoskeleton (Case et al., 2015). Vinculin-depleted cells demonstrate a reduction in attachment to the ECM, exhibit smaller and fewer focal adhesions, and display enhanced cell migration rates compared to WT cells (Coll et al., 1995; Saunders et al., 2006; Volberg et al., 1995; Xu et al., 1998). Interaction of vinculin and talin is necessary for vinculin to promote focal adhesion

formation and growth (Cohen et al., 2005; Humphries et al., 2007). Vinculin contains binding sites for actin as well as actin-associated proteins such as talin, α -actinin, Arp2/3, vinexin, VASP, and CAP (Carisey and Ballestrem, 2011). Inhibiting Arp2/3 binding to vinculin prevents efficient cell spreading and reduces cell migration (DeMali et al., 2002). Simultaneous binding of VASP to vinculin and zyxin, another focal adhesion protein, has been suggested to initiate an actin nucleation nodule in focal adhesions (Carisey and Ballestrem, 2011). Additional proteins bind to primary interactors of vinculin, which puts vinculin at the forefront of a molecular signaling network that controls many focal adhesion related processes (Carisey and Ballestrem, 2011).

p130Cas: Cas is a 130 kDa scaffolding protein which is a member of the Cas protein family along with three structurally similar proteins (Tikhmyanova et al., 2010). Cas comprises an N-terminal SH3 domain, a substrate domain (SD), a serine-rich region, a C-terminal Src binding domain, and a C-terminal Cas-family homology (CCH) domain (Janostiak et al., 2014b). These domains serve as docking sites for multiple focal adhesion proteins such as FAK, SFKs, tyrosine phosphatases, vinculin, Crk, Nck, and BCAR3 (Janostiak et al., 2014a; Polte and Hanks, 1995; Sakai et al., 1994; Schlaepfer et al., 1997).

Cas is also a mechanotransduction protein that is phosphorylated by SFKs at tyrosine residues in the SD that are exposed in response to mechanical stretching (Fonseca et al., 2004; Sawada et al., 2006). Upon integrin ligation, Cas translocates from the cytoplasm to focal adhesions where it is phosphorylated, and initiates molecular binding of adhesion proteins that mediate cell spreading, focal adhesion formation, migration, and reorganization of the actin cytoskeleton (Bouton et al., 2001; Cabodi et al., 2010; Fonseca et al., 2004; Honda et al., 1999).

Phosphorylation of Cas recruits the adapter protein Crk and Cas-Crk coupling stimulates actin polymerization at membrane protrusions to effect cell migration through a Rac-dependent mechanism (Fonseca et al., 2004; Klemke et al., 1998; Janostiak et al., 2011). Cas is involved in the adaptation of cyclic stretch, where stress fibers are realigned in the direction of the stretch (Lee et al., 2010). The reinforcement of focal adhesions during mechanical cellular strain also requires Cas (Carisey et al., 2013). Therefore, phosphorylation of Cas is a key integrin signaling event regulating many processes of cell migration (Fonseca et al., 2004).

1.3 Protein tyrosine phosphatases

Tyrosine phosphorylation is a reversible post-translational protein modification that is critical for a multitude of intracellular signal transduction events. Protein tyrosine kinases (PTKs) catalyze the phosphorylation of tyrosine, while protein tyrosine phosphatases (PTPs) remove phosphate groups. PTPs and PTKs act in concert to control tyrosine phosphorylation and activity of various signaling effectors in most physiological processes. Categorized by their structure and catalytic mechanism, the PTP superfamily comprises four subfamilies: Class I, Class II, Class III cysteine-based PTPs, and the Class IV Asp-based EyA PTPs (Fig. 1.3) (Alonso et al., 2004; Kim and Ryu, 2012; Tonks, 2006).

The Class I Cys-based PTPs, comprised of classical tyrosine-specific PTPs and dual specific protein phosphatases (DSPs), are the largest groups of PTPs. There are 38 classical tyrosine-specific PTPs that are further categorized into 21 transmembrane receptor-like proteins (RPTPs: i.e. PTP α , CD45, LAR) and 17 non-transmembrane, cytoplasmic PTPs (i.e. PTP1B, PTP-PEST, SHP2) (Kim and Ryu, 2012). Classical Tyr-specific PTPs contain a mobile acid/base loop (WPD) and a signature catalytic motif (HCX₅R). The cysteine residue in the catalytic motif

acts as a nucleophile during the removal of the phosphate group (Andersen et al., 2001; Kim and Ryu, 2012). The DSPs can also dephosphorylate phosphoserine (pSer) and phosphothreonine (pThr) in addition to phosphotyrosine (pTyr). An example of the cytoplasmic DSPs are the MAPK phosphatases (MKPs) that inactivate MAPK by dephosphorylating tyrosine and threonine residues (Kim and Ryu, 2012; Tonks, 2006).

The Class II Cys-based PTPs consist solely of the Cys-based low molecular weight (18kDa) PTP (LMPTP) in humans. The LMPTP is a cytosolic phosphatase composed of a single catalytic domain (Kim and Ryu, 2012; Madhurantakam et al., 2005) and its physiological role is not clear. The most notable distinguishing factor about this PTP is that the active site is located close to the N-terminus of the catalytic domain (Kim and Ryu, 2012), compared to other PTPs where the active sites reside near the C-terminus.

Class III Cys-based PTPs specifically dephosphorylate cyclin-dependent kinases at inhibitory sites, thereby promoting progression of the cell cycle (Alonso et al., 2004). They are known as the cell division cycle 25 (Cdc25) phosphatases and similar to the LMPTP, they share minor sequence homology with other PTPs (Kim and Ryu, 2012). Three members, Cdc25A, B, and C, comprise the Class III PTP family. Cdc25A and B have been implicated in several human cancers (Gasparotto et al., 1997; Kristjansdottir and Rudolph, 2004).

The Class IV Asp-based PTPs dephosphorylate phosphotyrosine and phosphothreonine and are unique as they contain an aspartate motif, rather than the signature cysteine residues present in the other three PTP classes (Okabe et al., 2009). These phosphatases can function as either transcription factors or enzymes (Jemc and Rebay, 2007).

1.3.1 Protein tyrosine phosphatase alpha

Protein tyrosine phosphatase alpha (PTP α) is a Class I transmembrane receptor-like PTP discovered in 1990. It is ubiquitously expressed, demonstrating the highest expression in the brain (Sap et al., 1990). PTP α -deficient mice are viable and have no visibly apparent abnormalities (Ponniah et al., 1999; Su et al., 1999), suggesting that PTP α function may be compensated for by other PTPs. PTP α knockout mice do however display spatial learning deficits, reduced activity levels, and decreased anxiety and fearfulness (Skelton et al., 2003). In addition, these mice show about a 50-70% reduction in Src and Fyn activity in the brain (Ponniah et al., 1999; Su et al., 1999), and a reduction in neuronal myelination in the CNS and PNS (Tiran et al., 2006; Wang et al., 2009). Hippocampal neuronal migration and long term potentiation have demonstrated requirements for PTP α (Petroni et al., 2003). Pathologically, PTP α overexpression has been implicated in human cancers such as breast, head and neck, colorectal, and gastric (Ardini et al., 2000; Berndt et al., 1999; Krndija et al., 2010; Tabiti et al., 1995; Wu et al., 2006).

PTP α is a 130 kDa protein with a short, glycosylated extracellular domain, a single transmembrane spanning region, and two catalytic D1 and D2 domains (Fig. 1.4). There is no known extracellular ligand for PTP α although PTP α does interact with a variety of other cell receptors (see section 1.3.2).

Many RPTPs contain a tandem arrangement of conserved PTP domains in their intracellular region. Typically, the membrane proximal (D1) domain is active, while the membrane distal (D2) domain usually has very low activity, or is inactive (Pallen, 2003; Tonks, 2006; Wang and Pallen, 1991). Like other PTPs, the majority of the catalytic activity of PTP α

resides in the D1 domain. However, the PTP α D2 domain is unusual in possessing low activity, the role of which remains elusive (Pallen, 2003). However, the structure of D2 contributes to the activity, specificity, and stability of the RPTP as well as its involvement in protein-protein interactions that regulate its dimerization (Blanchetot et al., 2002; Felberg and Johnson, 1998; Jiang et al., 2000; Streuli et al., 1990).

1.3.2 PTP α in receptor-mediated activation of Src family kinases and signaling

PTP α is an activator of SFKs which regulate many diverse signaling pathways underlying tumorigenesis, neuronal development, proliferation, T cell regulation, and integrin signaling and cell migration (Maksumova et al., 2007; Pallen, 2003). PTP α regulates the signaling of the receptor tyrosine kinase c-Kit, which controls cell migration and chemotaxis in bone-marrow derived mast cells (BMMCs) (Samayawardhena and Pallen, 2008).

PTP α -dependent SFK activation has also been implicated in neuronal development and signaling (Zeng et al., 1999). Contactin is a neuronal glycosyl phosphatidylinositol (GPI)-anchored receptor that associates with PTP α in a *cis*-membrane spanning complex through the extracellular domain of PTP α . The formation of a PTP α -contactin complex could provide the mechanism for the unknown linkage between contactin and Fyn, as well as a method of extracellular signal transduction by PTP α (Zeng et al., 1999).

PTP α -null mice display NMDA receptor-associated impairments in learning, memory, neuronal migration, and long-term potentiation (Le et al., 2006; Lei et al., 2002). PTP α -null mouse synaptosomes display reduced SFK activity, concomitant with a reduction in tyrosine phosphorylation of the NMDA receptor, suggesting an upstream role of PTP α in NMDA

receptor regulation (Le et al., 2006). PTP α phosphorylation also regulates neurite outgrowth through Fyn activation (Bodrikov et al., 2008).

PTP α and CD45 are PTPs that are abundantly expressed in T cells and regulate SFKs. CD45 regulates the phosphorylation of PTP α at tyrosine 789 (Tyr789), which is an important phosphosite for PTP α -dependent dephosphorylation of Fyn and Cbp, thereby regulating Fyn activation and restoring T cell receptor-induced signaling events (Maksumova et al., 2007).

This thesis focuses on yet another role of PTP α in receptor-mediated activation of SFKs through integrin signaling. Integrin signaling is an important early step in focal adhesion formation which involves the recruitment of many adhesion proteins to integrins in order to facilitate cellular processes that coordinate movement.

1.3.3 PTP α in integrin signaling

PTP α was first reported to be involved in cell adhesion in 1998, when ectopic expression of PTP α resulted in increased cell-substratum adhesion (Harder et al., 1998). PTP α is found in close proximity with activated integrins at the cell membrane, and has demonstrated transient co-localization and association with α_v integrins at the leading edge of spreading cells (von Wichert et al., 2003). Upon integrin ligation, PTP α mediates the phosphorylation and activation of many key focal adhesion proteins either directly or indirectly, such as Src, FAK, Cas, Paxillin, and ERK (Chen et al., 2006b; Harder et al., 1998; Ponniah et al., 1999; Su et al., 1999; von Wichert et al., 2003; Zeng et al., 2003).

Our lab has demonstrated that PTP α has two main roles in integrin signaling. The first role involves PTP α -mediated activation of Src, which promotes the interaction of Src and FAK

(Zeng et al., 2003). The resulting activated Src-FAK complex phosphorylates PTP α at Tyr789, giving rise to the second role of PTP α in regulating focal adhesion assembly, stress fiber organization, and cell migration (Chen et al., 2006b).

1.3.3.1 Catalytic signaling role of PTP α

Integrin engagement promotes the PTP α -mediated dephosphorylation of Src at Tyr527, resulting in Src activation (Ponniah et al., 1999; Su et al., 1999; von Wichert et al., 2003; Zeng et al., 2003). Integrin ligation also promotes autophosphorylation of FAK at Tyr397, which creates a high-affinity binding site for the SH2 domain of the Src or Fyn SFKs (Cary et al., 1996; Cobb et al., 1994; Schaller et al., 1994; Xing et al., 1994). Activated Src and FAK form a complex which mediates integrin signaling downstream of PTP α .

Integrin-stimulated PTP α -null MEFs and MEFs expressing catalytically inactive PTP α (lacking two cysteine residues in the active site of the D1 domain-C414S/C704S), show an increase in Src-pTyr527 and decrease in FAK-pTyr397 in comparison to WT MEFs (Chen et al., 2006b; Zeng et al., 2003). Taken together, these findings demonstrate a requirement for PTP α catalytic activity in Src activation and subsequent FAK phosphorylation in response to integrin stimulation.

1.3.3.2 Non-catalytic signaling role of PTP α

Activation of the Src-FAK complex is involved in regulating many downstream signaling events, including the phosphorylation of PTP α at Tyr789. PTP α is phosphorylated at Tyr789 in its C-terminal region in response to integrin stimulation, and dephosphorylated when cells are

detached from the substratum (Chen et al., 2006b). MEFs expressing catalytically inactive PTP α cannot mediate Src dephosphorylation and activation in response to integrin stimulation, and display minimal PTP α -Tyr789 phosphorylation unless Src is constitutively expressed (Chen et al., 2006b).

PTP α phosphorylation at Tyr789 is not involved in the integrin-mediated activation of Src or FAK, and does not affect PTP α catalytic activity. Furthermore, FAK-null fibroblasts show defective PTP α -Tyr789 phosphorylation in response to integrin engagement (Chen et al., 2006b). These observations confirm that PTP α phosphorylation at Tyr789 follows the formation of, and is mediated by, the Src-FAK complex. PTP α -pTyr789 plays a non-catalytic role in integrin signaling by serving as a binding site for proteins containing phosphotyrosine binding domains, thereby facilitating protein-protein interactions that regulate integrin signaling.

1.3.3.3 PTP α recruits focal adhesion proteins

PTP α -Tyr789 phosphorylation is involved in the recruitment of PTP α to integrin-induced focal adhesions, where it can interact with central focal adhesion signaling proteins (Lammers et al., 2000; Sun et al., 2012). Phosphorylation of PTP α at Tyr789 creates a binding site for SH2 domains in two important scaffolding proteins, Grb2 and BCAR3 (Cheng et al., 2014; Sun et al., 2012).

Our lab determined that the interaction of PTP α -pTyr789 with BCAR3 promotes the localization of BCAR3-bound Cas to focal adhesions, where Cas is phosphorylated by Src to enable downstream signaling (Sun et al., 2012). Cas phosphorylation recruits additional focal adhesion proteins to provide mechanical reinforcement of focal adhesions, stress fiber

coordination, and cell migration (Janostiak et al., 2011; Janostiak et al., 2014b). Therefore, PTP α -pTyr789 likely mediates focal adhesion formation and cell migration, at least in part, through its interaction with BCAR3 and indirect association with Cas.

Grb2 is another scaffolding protein that binds PTP α -pTyr789 through its SH2 and SH3 domains (den Hertog et al., 1994; denHertog and Hunter, 1996; Su et al., 1994; Su et al., 1996). Previous work in our lab demonstrated that Grb2-depleted cells displayed a reduction in PTP α -Tyr789 phosphorylation concomitant with abrogated FAK-Tyr397 phosphorylation and prohibition of the Src-FAK complex (Cheng et al., 2014). Grb2 was found to be involved in the autophosphorylation and activation of FAK following integrin signaling, demonstrating an upstream role of Grb2 in PTP α phosphorylation (Cheng et al., 2014). The SH2 domain of Grb2 binds FAK-pTyr925, which is phosphorylated by Src upon binding to FAK (Schlaepfer et al., 1994). Therefore, our lab proposed that the interaction of Grb2 with PTP α -pTyr789 may function to mediate coupling of the Src-FAK complex with PTP α -pTyr789. The proposed mechanism suggests that a Grb2 dimer could bind FAK-pTyr925 and PTP α -pTyr789 simultaneously, bringing the Src-FAK complex into proximity with additional PTP α receptors to produce maximal phosphorylation of Tyr789 (Cheng et al., 2014).

1.3.4 PTP α and migration

PTP α -deficient cells have previously shown a decrease in cell spreading in response to integrin stimulation on FN (Chen et al., 2006b; Herrera Abreu et al., 2008; Su et al., 1999; von Wichert et al., 2003; Zeng et al., 2003). This reduction in spreading is accompanied by a decrease in actin stress fiber assembly within the cell, as well as a reduction in focal adhesion

formation around the cell periphery (Chen et al., 2006b; Herrera Abreu et al., 2008; von Wichert et al., 2003; Zeng et al., 2003). Adhesions of PTP α -null cells appear larger and irregularly shaped, and are denoted as “supermature”, compared to the thin and elongated focal adhesions characteristic of WT cells (Chen et al., 2006b; von Wichert et al., 2003; Herrera Abreu et al., 2008; Zeng et al., 2003). The defects in cell spreading, actin stress fiber assembly, and focal adhesion formation observed in PTP α -null cells could be rescued by re-expressing WT PTP α , but not a catalytically inactive PTP α or an unphosphorylatable (PTP α -Y789F) mutant (Chen et al., 2006b).

Wound healing assays have revealed major migration defects in PTP α -deficient MEFs (Zeng et al., 2003). PTP α -null MEFs at the leading edge of the wound appear to have flattened cell edges that are relatively void of protrusions whereas WT MEFs exhibit several protrusions (Zeng et al., 2003). In addition to the migration defects observed in MEFs, PTP α -null hippocampal neurons exhibit abnormal radial migration during development (Petroni et al., 2003). PTP α has also been implicated in cellular invasion, a process requiring migration, demonstrated by the diminished ability of siRNA-mediated PTP α -depleted colon cancer cells to invade the stroma in an *in vivo* model (Krdija et al., 2010).

Haptotactic migration of PTP α -null cells towards FN is significantly defective compared to control WT MEFs (Chen et al., 2006b). This migration defect in PTP α -null MEFs cannot be rescued by expressing catalytically inactive mutant PTP α or unphosphorylatable mutant PTP α -Y789F, but is restored by re-expressing WT PTP α (Zeng et al., 2003). Therefore, PTP α expression and specifically, PTP α -Tyr789 phosphorylation, play significant roles in regulating the cellular processes that govern cell migration.

1.4 Rationale and hypothesis

PTP α regulates the activity of several focal adhesion proteins that play key roles in the process of cell migration. Src dephosphorylation and activation is catalyzed by PTP α in response to integrin engagement. Activated Src binds to FAK, leading to the formation of a Src-FAK complex which in turn phosphorylates PTP α at Tyr789 (PTP α -pTyr789).

PTP α -pTyr789 has been identified as a central regulator of PTP α -mediated focal adhesion formation, cell spreading, and actin cytoskeletal organization (Chen et al., 2006b). However, little is known about the role of PTP α -pTyr789 in the regulation of focal adhesion dynamics. Focal adhesion turnover is required for continuous cell migration (Wehrle-Haller, 2012) and interestingly, cells lacking PTP α or PTP α -pTyr789 present defective migration (Chen et al., 2006b; Krndija et al., 2010; Petrone et al., 2003; Zeng et al., 2003). **Thus, I hypothesize that PTP α and PTP α -pTyr789 are required to regulate focal adhesion dynamics and mechanisms that coordinate cell motility.**

The first aim in my project is to investigate the morphology, composition, and dynamics of developing adhesions in integrin-stimulated PTP α -null and PTP α -Y789F MEFs. The second aim of my study is to investigate parameters of cell motility to identify and distinguish how the focal adhesion dynamics of PTP α -null and PTP α -Y789F MEFs affect cell migration.

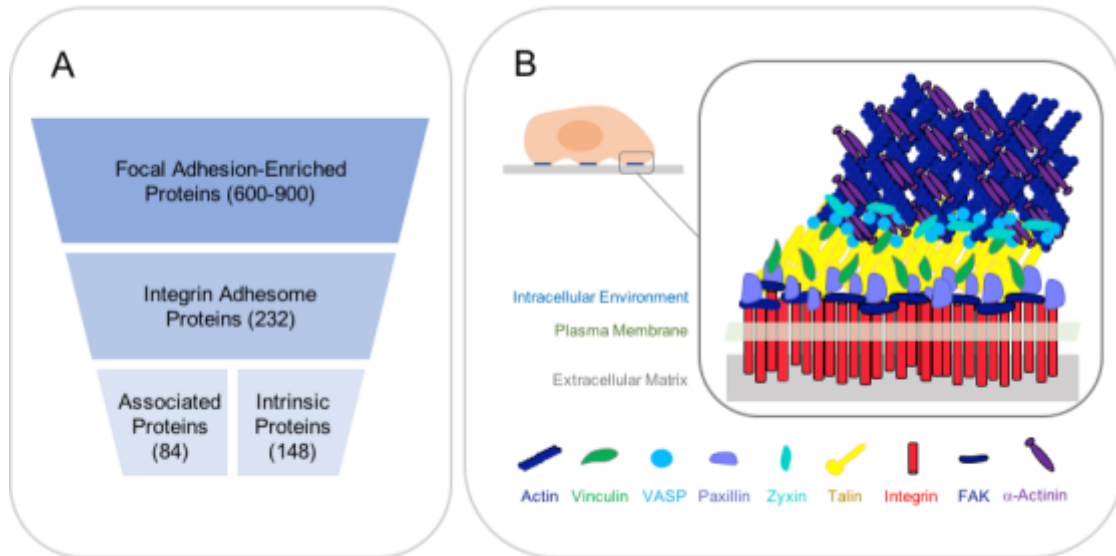


Figure 1.1 The focal adhesion complex. **A)** An overview of the increasing number of proteins identified as associated with the integrin-mediated focal adhesion. Of the 600-900 focal adhesion-enriched proteins found, 232 are known to be involved in the integrin adhesome. These proteins are further subdivided into intrinsic proteins (that are located mainly in the adhesion site) and associated proteins (that transiently interact with the adhesion). **B)** Focal adhesion proteins structurally link substrate-bound integrins to the actin cytoskeleton through many scaffolding and adaptor proteins. These proteins participate in a large network of protein-protein interactions within the focal adhesion complex that functions to coordinate cell shape and movement. (Adapted from Kanchanawong *et al.*, 2010)

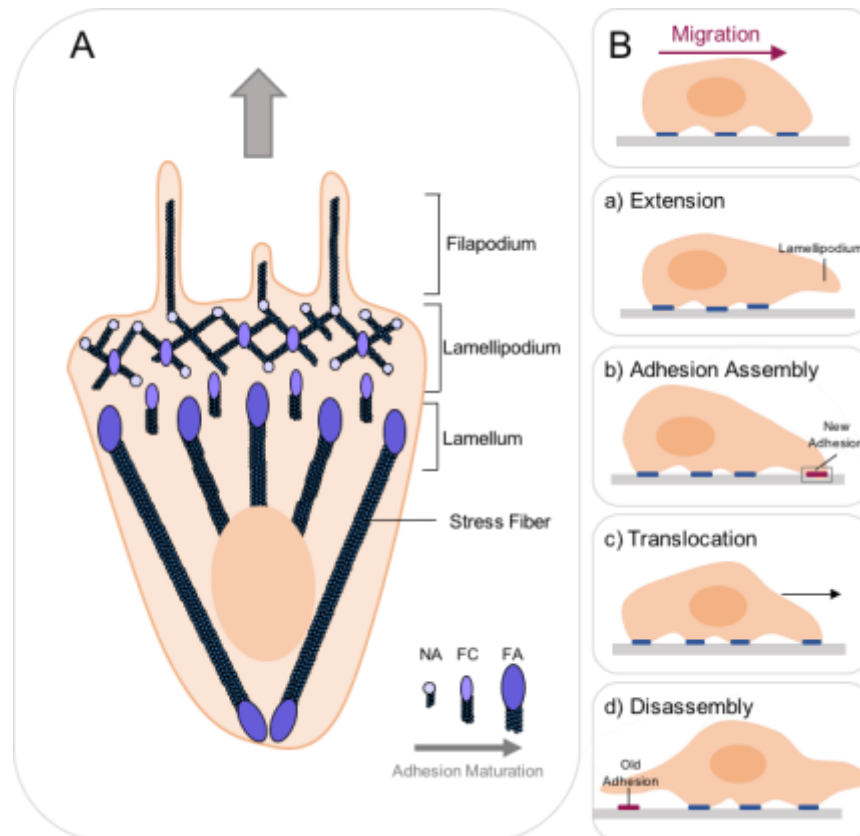


Figure 1.2 The focal adhesion cycle. **A)** Focal adhesion lifetime and actin coordination in the migrating cell: Dendritic actin polymerizes at the leading edge to push the membrane forward in finger-like projections (filopodium). Nascent adhesions form at the front of the cell protrusion (lamellipodium) at the ends of dendritic actin, and disassemble at the rear of the lamellipodium. Nascent adhesions that persist use actin filaments as a template to elongate and mature into focal complexes. Focal complexes can be quickly disassembled or further mature into focal adhesions, which requires bundling of actin filaments into stress fibers. **B)** The focal adhesion cycle: The cell extends a protrusion at the leading edge where a new focal adhesion assembles. The cell body contracts towards the new adhesion, and disassembly of adhesions at the trailing edge of the cell occurs to complete the movement. Abbreviations used include: NA (nascent adhesion), FC (focal complex), and FA (focal adhesion). (Adapted from Parsons *et al.* 2010 and Ladoux *et al.* 2012).

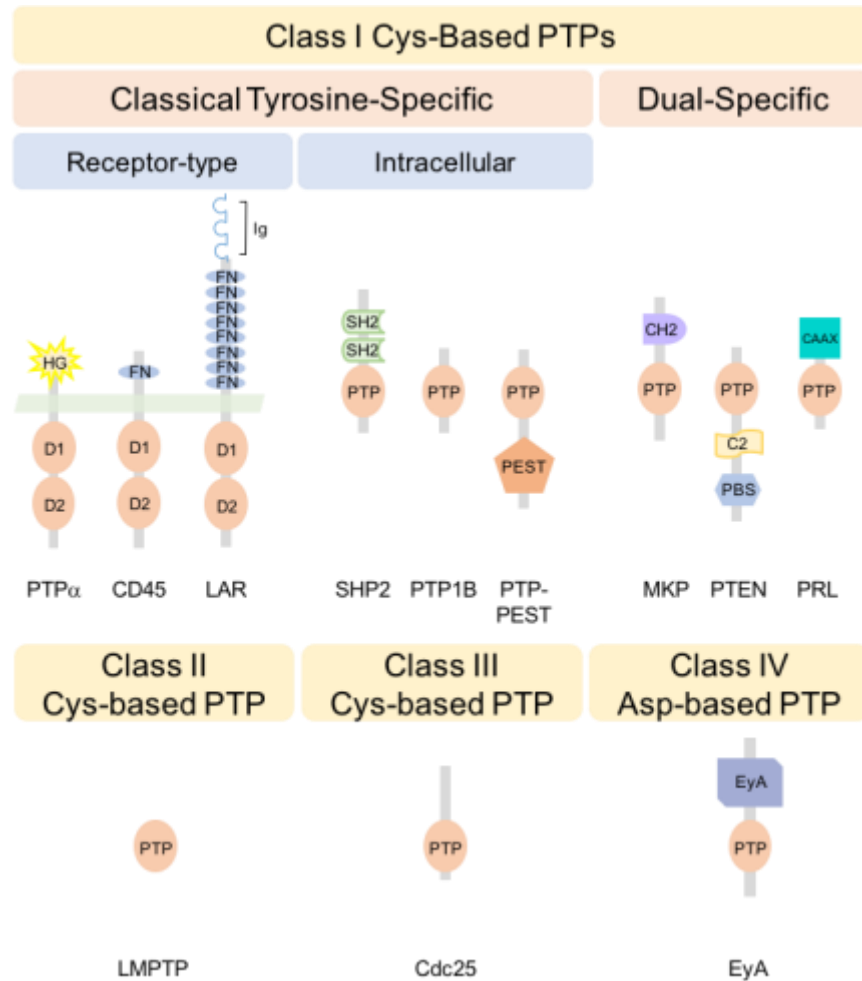


Figure 1.3. Overview of the protein tyrosine phosphatase (PTP) superfamily. The PTP superfamily is categorized into four subfamilies, according to structure and catalytic mechanism. The four subfamilies are: The Class 1 Cys-based PTPs, Class II Cys-based low molecular weight PTP (LMPTP), Class III Cys-based Cdc25 PTPs, and the Class IV Asp-based Eyes Absent (EyA) PTP. The Class 1 Cys-Based PTPs are further divided into classical tyrosine-specific and dual specific PTPs. Classical tyrosine specific PTPs are either receptor-type or intracellular phosphatases. Examples of PTPs belonging to each subfamily are shown in the figure. Abbreviations used include: HG (highly glycosylated), D1/D2 (PTP domains), FN (fibronectin-like), Ig (immunoglobulin-like), SH2 (Src-homology 2), CH2 (Cdc25 homology domain), C2 (C2 domain), PBS (PDZ-binding sequence), CAAX box (farnesylation signal), EyA (Eyes absent domain).

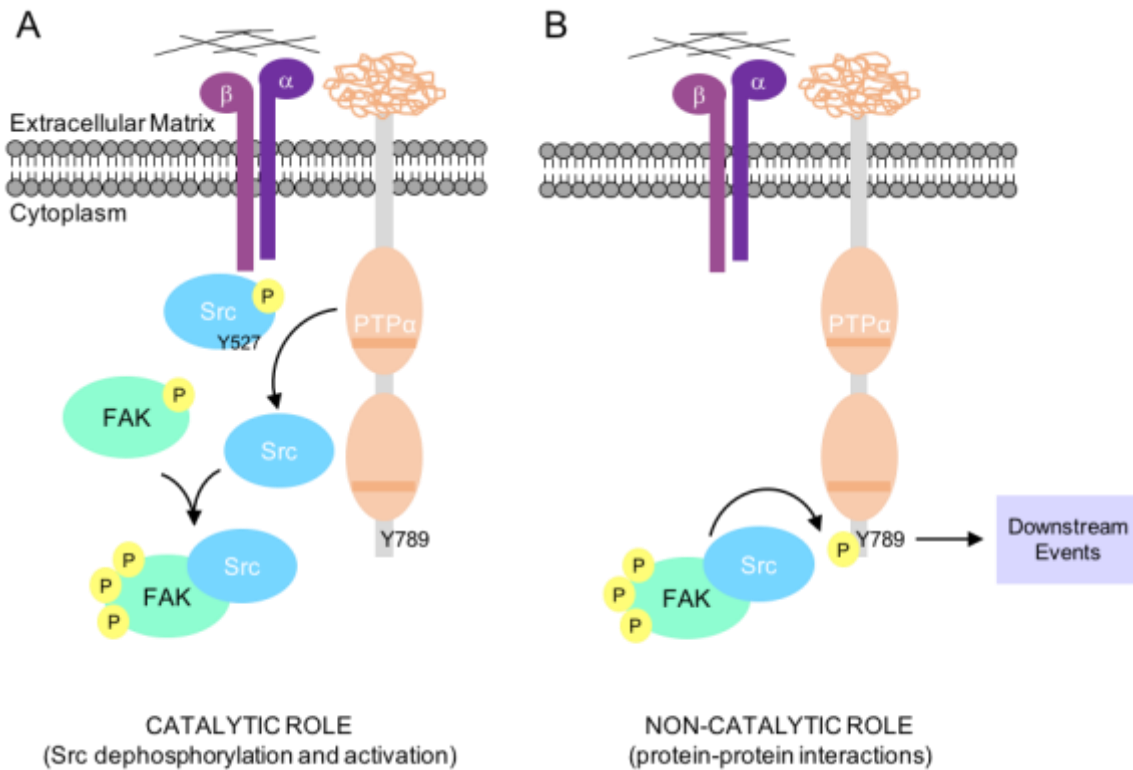


Figure 1.4. The two roles of PTP α in integrin signaling. **A)** Integrin engagement promotes the association of PTP α with integrins, where PTP α can dephosphorylate Src at the inhibitory Tyr527 phosphosite, activating Src and promoting the formation of the Src-FAK complex. **B)** The Src-FAK complex is involved in many downstream signaling events, including the phosphorylation of PTP α at Tyr789 which promotes focal adhesion formation, actin stress fiber assembly, and cell migration.

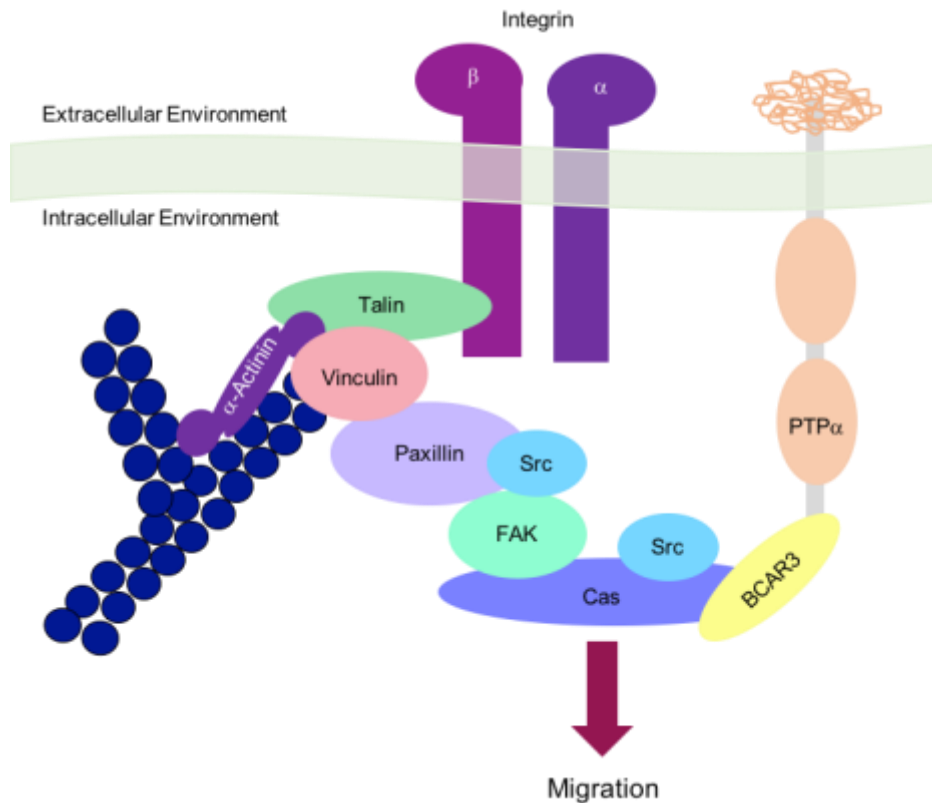


Figure 1.5 Key integrin-mediated adhesion proteins in focal adhesion signaling. Integrin ligation promotes the close proximity of PTP α with important adhesion signaling molecules. These scaffold and regulatory molecules physically and functionally connect substrate-bound integrins to the actin cytoskeleton to coordinate cell shape and movement. For instance, talin binds β -integrins, α -actinin, and vinculin to promote the association of the actin cytoskeleton with focal adhesions. In addition, vinculin interacts with talin and α -actinin through its head domain, and actin and paxillin via its tail domain. FAK is localized to focal adhesions through its association with paxillin and talin and interacts with Src in a Src-FAK complex. BCAR3 binds to PTP α -pTyr789 and promotes the localization of Cas to adhesions. Cas serves as a scaffolding protein for FAK, SFKs, vinculin, and other molecules that regulate migration. Abbreviations used include: FAK (focal adhesion kinase), SFKs (Src family kinases), Cas (Crk-associated substrate), and BCAR3 (breast cancer anti-estrogen resistance 3).

Chapter 2: Materials and Methods

2.1 Cell lines and cell culture

Spontaneously immortalized wild-type (WT601) and PTP α knockout (KO595) mouse embryonic fibroblast (MEF) cell lines were established previously by our lab as described (Chen et al., 2006b; Zeng et al., 2003). For this study, I generated new spontaneously immortalized MEF cell lines WT2 and KO8, according to procedures described in section 2.1.1. MDA-MB-231 human breast adenocarcinoma cells were obtained from the American Type Culture Collection (ATCC).

MEF lines expressing mutant PTP α -Y789F under control of the endogenous *Ptptra* promoter were generated in the Pallen lab by Dr. Hoa Le. Briefly, CRISPR/Cas9 gene editing technology was used with WT601 MEFs to mutate the codon in *Ptptra* for Tyr789, resulting in a mutant PTP α protein that has an unphosphorylatable Phe residue in place of Tyr789 being expressed by these cells. After editing, the cells were subjected to limiting dilution and single cells were expanded to produce clonal lines. Two mutant PTP α -Y789F (Y789F) cell lines (named 6-22 and 1-11) and two 'control' (CTRL) cell lines (named 6-24 and 1-13) were identified and verified by Western blotting and sequencing, to ascertain the presence or absence of PTP α -phosphoTyr789. The CTRL cell lines are cells that did not incorporate the CRISPR/Cas9-introduced Tyr-to-Phe-789 mutation.

All cell lines were cultured in HyClone™ Dulbecco's modified Eagle medium (DMEM) with high glucose (GE Healthcare Life Sciences) containing 10% fetal bovine serum (FBS) (Gibco or Hyclone) and 1% penicillin and streptomycin (P/S) (Gibco).

2.1.1 Spontaneous immortalization of MEFs

To obtain mouse embryonic fibroblasts, mouse embryos were dissected at embryonic day 14.5 (E14.5) using our lab protocol described in Min Chen's thesis dissertation (2007), the same protocol that was used to generate the WT601 and KO595 MEFs. The embryos were carefully extracted from the embryonic sac and washed in PBS. The top half of the brain (including the eyes) and the liver were removed, stored separately at 4°C, and were later used to confirm the genotype of each embryo by PCR. All blood-containing organs (liver, heart) were removed, and the embryo was rinsed thoroughly in PBS to remove any debris or blood. A sterilized razor blade was used to dice the remaining tissue of each embryo. Diced tissue from each embryo was collected in individual Falcon tubes containing trypsinization buffer [pH 7] (8g/L NaCl, 0.4g/L KCl, 1g/L glucose, 0.4g/L NaHCO₃, 0.24g/L Na-EDTA/dH₂O, 0.05% trypsin from bovine pancreas [Sigma]) and stored at 4°C overnight. The trypsin buffer was then aspirated, leaving a few milliliters (mL) above the settled tissue in the Falcon tube. The remaining tissue and trypsin buffer were incubated at 37°C for 30 min, with gentle shaking of the tube every 5 min. The trypsin was neutralized using DMEM containing 10% FBS and 0.1 mM β-mercaptoethanol and the tissue was dissociated by vigorous pipetting. The mixture was then centrifuged at 150g for 1 min. The supernatant was transferred to a new tube, taking care not to disturb or transfer any tissue debris, and was centrifuged at 1200 rpm for 5 min. The resulting supernatant was aspirated and cell pellets were resuspended in DMEM containing 10% FBS and plated in a tissue culture dish. After the cells had attached, the media was changed to remove any dead cells and debris. Two plates each of WT and PTP α KO mouse embryonic primary cells were cultured. These were passaged once they had reached confluency, or shortly before, until spontaneous immortalization was achieved (passage 20-25).

2.1.2 Depletion of PTP α from WT2 MEFs and MDA-MB-231 cells

WT2 MEFs and MDA-MB-231 cells were depleted of PTP α using the Lipofectamine[®] RNAiMAX Transfection Reagent and siRNA transfection protocol from ThermoFisher. MEFs and MDA-MB-231 cells were treated with 20 nM (per 6 cm dish) of ON-TARGET plus SMART pool siRNA targeting human PTP α (cat.# L-004519-00-0005; human PTP α siRNA also targets murine *Ptpa* with high efficiency) and non-targeting siRNA (siGENOME Non-targeting Pool #2, cat.#D-001206-14-50) purchased from Dharmacon. RNAiMAX and siRNAs were diluted separately in Opti-MEM and incubated at room temperature for 5 min before combining the mixtures and incubating at room temperature for 20 min. Cells were plated (7×10^5 and 3.5×10^5 cells for MDA-MB-231 and MEFs respectively, per 6cm plate) in culture dishes and immediately overlaid with the transfection media. Parental cells were incubated as above with the reagents in the transfection protocol, excluding only the siRNA. MDA-MB-231 cells and MEFs were cultured in antibiotic-free media for 48 h post-transfection before further experimentation. MDA-MB-231 cells required the siRNA-containing media to be changed to full media (with 10% FBS, 1% P/S DMEM) at 8 h post transfection. PTP α depletion was confirmed by Western blot and quantified by densitometry. On average over 6-8 experiments per cell type, MEFs and MDA-MB-231 cells demonstrated 80.5% and 91% PTP α knockdown efficiency, respectively.

2.2 Antibodies and immunological detection reagents

2.2.1 Primary antibodies

The following primary antibodies were used for immunoblotting as dilutions in phosphate-buffered saline (PBS) with 0.1% Tween (PBST) and 3% bovine serum albumin (BSA) as stated. In-house PTP α and PTP α -phosphoTyr789 antibodies have been previously described (Chen et al., 2006b) and these were used at a 1:3000 and 1:500 dilution, respectively. Mouse anti-phosphotyrosine antibody clone PY20 (BD Transduction Laboratories) was used at a dilution of 1:500, rabbit anti-FAKTyr397 (Cell Signaling Technology) at 1:500, mouse anti-FAK (BD Transduction Laboratories) at 1:1000, mouse anti- γ -tubulin (Sigma) at 1:3000, and rabbit anti-actin (Sigma) at 1:3000. For immunofluorescent imaging, mouse anti-paxillin (BD Transduction Laboratories) was used at a 1:300 dilution in PBS with 1% BSA, 1% normal goat serum (NGS), and 0.1% Triton X-100.

2.2.2 Secondary antibodies

HRP-conjugated goat anti-mouse and goat anti-rabbit secondary antibodies were obtained from Sigma and Bio-Rad, respectively, and diluted in PBST for immunoblotting. For immunofluorescent imaging, goat anti-mouse Alexa Fluor® 488 (Life Technologies) was diluted as specified in various experiments in PBS with 1% BSA, 1% NGS, and 0.1% Triton X-100.

2.3 Fibronectin stimulation of cells

2.3.1 Cell culture and stimulation

Cells cultured in plastic tissue culture dishes to ~70% confluency (termed ‘adherent’ cells) were starved in DMEM with 0.5% FBS and 1% P/S for 18 h and subsequently harvested

using 0.05% Trypsin-EDTA to detach cells. The trypsin was neutralized using DMEM with 0.5mg/mL soybean trypsin inhibitor (STI; Gibco) and everything was collected in a Falcon tube and centrifuged at 1200 rpm for 5 min. The cell pellet was resuspended in STI/DMEM, centrifuged again, and washed in serum-free DMEM. The cells were then centrifuged once more and resuspended in DMEM containing 0.1% BSA. Finally, this cell suspension was incubated at 37°C for 1 h, and the cells were kept in suspension by gently inverting the Falcon tube every 10 min during the incubation period.

Tissue culture plates were coated with 10µg/mL FN or 20µg/mL Poly-L-Lysine (PLL; Sigma) in PBS at 4°C overnight prior to stimulation. Pre-coated plates were washed twice with PBS to remove excess FN or PLL and incubated with serum-free (SF) DMEM at 37°C for 1 h prior to stimulation. Suspended cells (1.5×10^6) were harvested (0 min time point) or plated on FN- or PLL-coated 10 cm tissue culture plates and incubated at 37°C for 15 or 30 min as specified before being washed with PBS and lysed for immunoblotting.

2.3.2 Cell stimulation for imaging

Glass coverslips (18mm, 1.5, Electron Microscopy Sciences) were coated with 10µg/mL fibronectin (FN; Chemicon International, Inc) in PBS at 4°C overnight. The coverslips were washed twice with PBS and incubated in serum-free DMEM for 1 h prior to stimulation. Suspended cells (1.0×10^5) (see section 2.3.1) were plated on the FN-coated coverslips and incubated at 37°C for 15, 30, 60, or 120 min before fixation.

2.4 TIRF microscopy

Fibronectin-stimulated MEFs (section 2.3.2) were washed once with PBS and fixed using 4% paraformaldehyde (PFA) for 10 min at room temperature. The PFA was then discarded and coverslips were washed twice with PBS. Cells were permeabilized using 0.1% Triton X-100 in PBS for 5 min, washed twice in PBS, and incubated in blocking buffer (PBS with 1% BSA) for 1 h at room temperature. Subsequently, cells were washed with PBS and incubated with anti-paxillin antibody (1:300) overnight at 4°C. Cells were rinsed three times with PBS and incubated in Alexa Fluor® 488-conjugated anti-mouse secondary antibody (1:300) for 45 min at room temperature while protected from light. Cells were washed in PBS three times and imaged using the Olympus 1x81 Cell[^]TIRF (total internal reflection fluorescence) system equipped with a CoolSnap HQ2 CCD camera. Fluorescently labelled proteins were visualized with a 60x TIRF objective lens (NA 1.49) using a 488nm laser with a penetration depth of 75 nm.

In live cell imaging experiments, MEFs were transfected with enhanced green fluorescent protein (eGFP)-paxillin (a gift from Dr. James Lim) using Lipofectamine™ LTX (Invitrogen). Transfected cells were grown in antibiotic-free media for 30 h prior to further experimentation. Cells were serum-deprived overnight, harvested, and stimulated as described (section 2.3.1). TIRF imaging was used to visualize fluorescently labelled paxillin in real-time as described above, but with the 488nm laser set at a penetration depth of 65nm. All TIRF images were processed using ImageJ software.

2.5 Cell lysis and immunoblotting

Cells were lysed using RIPA buffer (50mM Tris-Cl [pH 7.4], 150mM NaCl, 1mM EDTA [pH 8.0], 1% Nonidet P-40, 0.5% sodium deoxycholate [NaDOC], 0.1% SDS, 10ug/mL

aprotinin, 10ug/mL leupeptin, 1mM phenylmethylsulfonyl fluoride [PMSF], and 2mM sodium orthovanadate [Na_3VO_4]). Cell lysates were cleared by centrifugation at 13500 rpm for 15 min at 4°C. Protein concentration was determined using the Bradford protein assay (Bio-Rad Laboratories) with absorbance measured at 595nm.

Protein samples were resolved by SDS-PAGE and transferred onto a polyvinylidene difluoride (PVDF) membrane at 110V for 80 min. The membrane was blocked with 3% BSA in 0.1% PSBT for 1 h at room temperature. The membrane was washed in 0.1% PBST three times, and then incubated with primary antibody overnight at 4°C. The primary antibody was removed and the membrane was washed three times with 0.1% PBST and incubated in HRP-conjugated secondary antibody for 1.5 h at room temperature. The membrane was then washed three times with PBST and protein bands were visualized using chemiluminescent ECL reagent.

2.6 Wound healing assay

Confluent cell monolayers were wounded using a P200 pipette tip. Cells were then washed with serum-free DMEM and incubated in serum-depleted (1% FBS) DMEM for the duration of the experiment. Each wound was imaged at four locations along its length at 0, 4, and 8 h post-wounding. Images were taken on an Olympus CKX41 microscope equipped with an Infinity2 camera, using a 4x (NA 0.13) objective. The area of the wound was measured at each of the four locations using ImageJ software, and these measurements were averaged to obtain the wound area at each timepoint. The wound area at 4 and 8 h was subtracted from the area at 0 h to calculate the wound closure (in arbitrary units) that had occurred at each timepoint in one independent experiment (n=1). The migration index was calculated by normalizing the amount of migration in the treatment group to the control, which was set to 1.

In wound healing experiments using MDA-MB-231 cells, PTP α was depleted according to the protocol described in section 2.1.2. At 72 h after transfection, when cells had formed a confluent monolayer, the Parental, siCTRL- and siPTP α -treated MDA-MB-231 cells were wounded using a P1000 pipette tip. The MDA-MB-231 cell wound healing assay and quantification followed the same protocol as described above, with the inclusion of a 16 h time point to accommodate the slower migration rates of these cells.

2.7 Transwell assay

2.7.1 Transwell assay for MEFs

Adherent cells (~70%) were serum-starved in DMEM containing 0.5% FBS for 18 h prior to harvesting. To coat the underside of the membrane, Transwell inserts (8 μ m pore size, Corning) were placed in wells containing 0.5 mL of 10 μ g/mL FN for 2 h at 37°C. The inserts were then washed twice with PBS and both the apical and basal chambers were incubated in DMEM containing 0.5% BSA at 37°C for 30 min. During this time, cells were harvested using the protocol outlined in section 2.3.1 and suspended in DMEM with 0.5% BSA (2.5 x 10⁵ cells/mL). The media in the apical chamber of the insert was aspirated and 100 μ L of cell suspension, corresponding to 2.5 x 10⁴ cells, were placed carefully in the center of the insert. Cells were incubated for 2 h at 37°C. Following the incubation period, the media was aspirated from the top chamber and a Q-tip moistened with DMEM was used to scrub off any cells that remained in the apical chamber. Transwell inserts were then placed in 70% ethanol for 15 min at room temperature to fix the cells. Membranes were removed from ethanol and air-dried for 15 min. The cells that had migrated through the membrane to the underside were stained using 0.2% crystal violet (Sigma) in dH₂O for 5 min at room temperature. The membranes were cut out of the

insert using a scalpel and mounted on a glass slide, and cells were imaged using a Axio Imager.A1 (Zeiss) upright microscope with a 20x (NA 0.5) objective and an Olympus DP72 camera. Alternatively, cells on membranes that were still intact within the insert were imaged on a Axio Observer.Z1 (Zeiss) inverted microscope with a 20x objective (NA 0.8) and Axiocam 105 colour camera.

2.7.2 Transwell assay for MDA-MB-231 cells

MDA-MB-231 cells were depleted of PTP α using PTP α -targeted siRNA (siPTP α), treated with a non-targeted control siRNA (siCTRL), or left untreated (Parental) for 48 h prior to harvesting (section 2.1.2). Transwell chambers (apical and basal) were incubated with serum-free DMEM at 37°C for 2 h prior to plating cells. Parental, siCTRL, and siPTP α cells were detached from plastic dishes using 0.25% Trypsin-EDTA. The trypsin was neutralized by the addition of DMEM with 10% FBS and the cell suspension was placed in a Falcon tube. The cells were centrifuged at 1200 rpm and washed with serum-free DMEM and then centrifuged again. The cell pellet was resuspended in DMEM with 0.5% BSA. The cells were counted and adjusted to a concentration of 6.25×10^4 cells/mL. The medium was aspirated from the Transwell chambers and the basal chamber was replenished with DMEM containing 10% FBS. Suspended cells (2.5×10^4) were slowly pipetted into the center of the Transwell insert. The cells were incubated at 37°C for 8 h to allow sufficient time for migration to occur. Following the incubation, cells that had not migrated were cleared from the upper surface of the membrane, and the membrane was fixed, stained, and imaged as described above in section 2.7.1.

2.8 Directionality assay

Wound healing assays were performed as described in section 2.6. WT2, KO8, CRISPR CTRL, and Y789F MEFs were plated ($3.5\text{-}4.0 \times 10^3$ cells/well) in 96-well plates 48 h prior to experimentation. Confluent monolayers were wounded (very lightly) using a P200 pipette tip. The cells were washed twice with serum-free DMEM and incubated in serum-depleted DMEM containing 1% FBS and 1% P/S for the duration of the experiment. Cells were imaged every 20 min for 24 h using the ImageXpress Micro XL microscope (Molecular Devices Inc) with a 4x (NA 0.20) objective. The ImageJ plugin, MTrackJ, was used to track cell location at each time point. Cell location coordinates were graphed and used to determine the total distance (total length of track, μm) and the net distance (length from start to finish, μm) travelled by each cell.

2.9 MTOC polarization assay

WT2 MEFs were seeded onto 18 mm coverslips (Electron Microscopy Sciences) pre-coated with $10 \mu\text{g}/\text{mL}$ fibronectin, and transfected with non-targeting or PTP α -targeting siRNA as described in section 2.1.2. Transfected cells were incubated in antibiotic-free DMEM for 48 h before further experimentation. Confluent cell monolayers were scratched using a P200 pipette tip, washed in serum-free DMEM, and placed in serum-deprived DMEM with 1% FBS for the duration of the experiment. Cells were incubated at 37°C for 4 and 8 h, and subsequently fixed using 4% PFA for 10 min. Coverslips were then washed in PBS and incubated in ice cold methanol (pre-cooled at -20°C) for 12 min. The cells were then permeabilized using PBS with 0.1% Triton X-100 and blocked for 1 hour in PBS with 1% BSA, before being incubated with anti- γ -tubulin (1:3000 in 1% PBS/BSA) primary antibody at 4°C overnight. The following day, coverslips were incubated in Alexa Fluor[®] 488-conjugated goat anti-mouse secondary antibody

(1:500) for 45 min at room temperature while protected from light. Coverslips were mounted on a glass slide using 10 μ L of Prolong Gold Antifade Reagent containing DAPI to stain the nuclei. Coverslips were imaged using a 20x (NA 0.45) objective on an Olympus 1x81 inverted microscope equipped with a CoolSnap HQ2 CCD camera. The orientation of the MTOCs was analyzed and scored using ImageJ.

2.10 Statistical analysis

Quantification of immunoblot signals from at least three independent (n=3) experiments was performed using the Quantity One® program (Bio-Rad Laboratories) and statistically analyzed using the Student's t-test. For the directionality assay, a two-way Analysis of Variance (ANOVA) and a one-way ANOVA were performed to determine the significance of the distance travelled and migration efficiency of each cell type, respectively. A two-way ANOVA was also performed with data from the MDA-MB-231 wound healing assay to determine whether differences in migration between each cell type at each time point were statistically significant. The Student's t-test was applied to all other data, and at least three independent experiments were analyzed. The number of independent replicates per experiment is given by n=x in each figure legend.

Chapter 3: The Role of PTP α and PTP α -Y789 Phosphorylation in Integrin-Stimulated Focal Adhesion Formation, Morphology, and Turnover

3.1 Rationale

Integrins bind components of the ECM, initiating a cascade of intracellular molecular signaling and protein-protein interactions and resulting in the formation of focal adhesions, multiprotein structures that link the ECM to the actin cytoskeleton to regulate cell movement (Zaidel-Bar et al., 2004). Integrin engagement promotes PTP α -mediated dephosphorylation and activation of Src (Ponniah et al., 1999; Su et al., 1999; von Wichert et al., 2003; Zeng et al., 2003). FAK is autophosphorylated in response to integrin engagement, which enables PTP α -activated Src to bind FAK thereby establishing an active Src-FAK complex (Ruest et al., 2000; Schlaepfer et al., 2004; Sieg et al., 2000; Toutant et al., 2002). The Src-FAK complex functions to recruit many early focal adhesion proteins, such as Cas, paxillin, Crk, Nck, and Grb2 to maturing focal adhesions (Hanks et al., 2003; Schlaepfer et al., 1997). Thus, PTP α plays an important upstream catalytic role in integrin-mediated signaling to regulate focal adhesion formation. Subsequent to PTP α -mediated Src-FAK activation, PTP α itself is phosphorylated by the activated Src-FAK complex at Tyr789 (Chen et al., 2006b). This is important for rearrangement of the actin cytoskeleton, focal adhesion formation and cell migration (Chen et al., 2006b). PTP α -pTyr789 is involved in the recruitment of PTP α to integrin-induced focal adhesions, placing PTP α in close proximity to central focal adhesion signaling proteins (Lammers et al., 2000; Sun et al., 2012). Indeed, PTP α -pTyr789 binds BCAR3 to promote the

recruitment of Cas to focal adhesions, and thereby mediates Cas downstream signaling events critical for cell migration (Sun et al., 2012).

Focal adhesion dynamics (formation, disassembly and turnover) are vital to the process of cell migration. Formation of new focal adhesions at the leading edge and simultaneous disassembly of focal adhesions at the trailing edge are required for translocation of the cell body (Wehrle-Haller, 2012). Given the dual catalytic and non-catalytic roles of PTP α and PTP α -pTyr789, respectively, in regulating integrin-stimulated focal adhesion signaling and formation, I set out to more precisely define and distinguish the roles of PTP α and PTP α -pTyr789 in these processes. To this end, my study aimed to characterize and compare the morphology and kinetics of focal adhesions formed upon integrin-stimulation of WT MEFs that express PTP α , KO MEFs that lack PTP α , and mutant Y789F MEFs engineered to endogenously express PTP α lacking the phosphorylatable Tyr789 site.

3.2 Wild-type (WT) and PTP α knockout (KO) MEF cell lines

Investigations of WT601 and KO595 MEF focal adhesion morphology and dynamics were carried out at the beginning of this project. Around this time, others in the lab informally observed unusually ‘better’ migration abilities of the KO595 cells (W Hong, personal communication). As the lab had lost earlier passages of these cells, we decided to generate new WT and PTP α KO MEFs for this study (named WT2 and KO8, respectively), as new cell lines would not as yet have been subjected to acquiring potential mutations over time in culture. WT and PTP α KO MEF cell lines were generated through spontaneous immortalization of cells from digested tissue of dissected WT and PTP α KO mice embryos (see Materials and Methods,

section 2.1.1). These cells were investigated alongside our lab's previously established WT601 and KO595 MEFs to validate the phenotypes of the new cells. PTP α expression or absence was confirmed in WT601/KO595 and WT2/KO8 MEFs through an immunoblot analysis (Fig. 3.1A).

The new WT2 and KO8 MEFs were grown in culture alongside the established WT601 and KO595 MEFs. Comparisons of the cell cultures revealed that they possess differences in morphological phenotype (Fig. 3.1B). The original WT601 and KO595 MEFs appear more rounded or spread in culture than the WT2 and KO8 MEFs, which look more elongated and less spread. In lower density conditions, WT601 and KO595 cells grow in clumps whereas the WT2 and KO8 cells tend to grow more individually, suggesting less contact with surrounding cells. These findings indicate differences between the two cell lines in terms of morphology and growth patterns.

3.3 Focal adhesion formation in established WT and PTP α KO MEF cell lines

In order to investigate the properties of focal adhesions formed in WT and PTP α KO MEFs, cells were stimulated on fibronectin-coated coverslips to induce focal adhesion formation through integrin stimulation, and imaged using TIRF microscopy. TIRF microscopy allows precise imaging at the cell-substrate interface where focal adhesions form. TIRF microscopy is commonly used to study focal adhesion dynamics, as it involves the reflection of the excitation light, creating evanescent waves with limited penetration depth that only excite the fluorophores within the first hundred ventral nanometers of the cell (Fish, 2009), which is where focal adhesions are located. Paxillin is one of the first proteins recruited to focal adhesions (Choi et al. 2008), and thus paxillin was labelled using immunofluorescent staining to detect focal adhesions in cells at different times following integrin engagement (plating on fibronectin).

The WT601 and KO595 MEFs previously established in our lab showed obvious differences in focal adhesion formation (Fig. 3.2A). At early times (up to 30 min), the WT601 cells form small focal adhesions that are uniformly distributed around the cell periphery. As the cells spread, the focal adhesions become bigger and farther apart; however, they maintain a linear, elongated shape and a uniform distribution around the edge of the cell. With regards to cell shape, the WT601 cells are round in comparison to the more irregular shape of the KO595 MEFs, and this is especially apparent from 30 min onwards. The KO595 MEFs exhibit a more random organization of focal adhesions that are not as localized to the cell periphery in comparison to WT601 cells, especially at 15 and 30 min on fibronectin. As the KO595 cells spread, their focal adhesions become larger and are more randomly distributed along the cell edge, as depicted by the aggregated adhesions in the KO595 MEFs at 120 min, in contrast to the long, fibrillar focal adhesions of the WT601 MEFs (Fig. 3.2A, see insets at 120 min).

3.4 Focal adhesion formation in newly generated WT and PTP α KO MEF cell lines

To validate the PTP α -dependent focal adhesion formation phenotypes demonstrated by the WT601 and KO595 MEFs in the new cell lines, the WT2 and KO8 MEFs were stimulated on fibronectin, immunostained for paxillin, and imaged using the same methodology as in experiments shown in Fig. 3.2A. After 15 min on fibronectin, the WT2 and KO8 MEFs both showed a uniform distribution of focal adhesions around the cell edge, with the WT2 MEFs forming a visibly thicker cell edge (Fig. 3.2B). As the WT2 and KO8 MEFs spread, the focal adhesions matured and became larger (30 min). By 120 min on fibronectin, the WT2 MEFs exhibited thinner and elongated adhesions, while the KO8 MEFs displayed thicker and rounder adhesions. However, both these morphological types were observed in each of the WT2 and

KO8 MEF cultures, making it difficult to clearly identify a PTP α -dependent phenotype in these cell lines.

A noteworthy difference between the new WT2/KO8 and the established WT601/KO595 cell lines is the extent of cell spreading on fibronectin. Unusually, the WT2 and KO8 MEFs demonstrate a more persistent rounded shape; the cells do not flatten and the cell body does not greatly change in shape or increase as much in size with time on fibronectin. This is in contrast to the readily observed spreading of the WT601 and KO595 MEFs (compare Fig. 3.2A with B). The new WT2 and KO8 MEFs exhibit reductions in cell spreading compared to the WT601 and KO595 MEFs that is not distinguished by a lack of PTP α expression. Thus, PTP α -dependent differences in focal adhesion formation, morphology, and cell spreading are less obvious between the newly generated WT2 and KO8 MEFs, compared to the clearly evident differences between the WT601 and KO595 MEF lines.

3.5 Focal adhesion dynamics in established and newly generated WT and PTP α KO MEFs

Focal adhesion turnover and remodeling must occur in a continuous, dynamic manner in order for cell movement to take place. Focal adhesion turnover can be assessed using essentially the same methodology used to assess focal adhesion morphology, but with monitoring the fluorescently labelled focal adhesion component paxillin in real time (without cell fixation). Therefore, MEFs were transfected with eGFP-paxillin in order to detect focal adhesions. Focal adhesion formation was stimulated by plating MEFs on fibronectin-coated coverslips, and live-cell imaging was conducted using TIRF microscopy. Individual cells (1-4 cells) were selected for imaging based on their attachment and spreading within the first 5-10 min. The time that cell

imaging was initiated was designated as ‘0 min’, which occurred 15 min after plating/FN stimulation and imaging was carried out for 45 min. Focal adhesion “footprints” were generated to enable ready visualization of the temporal formation of eGFP-paxillin-containing focal adhesions in a single image. To create a “footprint”, live-cell images were selected at approximately 5 min intervals, each image was assigned a distinct colour corresponding to time, and the coloured images were overlaid to create a single image (the “footprint”) in which the sequence of focal adhesion development can be seen (Fig. 3.3A). Focal adhesions that persist throughout all overlaid frames (i.e. no disassembly) appear white due to the merge of the colour spectrum.

Footprint images of WT601 cells reveal early small focal adhesions (0-10 min, orange-light green) that mature with time (green-to-blue at 15-to-25 min, then blue-to-pink/red at 25-45 min), with the largest focal adhesions forming toward the end of the video time-lapse (Fig. 3.3A, top left panel). The focal adhesions are uniformly distributed around the periphery, and are elongated and thin, particularly after 20 min on fibronectin (the blue-pink spectrum of adhesions). In contrast, KO595 MEFs form rounder and thicker focal adhesions that are more randomly organized in clumps around the cell periphery (Fig. 3.3A, top right panel). Even at early times, there are fewer but larger focal adhesions (orange) present in the KO595 MEFs, and several of these focal adhesions persist without being disassembled (white).

In contrast to the WT601 and KO595 MEFs, focal adhesion progression in the newly generated WT2 and KO8 MEFs is localized to a very distinct edge encircling a cell body that is largely devoid of adhesions at any time. Compared to the WT601 MEFs, focal adhesions in the WT2 MEFs are larger (‘chunkier’) and more mature adhesions form at earlier time-points (note the many large green adhesions visible at 10-15 min) (Fig. 3.3A, bottom left panel). There is also

evidence of delayed focal adhesion turnover as indicated by the presence of some long white adhesions. The KO8 MEFs have smaller focal adhesions than the KO595 MEFs. Nevertheless, many KO8 cell adhesions at early-intermediate times (green, 10-15 min) appear thickened and non-fibrillar in nature, while some are elongated (Fig. 3.3A, bottom right panel). These cells exhibit focal adhesion turnover as there are no white adhesions. These differences are highlighted in the montages beside each footprint image, which display the area of the cell outlined in white at each 5 min interval used to create the footprint. A static image of each cell that was live-imaged in the footprint analyses is shown at 30 min on fibronectin (Fig. 3.3B), as another form of direct comparison between the cell lines. The focal adhesion footprint images are not only consistent with their respective overall fixed-cell images (Fig. 3.2), but readily delineate a snapshot of the differences between the established and newly generated cell lines, as well as between the wild-type (WT601 and WT2) and the knockout (KO595 and KO8) MEFs.

3.6 Role of PTP α -pTyr789 in focal adhesion morphology and turnover in MEFs

To investigate the role of PTP α -Tyr789 phosphorylation in focal adhesion dynamics, I assessed focal adhesion morphology and turnover in MEFs that had undergone gene editing to mutate the gene encoding PTP α , *Ptp α* . CRISPR/Cas9 gene editing technology was used with WT601 cells (carried out by Dr. Hoa Le) to target endogenous *Ptp α* and modify the bases encoding the Tyr789 phosphosite to those encoding a Phe residue, thereby producing MEFs that endogenously express unphosphorylatable PTP α protein. A PTP α -Y789F cell line derived post-editing from a single cell clone and named cell line 6-22 (also referred to as Y789F) was used in my experiments. A control cell line (cell line 6-24, also referred to as CTRL) that had undergone *Ptp α* -targeted gene editing that was confirmed to be unsuccessful, also expanded from a single

cell clone, was used in my experiments as well. I confirmed the expression of mutant unphosphorylatable PTP α -Y789F in the 6-22 cells and unmutated, phosphorylatable PTP α (wild-type) in the control 6-24 cells (Fig. 3.4).

The CRISPR CTRL and Y789F MEFs were stimulated by placing the cells on fibronectin with fixation after 15, 30, 60, and 120 min (Fig. 3.4B). Focal adhesions were identified by immunofluorescent labelling of paxillin. The CTRL MEFs show smaller, linear focal adhesions consistent with the WT601 MEFs, although the control 6-24 cells were more irregularly shaped during spreading and the focal adhesions around the cell periphery were less uniformly distributed. The Y789F MEFs show a more uniform organization of focal adhesions around the periphery at early times on fibronectin compared to the KO595 MEFs, but consistent with KO595 MEFs, these focal adhesions aggregate in globular clusters at later times. The differences in focal adhesion morphology between the CTRL and Y789F cells are most distinct at later time points (Fig. 3.4B, 60 and 120 min on fibronectin).

The CTRL and Y789F MEFs were transfected with eGFP-paxillin, stimulated on fibronectin-coated coverslips, and live-cell imaging was conducted as described in section 3.5. The time that cell imaging was initiated was designated as '0 min', which occurred 10 min after plating/FN stimulation. Focal adhesion footprints were created by overlaying temporally coloured images at approximately 5 min intervals from time-lapse videos taken of the cells after placing them on fibronectin-coated coverslips (Fig. 3.5A). The montages beside each footprint image show the 5 min interval images of the areas outlined by the white box. The CTRL 6-24 cell footprint reveals elongated, thin and linear focal adhesions consistent with those seen in the fixed images, and the montage images demonstrate remodelling of peripheral focal adhesions in these CTRL MEFs. In contrast, the 6-22 Y789F MEF footprint shows thicker, more clumped

focal adhesions that are mainly formed at later times on fibronectin (indicated by purple/pink adhesions formed at 35-45 min). Montage images of the Y789F cell footprint highlight this delay in forming larger, more mature focal adhesions. (Fig. 3.5A). An image of each cell used in the footprint analyses is shown at 30 min on fibronectin (Fig. 3.5B). At this time, small, thin focal adhesions localize to the cell periphery in CTRL MEFs, and display a more random, disorganized distribution throughout the cell in the Y789F MEFs.

3.7 Investigation of the molecular responses of newly generated MEFs to integrin stimulation

The inconsistencies observed between integrin-stimulated focal adhesion formation in the newly generated WT2/KO8 MEFs compared to the established WT601/KO595 MEFs prompted me, at the end of my study, to investigate whether these differences were reflected in the early, key molecular events of integrin signaling in these cells. In the absence of PTP α , Src is not properly dephosphorylated at the inhibitory Y527 site in response to integrin stimulation (Su et al., 1999; Zeng et al., 2003; Chen et al., 2006b). Therefore, Src activation, its interaction with FAK, and the subsequent phosphorylation and activation of FAK are defective in PTP α -null cells (for example see Fig. 3.6A). FAK activation is essential for integrin-mediated cell migration (Owen et al., 1999; Schaller et al., 1994; Sieg et al., 1999).

To investigate integrin-mediated FAK activation in the WT2 and KO8 MEFs, cells were placed in suspension to terminate integrin signaling, and then plated on fibronectin-coated dishes to initiate integrin signaling. Lysates were prepared from cells stimulated on fibronectin for various times, and FAK phosphorylation at its key Tyr397 site, a widely used indicator of FAK activation, was analyzed by immunoblotting. This revealed that upon integrin engagement, FAK-

Tyr397 phosphorylation was induced in both WT2 and KO8 cells, with equivalent phosphorylation detected at 5, 15, and 30 min of fibronectin stimulation (Fig. 3.6B). Also, FAK-Tyr397 phosphorylation was similar in both cell lines cultured on uncoated plastic dishes (Fig. 3.6B, 'Ad'[adherent] lanes), and was not induced in either cell line when suspended cells were plated on dishes coated with poly-L-lysine, a non-specific substrate that does not stimulate integrin signaling (Fig. 3.6B, '30^{PLL}' lanes). These results suggest that the KO8 MEFs, despite lacking PTP α , do not exhibit at least some of the major integrin signaling defects characterized in the KO595 and other lines of PTP α knockout cells (Chen et al., 2006b; Su et al., 1999; Zeng et al., 2003).

To provide a direct side-by-side comparison with the established WT601 cells, integrin-stimulated FAK activation was assessed as above using the three cell lines WT601, WT2 and KO8. Lysates prepared from cells in Ad, 0, and 5 min FN-stimulated conditions were analyzed by immunoblotting for FAK-Tyr397 phosphorylation. All cell types exhibited integrin-stimulated FAK-Tyr397 phosphorylation (Fig. 3.6C, compare the 0 and 5 min lanes). Moreover, densitometric quantification confirmed that FAK phosphorylation occurred to similar levels in the WT2 and KO8 cells, and was slightly more robust in the WT601 cells (Fig. 3.6D). This indicates that a major difference between the established WT601/KO595 cells and the newly generated WT2/KO8 cells is due to an inconsistency between the KO595 and KO8 cells, where the latter cell line does not exhibit the well-characterized defect in FAK activation arising from the ablation of PTP α .

Integrin-stimulated PTP α -deficient MEFs on average exhibit 50% higher phosphorylation at the C-terminal inhibitory site of the SFKs Src (Tyr527) and Fyn (Tyr528) at 15-30 min after integrin stimulation, compared to wild-type MEFs (Chen et al., 2006b; Su et al.,

1999), reflecting the impaired dephosphorylation of this site and consequently defective activation of SFKs in the absence of PTP α . I investigated Src-Tyr527 phosphorylation in WT601, WT2, and KO8 MEFs plated on fibronectin for 5 min, or cultured on uncoated plastic dishes ('Ad'). WT601 MEFs showed a 55% decrease in Src-Tyr527 phosphorylation after 5 min on fibronectin, relative to phosphorylation levels observed in 'Ad' MEFs (taken as 100%). In comparison, WT2 MEFs showed a lesser 25% decrease, while the KO8 MEFs displayed approximately a 55% decrease in Src-Tyr527 phosphorylation (Fig. 3.6E). This indicates that differences between the established WT601/KO595 cells and the newly generated WT2/KO8 cells comprise a potential impairment in the ability of WT2 MEFs to effectively dephosphorylate Src despite the presence of PTP α ; and conversely, in the ability of the KO8 MEFs to effectively dephosphorylate Src in the absence of PTP α .

3.8 Discussion

PTP α expression and PTP α -Y789 phosphorylation play important roles in cell spreading, focal adhesion formation, and cytoskeleton rearrangement in response to integrin stimulation (Chen et al., 2006b; Herrera Abreu et al., 2008; Su et al., 1999; von Wichert et al., 2003; Zeng et al., 2003). Here, I have investigated these PTP α -dependent characteristics, specifically as to their effects on focal adhesion dynamics, in wild-type, knockout and unphosphorylatable mutant PTP α -Y789F MEFs.

Newly generated WT2 and KO8 MEFs were characterized in culture and FN-stimulated conditions using the previously established WT601 and KO595 cell lines as comparative controls. In unstimulated conditions, WT2 and KO8 MEFs showed an overall decrease in cell

spreading in comparison to WT601 and KO595 MEFs. Upon FN stimulation, WT601 MEFs displayed thin, elongated, and evenly distributed focal adhesions that underwent rapid turnover. These findings were consistent with reports from Herrera Abreu et al. (2008) that WT MEFs exhibited small peripheral focal adhesions that localized to the periphery and matured over time. In contrast, KO595 MEFs demonstrated thick, aggregated focal adhesions that displayed defective turnover, congruent with the “supermature” (large and thickened) focal adhesions observed in PTP α KO MEFs by Herrera Abreu et al. (2008). In addition, KO595 MEFs displayed a delay in early focal adhesion formation, consistent with previous findings (Chen et al., 2006b; Herrera Abreu et al., 2008).

Interestingly, the distinct phenotypes associated with WT and PTP α KO MEFs were not observed in the newly generated lines of WT2 and KO8 MEFs. The reduced focal adhesion turnover observed in KO595 MEFs was observed in WT2, but not in the KO8 MEFs. This suggested that the newly generated WT2 and KO8 MEFs must be fundamentally distinct from the WT601 and KO595 MEFs as well as from other established PTP α -deficient lines of MEFs described in the literature (Chen et al., 2006b; Herrera Abreu et al., 2008; Su et al., 1999; von Wichert et al., 2003; Zeng et al., 2003).

The CRISPR-edited Y789F MEFs displayed a reduction in focal adhesion formation, and the adhesions were large and aggregated, characteristic of the KO595 MEFs and MEFs expressing mutant PTP α -Y789F (Chen et al., 2006b; Herrera Abreu et al., 2008). Contrary to the impaired dynamics of focal adhesions in KO595 MEFs, my study did not find focal adhesion turnover to be obviously defective in Y789F MEFs. This suggests that this process may require PTP α expression but not phosphorylation of Tyr789, or that other changes in the cells subvert or

dominate the defects attributed by others (Chen et al., 2006b) to the abrogation of this post-translational modification.

The WT2 and KO8 MEFs failed to recapitulate the previously reported PTP α -dependent changes in focal adhesion formation and morphology. Therefore, after completing further experimentation as described in Chapter 4, I initiated additional experiments to verify whether these cell lines exhibited abnormalities in defined PTP α -mediated integrin signaling events that might underlie their atypical focal adhesion phenotypes. WT2 and KO8 MEFs showed no difference in FAK-Tyr397 phosphorylation in response to integrin stimulation, contrary to the well-established defect in FAK-Tyr397 phosphorylation characteristic of PTP α KO cell lines (Chen et al., 2006b; Su et al., 1999; Zeng et al., 2003). When the WT601 cells were included in these experiments as a benchmark ‘normal’ control, FAK-Tyr397 phosphorylation was somewhat lower in the WT2 cells (~15%) and the KO8 cells (~30%) compared to the established WT601 cells. In addition, KO8 MEFs demonstrated substantial Src dephosphorylation at Tyr527, which was equivalent to that observed in the WT601 cells and exceeded the dephosphorylation shown by WT2 MEFs. Given that integrin-induced PTP α -mediated dephosphorylation and activation of Src is a widely validated mechanism of PTP α action (Chen et al., 2006b; Harder et al., 1998; Ponniah et al., 1999; Su et al., 1999; von Wichert et al., 2003; Zeng et al., 2003), these results suggest that KO8 MEFs do not exhibit the characteristic tandem Src-FAK signaling defects of cells that lack PTP α expression. Furthermore, WT2 MEFs do not exhibit the well-documented integrin-induced and PTP α -mediated dephosphorylation of Src. In hindsight, it would have been beneficial to have conducted these experiments earlier in my study, with the inclusion of the KO595 cells to allow a full comparison of both pairs of genotypic cell lines and

with time in hand to have conducted (and perhaps extended) these signaling experiments in triplicate to allow definitive and quantitative comparisons.

My results reveal distinct differences in the integrin signaling responses of the newly generated WT2 and KO8 MEFs compared to the established WT and PTP α KO cell lines of our lab and others, which likely underlie the phenotypic abnormalities described in this chapter. These inconsistencies do not appear to result from alterations peculiar to only one of the counterpart WT or KO cell lines, but instead seem to reflect irregularities in both cell lines. The KO8 MEFs appear effective in promoting integrin-stimulated molecular events despite lacking PTP α , and conversely, the WT2 MEFs appear less effective in promoting PTP α -mediated integrin signaling in comparison to the reported responses of established PTP α cell lines.

Cell migration is a process that is dependent on integrin signaling and focal adhesion dynamics, and consistent findings from several labs demonstrate defects in the migration ability of PTP α KO cell lines (Chen et al., 2006b; Krndija et al., 2010; Petrone et al., 2003; Zeng et al., 2003). The impaired migration observed in PTP α -null MEFs was not rescued by introduction of mutant PTP α -Y789F, indicating the importance of PTP α phosphorylation in this process (Chen et al., 2006b). Therefore, I next investigated the migratory abilities of the WT2, KO8, CTRL, and Y798F MEFs to determine if the atypical properties that I observed in integrin signalling and focal adhesion formation would be reflected by changes in the migratory ability of these cells.

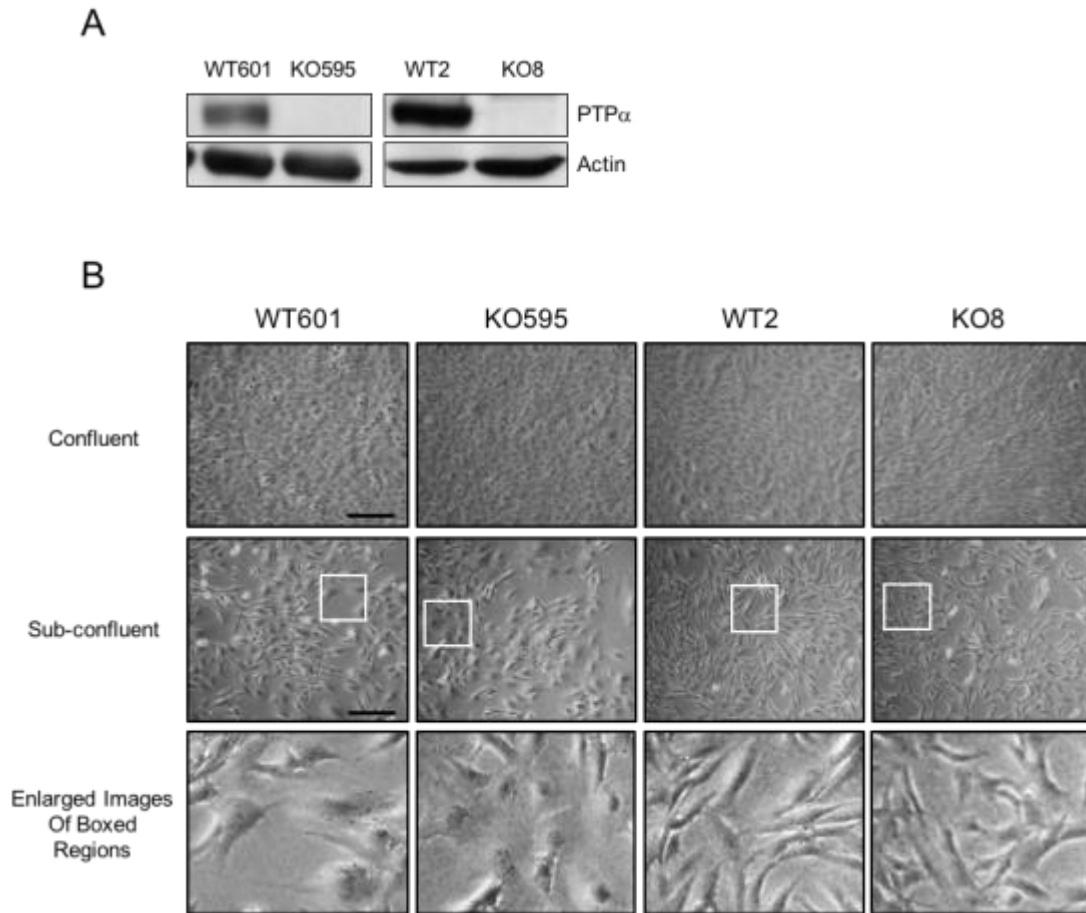


Figure 3.1 PTP α expression and morphology of WT and PTP α KO cell lines. A) A representative Western blot confirms the absence of PTP α in the KO595 and KO8 MEFs. **B)** Representative images of WT601 and KO595 MEFs versus WT2 and KO8 MEFs. Cells were grown to confluency (top panels) or to sub-confluent densities (middle panels) in uncoated plastic culture dishes. The bottom panels show magnified images of the boxed regions of the images of sub-confluent cells above. Scale bars represent 200 μ m.

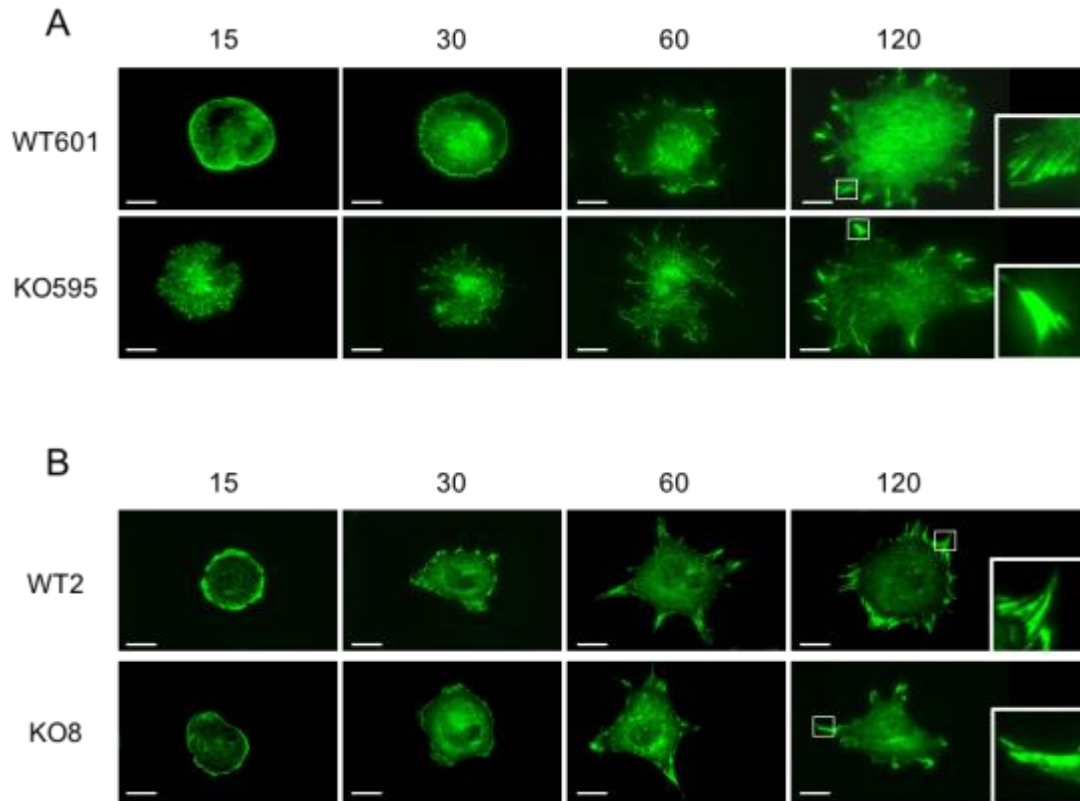


Figure 3.2 PTP α regulates focal adhesion morphology in integrin-stimulated MEFs. Focal adhesion morphology in spreading cells was investigated in response to integrin stimulation of WT and PTP α KO MEF cell lines: WT601 and KO595, and WT2 and KO8. Cells were harvested and plated on FN-coated coverslips for 15, 30, 60, or 120 min before fixation and immunofluorescent staining with anti-paxillin antibody. Cells were imaged using TIRF microscopy. **A)** Representative images of WT601 and KO595 MEFs. **B)** Representative images of WT2 and KO8 MEFs. The insets show a magnified view of focal adhesions from the boxed regions in the 120 min images. Scale bars represent 20 μ m.

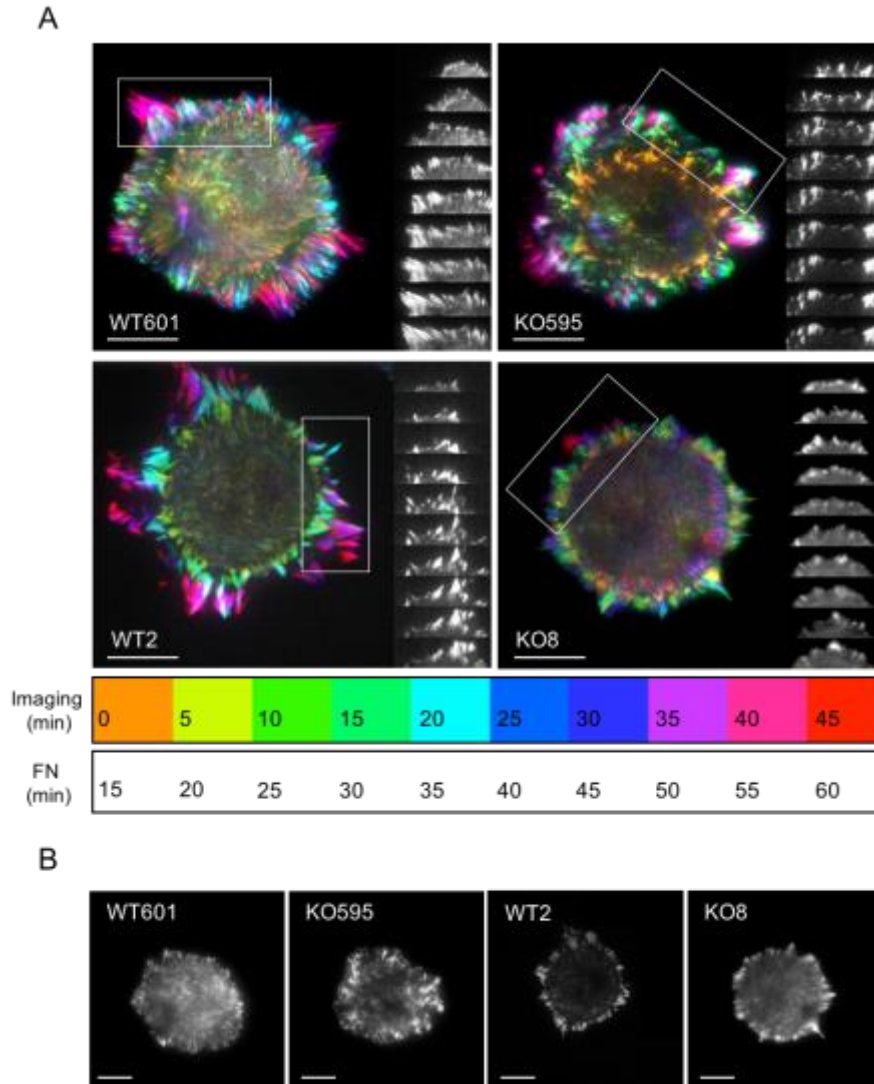


Figure 3.3 PTP α plays a role in focal adhesion formation and dynamics in integrin-stimulated MEFs. Focal adhesion formation and dynamics were investigated in two separate pairs of WT and PTP α KO MEF cell lines: WT601/KO595 and WT2/KO8 MEFs. Cells were transfected with eGFP-paxillin, plated on FN-coated coverslips, and imaged every 20-30 s for 45 min using TIRF microscopy. **A)** Focal adhesion footprints were created by compiling images taken at 5 min intervals, with time 0 representing 15 min on fibronectin. Individual images were temporally coloured according to the time-scale shown below the cell images (the lower time-scale depicts actual time of cell contact with FN), and then overlaid to create a focal adhesion “Footprint” which displays the temporal progression of focal adhesion assembly and disassembly in the FN-stimulated cell. The black and white montage images appearing to the right of each footprint image show frame-by-frame appearance of eGFP-paxillin-containing focal adhesions in the boxed region of the footprint image, at each time depicted on the colour key. **B)** An image of each cell in (A) at 30 min on fibronectin (15 min imaging). Scale bars represent 20 μ m.

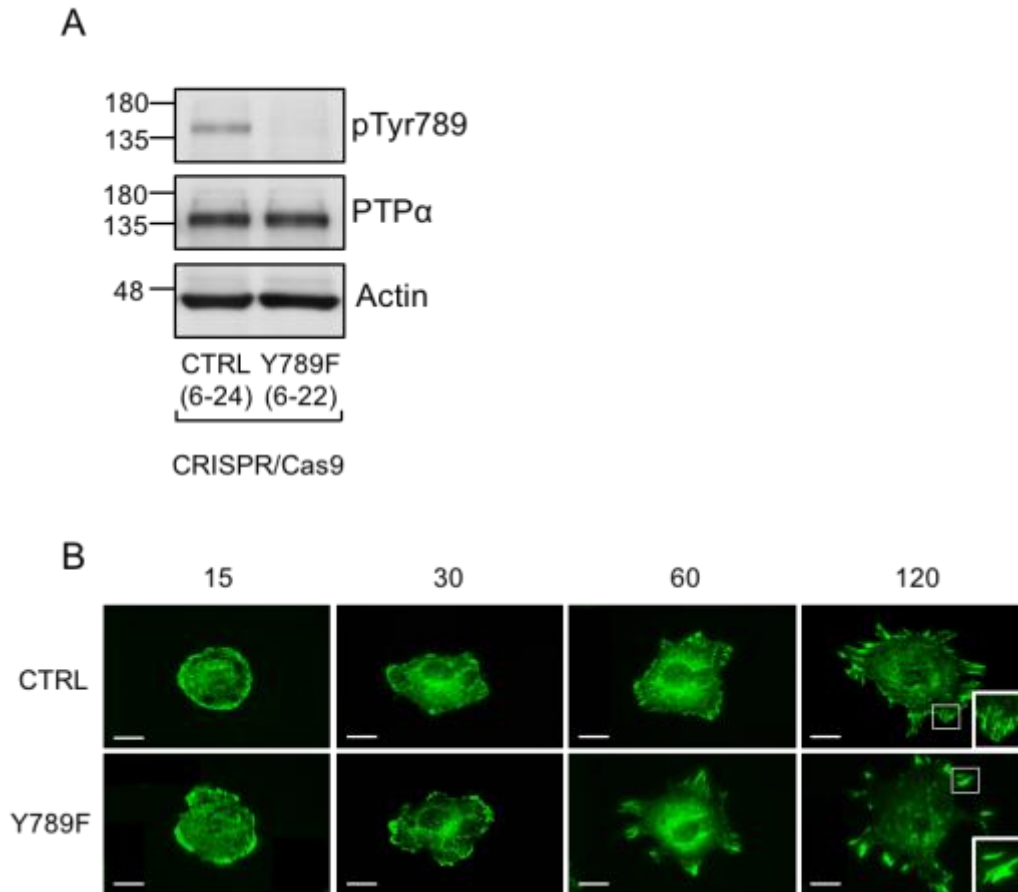


Figure 3.4 Focal adhesion morphology is affected by the absence of PTP α -Tyr789 in integrin-stimulated MEFs. **A)** A representative Western blot confirms the presence of PTP α and absence of phosphorylation at PTP α -Tyr789 in CRISPR-edited cell lines (cell line 6-24, CTRL; cell line 6-22, Y789F). **B)** CTRL and Y789F MEFs were plated on fibronectin (FN)-coated coverslips for 15, 30, 60, and 120 min. At these times, cells were fixed, immunostained for paxillin, and imaged using TIRF microscopy. The insets in (B) at 120 min show a magnified view of focal adhesions in the boxed regions. Scale bars represent 20 μ m.

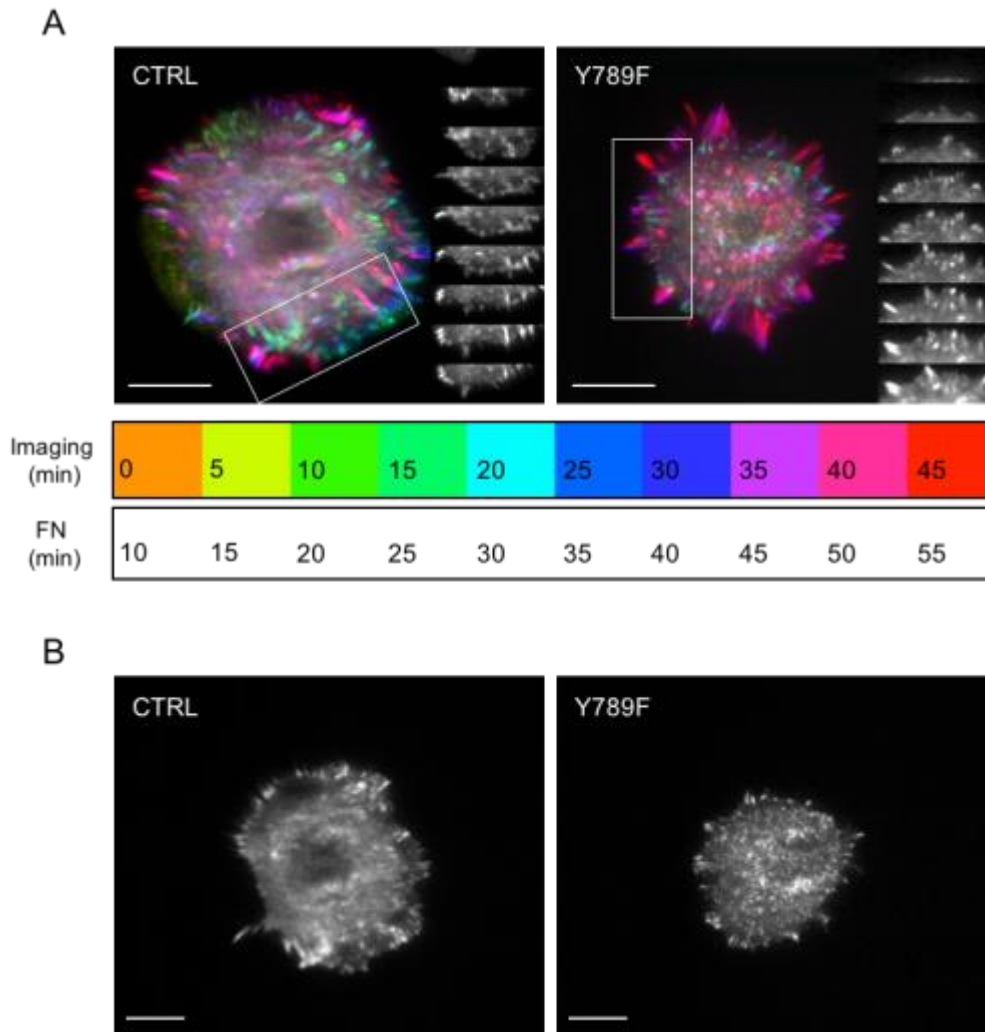


Figure 3.5 Focal adhesion dynamics are affected by the absence of PTP α -Tyr789 in integrin-stimulated MEFs. Focal adhesion formation and turnover were investigated in CRISPR/Cas9-edited MEFs expressing control (cell line 6-24, CTRL) or unphosphorylatable mutant PTP α -Y789F (cell line 6-22, Y789F). Cells were transfected with eGFP-paxillin, plated on FN-coated coverslips, and imaged every 20 s for 45 min, using TIRF microscopy. **A**) Focal adhesion footprints were created by compiling images taken at 5 min intervals, with time 0 representing 10 min on FN. Individual images were temporally coloured according to the time-scale shown below the cell images (the lower time-scale depicts actual time of cell contact with FN), and then overlaid to create a focal adhesion “Footprint” which displays the temporal progression of focal adhesion assembly and disassembly in the FN-stimulated cell. The black and white montage images appearing to the right of each footprint show frame-by-frame appearance of eGFP-paxillin-containing focal adhesions in the boxed region of the footprint image, at each time depicted on the colour key. **B**) An image of each cell in (A) at 30 min on fibronectin (20 min imaging). Scale bars represent 20 μ m.

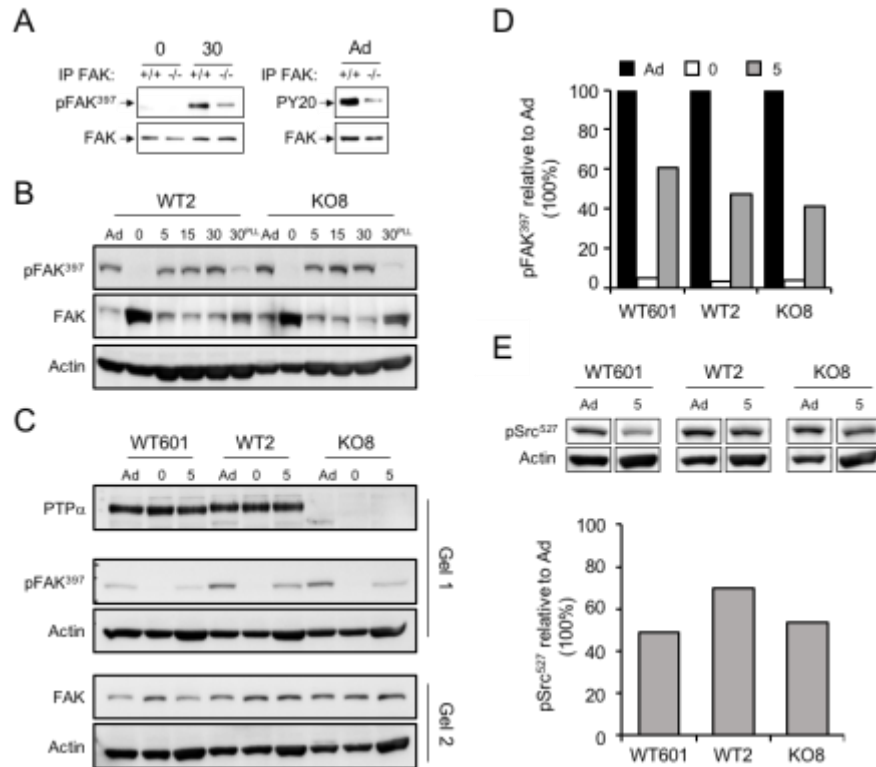


Figure 3.6 Early integrin-stimulated signaling events in WT and PTP α KO MEFs. WT601 MEFs and the newly established lines of WT2 and KO8 MEFs were cultured on plastic dishes (adherent, Ad), trypsinized and placed in suspension for 1 h to terminate integrin signaling (0), and then re-plated on FN-coated dishes for the indicated times (min). Cell lysates were analyzed by Western blotting. **A**) Results reproduced from Zeng et al. (2003) showing the reduced phosphorylation of FAK in KO595 MEFs (-/-) compared to WT601 MEFs (+/+). Cell lysates were probed with anti-FAK-pTyr397 (pFAK³⁹⁷) and FAK antibodies (left panels) or with anti-phosphotyrosine antibody PY20 and FAK antibody (right panels). **B**) Lysates of WT2 and KO8 cells were probed with anti-FAK-pTyr397, FAK and actin antibodies. Some cells were also cultured on poly-L-lysine for 30 min (30^{PLL}), a substratum that does not stimulate integrin signaling. The blot shown is representative of 3 independent experiments. **C**) Lysates of WT601, WT2 and KO8 cells were probed with PTP α , anti-FAK-pTyr397, FAK and actin antibodies. The blot shown is from one experiment. **D**) Densitometric quantification of FAK-pTyr397 and FAK from (C). The FAK-pTyr397 signal was normalized to that of actin detected on the same blot (Gel 1), and the FAK signal was normalized to that of actin detected on the same blot (Gel 2), and these values were used to determine FAK-pTyr397 per unit FAK. Values are shown relative to that in adherent (Ad) cells, with the latter taken as 100%. **E**) Lysates of WT601, WT2 and KO8 cells were probed with anti-Src-pTyr527 (pSrc⁵²⁷) and actin antibodies (top panels). Following densitometric quantification, the Src-pTyr527 signals were normalized to those of the corresponding actin signals. The values from cells at 5 min on FN are shown in the graph, and are presented relative to the value of the adherent cells (Ad) taken as 100% for each cell line.

Chapter 4: The Role of PTP α and PTP α -Y789 Phosphorylation in Migration Ability, Directionality, and Cell Polarity

4.1 Rationale

The focal adhesion cycle of assembly and disassembly is important to the ability of a cell to migrate. Previous studies of WT601 and KO595 MEFs showed defects in focal adhesion formation and migration in the KO595 MEFs (Chen et al., 2006b; Zeng et al., 2003). However, the newly generated line of KO8 MEFs does not exhibit defects in cell spreading or focal adhesion dynamics in comparison to the WT2 MEFs. Thus, I next investigated the migratory abilities of these MEFs to determine how this related to their integrin signalling and focal adhesion formation phenotypes. The CRISPR/Cas9-edited Y789F MEFs display large, aggregated focal adhesions, similar to focal adhesions formed in the KO595 MEFs. Previous studies have demonstrated that the defective migration ability of PTP α -null MEFs is not rescued by introduction of exogenous mutant PTP α -Y789F (Chen et al., 2006b), indicating that PTP α -Tyr789 phosphorylation is required for proper cell migration. Therefore, I also investigated the migratory abilities of the CRISPR CTRL and Y798F MEFs to determine if the endogenous expression of unphosphorylatable mutant PTP α altered the migration of MEFs.

The migration abilities of WT2, KO8, CTRL, and Y789F MEFs were assessed using two different types of assays: a ‘wound healing’ assay that measures the ability of cells to repair a break or ‘wound’ in a cell monolayer by moving into and filling the wound area; and a Transwell assay that measures the motile ability of individual cells in a process known as haptotaxis or chemotaxis. Two key linked parameters of cell migration, directionality and polarity, were also

investigated to determine if these were specifically affected in a PTP α -dependent manner. The directional movement of a migrating cell reflects its persistence and determines its efficiency in arriving at a final destination. Cell polarity establishes asymmetry in a migrating cell that differentiates its leading and trailing edges, where distinct molecular and structural events occur to establish forward movement of the cell (Ridley et al., 2003). Using these assays and analyses, I sought to determine whether the migratory properties and abilities of the new WT2, KO8 and Y789F MEFs were consistent with the properties of focal adhesion formation and turnover that I had characterized in these cell lines (as described in Chapter 3).

4.2 The role of PTP α in wound healing

I conducted wound healing assays to characterize the PTP α -dependent migration ability of the newly generated wild-type (WT2) and PTP α knockout (KO8) MEFs. Confluent monolayers of cells were ‘wounded’ by scratching the monolayer with a pipette tip to introduce a long thin area devoid of cells. This wound area in the monolayer was imaged over 8 hours to investigate the wound closure ability of the MEFs, and determine how the presence or absence of PTP α affects the migration of cells into the empty area.

Wound closure was measured in the WT2 and KO8 MEF cultures, and statistical analyses confirmed there was no significant difference between the two cell types at early (4 h) or later (8 h) times (Fig. 4.1A, B). Representative images of the wound in WT2 and KO8 MEF cultures at 0 and 8 h are shown in Fig. 4.1C. My finding that WT2 and KO8 cells exhibited similar migratory abilities in these assays was unexpected as our lab previously demonstrated a significant reduction in the migration of MEFs lacking PTP α (Chen et al., 2006b; Zeng et al., 2003).

To investigate the role of PTP α in wound healing using a different approach, WT2 MEFs were depleted of PTP α using siRNA. Wound healing assays were performed using these cells (siPTP α) as well as WT2 MEFs treated with non-targeting control (siCTRL) siRNA. Statistical analyses showed that the wound closure ability of the siPTP α -MEFs was not significantly different from that of the siCTRL MEFs at early (4 h) or later (8 h) times (Fig. 4.2A, B). The depletion of PTP α was confirmed through Western blotting (Fig. 4.2A, inset).

Since neither the absence nor the depletion of PTP α in MEFs resulted in impaired migration, I investigated whether or not this effect was specific to the MEFs (i.e. reflected an abnormality in one or both of these particular cell lines) by testing the effect of depleting PTP α on the migratory ability of another cell line. I chose to use the metastatic human breast adenocarcinoma cell line MDA-MB-231, as these commercially available cells are widely used to investigate the molecular regulation of cell motility. MDA-MB-231 cells were treated with PTP α -targeted siRNA, a non-targeted control siRNA (siCTRL), or left untreated (Parental) and the wound closure abilities of these cells were investigated. The wound healing assay was extended to 16 hours to account for the slower migration of the MDA-MB-231 cells. No significant differences in wound closure were observed between the treatment groups at 4, 8, or 16 h, suggesting that the absence of PTP α has no effect on the migratory ability of MDA-MB-231 cells (Fig. 4.3A, B). PTP α depletion was confirmed by Western blotting (Fig. 4.3B, inset).

4.3 The role of PTP α -pTyr789 in wound healing

Wound closure abilities of the CRISPR/Cas-edited CTRL and Y789F MEFs were assessed to determine if the presence of this phosphorylatable residue of PTP α is required for

proper migration, as previously shown using KO595 MEFs re-expressing mutant PTP α -Y789F (Chen et al., 2006b). Contrary to these previous results, CRISPR/Cas-mutated PTP α -Y789F MEFs showed a significant increase in their ability to close the wound in contrast to the CTRL MEFs (Fig. 4.4A, B).

4.4 Investigating the role of PTP α in Transwell migration

The unexpected results from the wound healing assays prompted further investigation of the migratory abilities of the MEFs and MDA-MB-231 cells. I used a different type of assay in order to determine if the motility of individual cells might differ from that observed with cells in tight contact with one another as in the wounded cell monolayers described above. In the Transwell assay, a cell suspension is placed in a chamber insert containing a permeable bottom membrane, with pores that allow transit of single cells. The cells that move through the pores to the underside of the insert can be detected and quantified (Materials and Methods, section 2.1.1). Transwell assays were performed using WT2 and KO8 MEFs as well as PTP α -depleted MDA-MB-231 cells.

The WT and PTP α KO MEFs were placed in the apical chambers of Transwell inserts and incubated to allow migration through the membrane to the fibronectin-coated side of the membrane in the basal chambers. No significant difference in the migration of WT2 and KO8 MEFs was detected (Fig. 4.5A, B).

MDA-MB-231 cells were depleted of PTP α or treated with non-targeting control siRNA as described above (section 4.2) and Parental, siCTRL, and siPTP α cell suspensions were placed in Transwell inserts to migrate towards FBS-supplemented DMEM in the basal chamber.

Statistical analysis found no significant difference in the migration of Parental, siCTRL, or siPTP α MDA-MB-231 cells (Fig. 4.5C). PTP α expression was determined in each cell type, confirming that PTP α was successfully depleted in the siPTP α MDA-MB-231 cells (Fig. 4.5D, inset).

The Transwell assay results are consistent with the findings from the wound healing assays, which suggests that the absence of PTP α has no effect on the migration abilities of KO8 MEFs or PTP α -depleted MDA-MB-231 cells.

4.5 The role of PTP α and PTP α -pTyr789 in directional cell movement

To investigate whether the expression of PTP α and phosphorylation at Tyr789 affect other aspects of cell migration, directionality and polarity were assessed in cells at the wound edge in wound healing assays. Cells were live-imaged for 24 hours following wounding in order to follow the movement of WT2, KO8, CTRL, and Y789F MEFs into the wound. Using the MTrackJ plugin in ImageJ, the location of individual cells can be recorded at each time-point to determine the total length of their tracks, as well as the net distance travelled by each selected cell (direct distance from start to finish). This allows a closer look as to whether a cell travels in a direct path or in a random, less efficient path to/in the wounded area.

The coordinates of the cell tracks were graphed in order to qualitatively visualize the movement of cells of each type. When comparing the tracks of WT2 MEFs to those of KO8 MEFs (Fig. 4.6A and B), the KO8 MEFs have more indirect and inefficient migration tracks compared to the tracks of the WT2 MEFs. The KO8 MEFs change direction, and occasionally migrate in circles, suggesting that the migrating KO8 MEFs have decreased directionality at the

wound edge. A qualitative comparison of the tracks of the CTRL and Y789F cells suggests that more of the Y789F cells tend to move straight across the wound area, whereas more CTRL cells seem to move into the wound area and stay relatively closer to the wound edge where they originated (Fig. 4.6C and D).

The total and net distances travelled by WT2, KO8, CTRL, and Y789F MEFs were measured in three independent experiments and averaged (Fig. 4.6E). Statistical analysis showed no significant difference between the total distance travelled by each cell type, nor was there a significant difference in the net distance travelled by each cell type. However, there was a significant difference between the total distance and the net distance travelled by the KO8 MEFs that was not apparent for any of the other cell lines, possibly reflecting a more random movement of the KO8 MEFs that is not directed properly towards the wound area. Such reduced directionality might be expected to translate to a decrease in migration, however as shown in Figs. 4.1 and 4.5A, the KO8 MEFs possess wound closure and Transwell migration abilities comparable to the WT2 MEFs. In accord with this, migration efficiency, calculated by dividing the net distance by the total distance, was not significantly impaired in KO8 cells or in any of the other cell types when compared to the WT cell efficiency (Fig. 4.6F).

4.6 The role of PTP α in cell polarization at the wound edge

Alignment of the microtubule organizing center (MTOC) with the nucleus in the direction of cell migration is important for cell polarity and directional cell migration (Francis et al., 2011; Kupfer et al., 1982; Magdalena et al., 2003). I investigated the polarity of PTP α -depleted WT2 MEFs at the wound edge, according to the method of Francis *et al.* (2011). WT2 MEFs were treated with PTP α -targeted siRNA (siPTP α) or a non-targeting control siRNA

(siCTRL), and a wound healing assay was performed on fibronectin-coated coverslips. After 4 and 8 hours of incubation, cells on the coverslip were fixed and stained with DAPI to visualize the nucleus and immunostained to detect γ -tubulin, a component of the MTOC. Cell polarity was determined by analyzing the location of the perinuclear MTOC relative to the leading edge of the cells. To quantify this, if the MTOC was positioned in the 120° sector of the cell facing the wound edge the cell was scored positive for polarization, whereas its positioning in the remaining 240° side/rear sector resulted in a negative score for polarity (Fig. 4.7A, B). Examples of siCTRL and siPTP α cells at the wound edge that scored positive (green arrows) or negative (red arrows) for polarity are shown in Fig. 4.7C and D. At 4 h after wounding, about 66% of siCTRL MEFs and about 76% of siPTP α MEFs exhibited polarization, with MTOCs oriented towards the leading edge of the cell, but with no significant difference in this measure arising due to the depletion of PTP α (Fig. 4.7E). At 8 h after wounding, the siCTRL cells showed no further change in polarity. However, PTP α -depleted MEFs underwent a significant reduction in polarization from 4 to 8 hours (from 76% \pm 8 to 53% \pm 6, respectively, $p < 0.05$), as well as in comparison to the CTRL MEF polarity at 8 h (Fig. 4.7E). PTP α -depletion was confirmed by Western blotting (Fig. 4.7F). These results suggest that PTP α may play a role in regulating cell polarity in migrating cells at the wound edge, specifically after 4 hours when cells have already started infiltrating the wound area. Thus, some migration-related defects in the PTP α -depleted WT2 MEFs are perhaps being compensated for in the wound healing assays such that defective cell motility is not readily observed.

4.7 Discussion

It has previously been established that cells lacking PTP α expression display defects in focal adhesion formation, cell spreading, and migration (Chen et al., 2006b; Su et al., 1999; Zeng et al., 2003). Investigation of the newly generated WT2 and KO8 MEFs demonstrated that unlike the previously studied WT601 and KO595 MEFs, WT2 and KO8 MEFs displayed less profound or no detectable differences in adhesion morphology, assembly, turnover, and cell spreading. This indicates that PTP α -dependent mechanisms that are known to affect migration may not be operative in the KO8 cells. Instead of continuing to study the dynamics and molecular activity of the adhesions in these cells, I focused on verifying PTP α -dependent migration in the new cell lines, and defining additional migration parameters such as cell polarity and directionality, to better characterize the KO8 and Y789F MEFs.

My findings described in Chapters 3 and 4 are summarized in Table 4.1. Wound healing and Transwell assays involving WT2 and KO8 MEFs demonstrated that there was no significant reduction in the migratory ability of KO8 MEFs, contrary to expectations based on the migration defects exhibited by KO595 MEFs (Chen et al., 2006b; Zeng et al., 2003). However, the apparently normal migration of KO8 MEFs is in accord with their lack of recapitulation of the morphological and functional defects associated with focal adhesions of PTP α KO cell lines. Together, this suggests that the atypical integrin signaling response and focal adhesion formation observed in KO8 MEFs underlie the abnormal migration phenotype of these cells. To discern whether this was an issue with either or both of the WT2 and KO8 cell lines, I repeated the wound healing assay with WT2 MEFs depleted of PTP α . PTP α -depleted MEFs also showed no significant difference in migration ability from siCTRL MEFs, which suggests that the similar

migration abilities of the WT2 and KO8 MEFs are likely attributed to abnormalities in the WT2 MEFs. Perhaps the WT2 MEFs are inherently less motile compared to previous WT cell lines, and therefore depleting PTP α does not further reduce their motility. Alternatively, the WT2 MEFs may have acquired changes that involve a dominant or compensatory mechanism driving migration regardless of PTP α expression.

In order to understand whether this PTP α -independent migration ability was specific to the WT2 and KO8 MEFs, I investigated the PTP α -dependent migration ability of the metastatic MDA-MB-231 cell line. PTP α -depleted MDA-MB-231 cells also failed to effect a significant reduction in migration in wound healing and Transwell assays. This suggested that PTP α may not play a prominent role in MDA-MB-231 cell migration.

CRISPR-edited Y789F MEFs surprisingly displayed a significant increase in migration over the CTRL MEFs in wound healing assays. This was unexpected as it has previously been reported that migration ability is reduced in KO595 MEFs with exogenous mutant PTP α -Y789F expression. Impaired focal adhesion turnover is characteristic of the KO595 MEFs (Fig. 3.3A, top right panel) and likely plays a large role in the defective migration observed in KO595 MEFs. In contrast, the dynamic peripheral adhesion turnover in Y789F MEFs (Fig 3.5A, top right panel) could contribute to the increased migration exhibited by these cells. In addition, the Y789F MEF migration ability could potentially be attributed to off-target effects of CRISPR/Cas gene editing that have resulted in the upregulation of a signaling network or protein involved in promoting migration.

The unexpected migration abilities of the WT2, KO8, CTRL, and Y789F MEFs prompted further investigation into additional parameters of migration in order to understand

some of the mechanisms that might feature in their abnormal migration phenotype. Investigating motile cell directionality revealed a significant reduction in the net migration distance compared to total distance travelled by the KO8 MEFs. This suggests that although the KO8 MEFs are very motile, they exhibit more random and inefficient movement into the wound area. Perhaps the high motility of these KO8 MEFs compensates for their lack of direction and increases their ability to close the wound or migrate through the Transwell membrane by random rather than directed cell movement. In addition, compared to siCTRL MEFs, PTP α -depleted WT2 MEFs showed a significant decrease in polarity of migrating cells at the wound edge at 8, but not at 4 h. This suggests a loss of polarity occurs after cells have begun migrating into the wound and that this could contribute to the lack of directional movement by the KO8 MEFs.

To conclude, the findings described in Chapters 3 and 4 further highlight the anomalous properties of the WT2 and KO8 MEFs. The PTP α -independent focal adhesion morphology, formation and turnover ability observed in the WT2 and KO8 MEFs are reflected in the inability of these MEFs to demonstrate PTP α -dependent alterations in cell motility. My results demonstrate that there are PTP α -dependent defects in cell polarity and directionality in the KO8 MEFs, but these defects are not significant enough to substantially affect their motility. Therefore, it is likely that the WT2 and KO8 MEF lines have both acquired important changes that supersede PTP α -dependent regulation of focal adhesion dynamics and cell migration. Possible reasons for the phenotypic differences characterized in these MEFs are discussed in the next chapter.

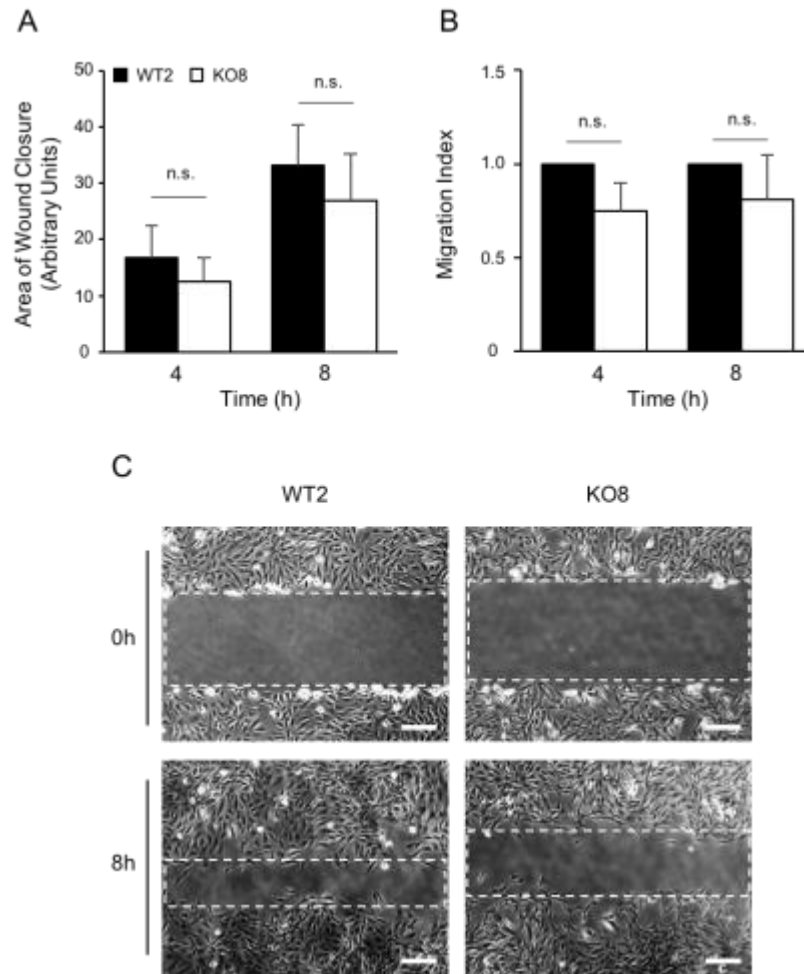


Figure 4.1 Wound healing abilities of WT and PTP α KO MEFs. Shortly after reaching confluency, monolayers of WT2 and PTP α KO8 MEFs were ‘wounded’ (a wound area was created by scratching with a pipette tip) and placed in serum-depleted media for the duration of the experiment (8 h). Each wound was imaged at 0, 4, and 8 h post-wounding. The wound area at each time point was measured using ImageJ. The area of wound closure was determined by subtracting the wound areas at 4 and 8 h from that at 0 h. **A)** The area of wound closure achieved by the MEFs is displayed in arbitrary units. **B)** The migration index was calculated using data obtained in experiments as in (A), and normalized to the WT2 MEF migration index that was set at 1. Bars in all graphs show the mean \pm S.D., n=6. Statistically non-significant differences are depicted as n.s., as determined by a two-tailed, equal variance Student’s t-test. **C)** Representative images of WT and PTP α KO MEFs at 0 and 8 h post-wounding. Cells were visualized at 4x magnification. Scale bar represents 200 μ m.

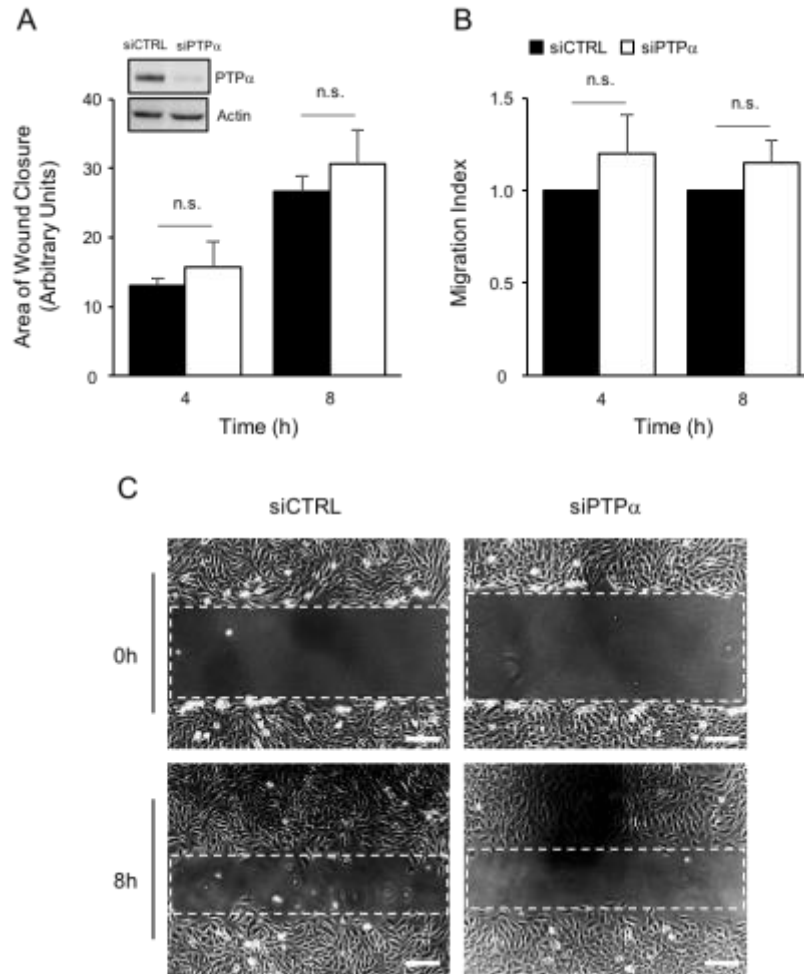


Figure 4.2 Wound healing ability of PTP α -depleted MEFs. Wound closure ability was assessed in WT2 MEFs that were depleted of PTP α using PTP α -targeted small interfering RNA (siPTP α) versus WT2 MEFs treated with non-targeted control siRNA (siCTRL). Shortly after reaching confluency, monolayers of these cells were ‘wounded’ (a wound area was created by scratching with a pipette tip) and placed in serum-depleted media for the duration of the experiment (8 h). Each wound was imaged at 0, 4, and 8 h post-wounding. The wound area at each time point was measured using ImageJ. The area of wound closure was determined by subtracting the wound areas at 4 and 8 h from that at 0 h. **A**) The area of wound closure in siCTRL and siPTP α MEFs is displayed in arbitrary units and a representative Western blot shows PTP α and actin expression in lysates of siCTRL and siPTP α cells. **B**) The migration index was calculated for siCTRL and siPTP α MEFs using data obtained in experiments as in (A), and normalized to the siCTRL MEF migration index that was set at 1. Graphs represent the mean \pm SD, n=4. Statistically non-significant differences are depicted as n.s., as determined by a two-tailed, equal variance Student’s t-test. **C**) Representative images of siCTRL and PTP α -depleted MEFs at 0 and 8 h post-wounding. Scale bar represents 200 μ m.

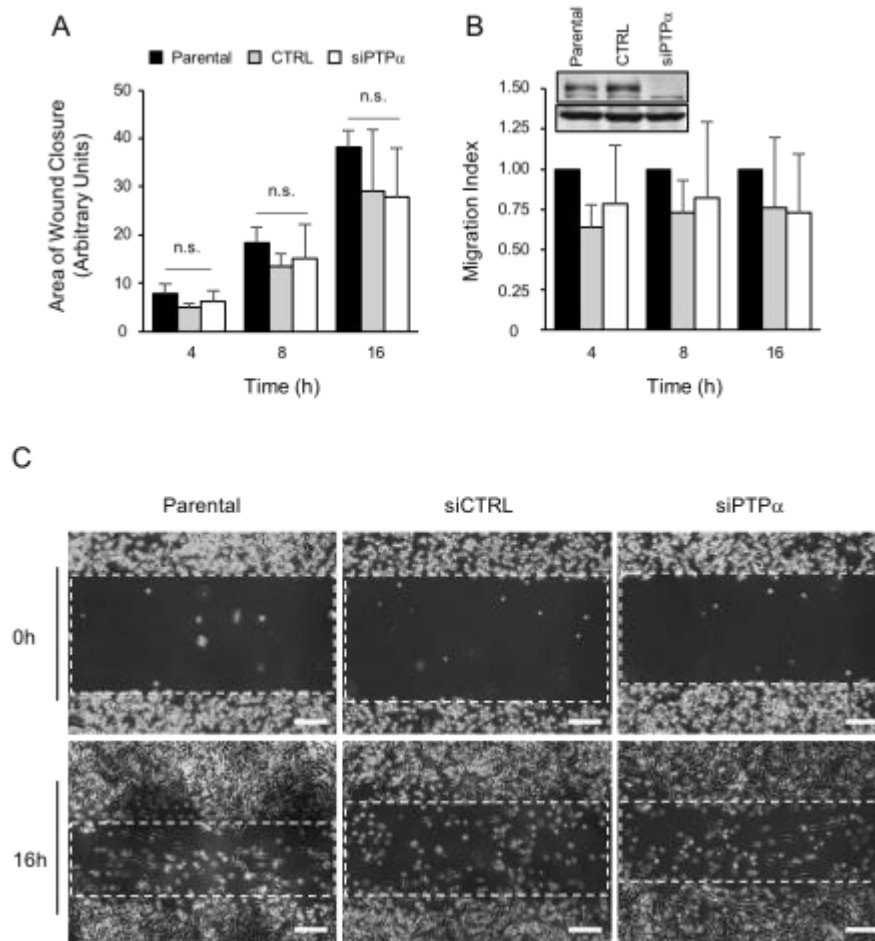


Figure 4.3 Wound healing ability of PTP α -depleted MDA-MB-231 Cells. Wound closure ability was assessed in MDA-MB-231 cells that were depleted of PTP α using PTP α -targeted siRNA (siPTP α), treated with a non-targeted control siRNA (siCTRL), or left untreated (Parental). Shortly after reaching confluency, monolayers of these cells were wounded and placed in serum-depleted media for the duration of the experiment (16 h). Each wound was imaged at 0, 4, 8 and 16 h post-wounding. The wound area at each time point was measured using ImageJ. The area of wound closure was determined by subtracting the wound areas at 4, 8 and 16 h from that at 0 h. **A**) The area of wound closure in Parental, siCTRL and siPTP α MDA-MB-231 cells is displayed in arbitrary units. **B**) The migration index was calculated for Parental, siCTRL and siPTP α MDA-MB-231 cells using data obtained in experiments as in (A), and normalized to the Parental MDA-MB-231 cell migration index that was set at 1. Graphs represent the mean \pm SD, n=3. Statistically non-significant differences are depicted as n.s., as determined by a two-way ANOVA with a Tukey's multiple comparisons test. A representative Western blot shows PTP α and actin expression in lysates of Parental, siCTRL, and siPTP α cells. **C**) Representative images of Parental, siCTRL and siPTP α -depleted MDA-MB-231 cells at 0 and 16 h post-wounding. Scale bar represents 200 μ m.

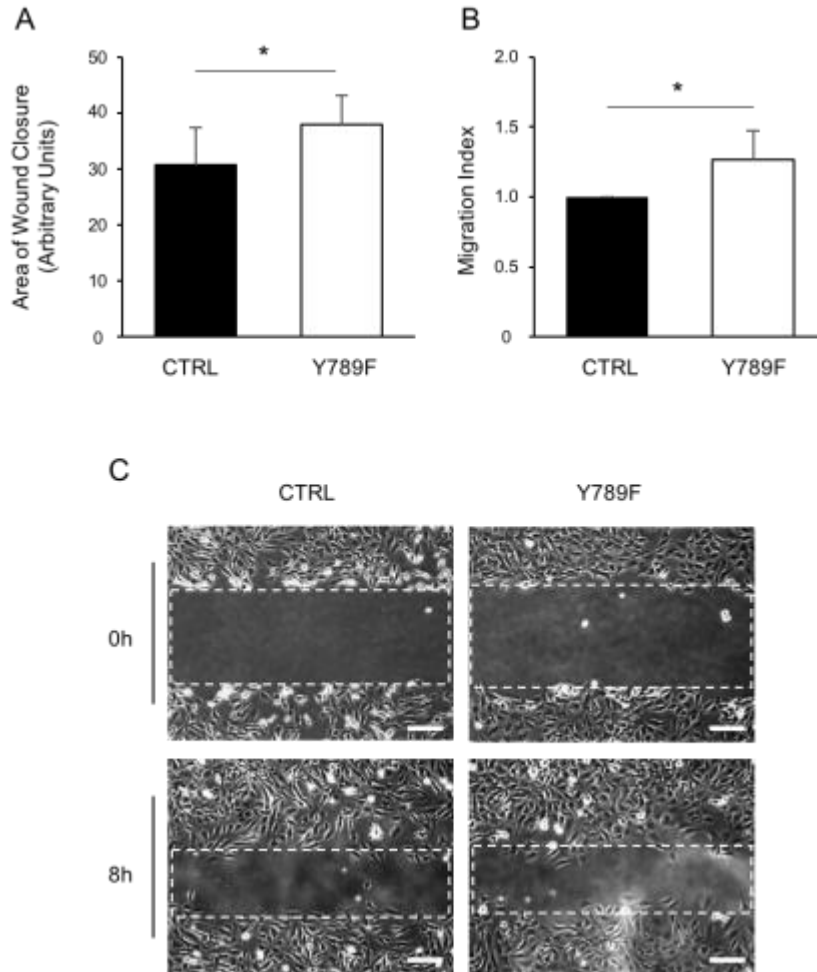


Figure 4.4 Wound healing ability of mutant MEFs expressing PTP α -Y789F. Wound closure ability was assessed in MEFs that had been successfully (cell line 6-22, PTP α -Y789F; Y789F) or unsuccessfully (cell line 6-24, control; CTRL) edited using CRISPR/Cas9 technology to target endogenous *Ptpra* so as to alter Tyr789 to Phe in the expressed PTP α protein. Shortly after reaching confluency, monolayers of CTRL and Y789F MEFs were ‘wounded’ (a wound area was created by scratching with a pipette tip) and placed in serum-depleted media for the duration of the experiment (8 h). Each wound was imaged at 0 and 8 h post-wounding. The wound area at each time point was measured using ImageJ. The area of wound closure was determined by subtracting the wound area at 8 h from that at 0 h. **A**) The area of wound closure achieved by CTRL and PTP α -Y789F MEFs is displayed in arbitrary units. **B**) The migration index was calculated for CTRL and PTP α -Y789F MEFs using data obtained in experiments as in (A), and normalized to the CTRL MEF migration index that was set at 1. Bars in all graphs show the mean \pm S.D., n=7. Asterisks depict $p < 0.05$, as determined by a two-tailed, equal variance Student’s t-test. **C**) Representative images of CTRL and PTP α -Y789F MEFs at 0 and 8 h post-wounding. Scale bar represents 200 μ m.

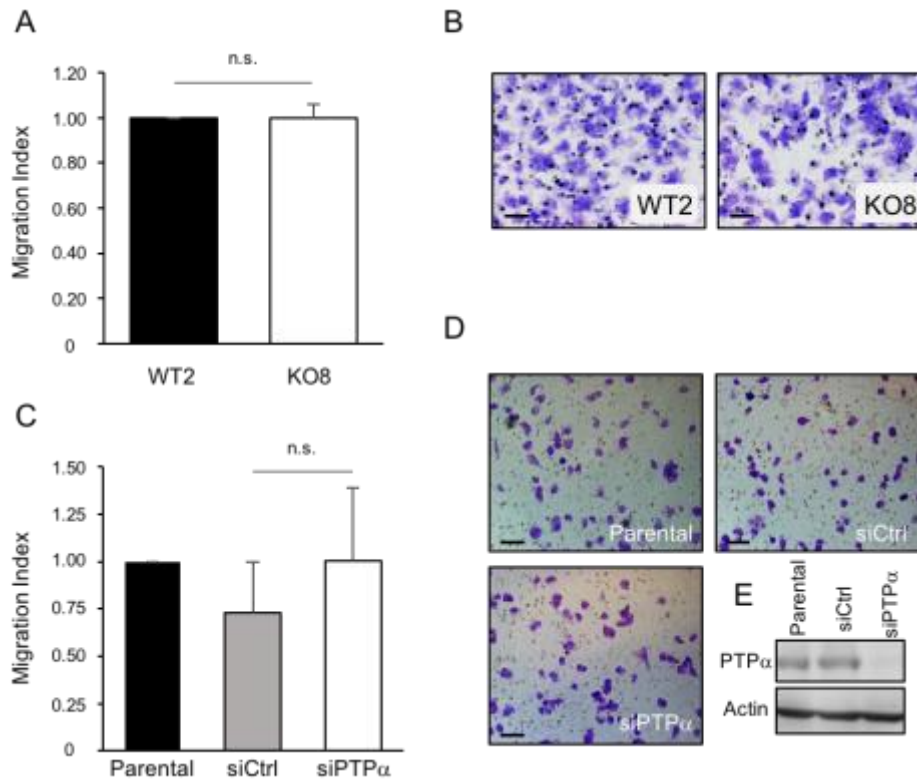


Figure 4.5: Migration ability of PTP α KO MEFs and PTP α -depleted MDA-MB-231 Cells. Migration ability of PTP α KO MEFs and PTP α -depleted MDA-MB-231 cells were investigated using Transwell migration assays. **A, B**) WT2 and KO8 MEFs were plated in the apical chamber of a Transwell assay and allowed to migrate across the membrane to the fibronectin coating on the bottom of the insert membrane. Following a 2h incubation, MEFs that had successfully migrated onto the basal surface of the membrane were fixed, stained, imaged and counted. **A**) Migration indices of WT2 and KO8 MEFs were calculated using average number of cells per field and normalized to the WT2 migration index that was set to 1. **B**) Representative images of WT2 and KO8 MEF Transwell membranes stained with crystal violet. **C, D**) MDA-MB-231 cells were treated with PTP α -targeted siRNA (siPTP α), non-targeting siRNA (siCTRL), or no siRNA (Parental), and migration ability was assessed over 8 h in a Transwell migration assay with 10% FBS as the migratory chemoattractant in the basal chamber. Following 8 h incubation, migratory MDA-MB-231 cells were fixed on the membrane, stained, counted and imaged. **C**) Migration indices of Parental, siCTRL, and siPTP α calculated as in (A) and normalized to the Parental migration index that was set to 1. **D**) Representative images of Parental, siCTRL, and siPTP α Transwell membranes stained with crystal violet, and a representative Western blot showing PTP α expression in MDA-MB-231 siRNA-treated cells. Bars in all graphs show the mean \pm S.D., n=3 (A), n=5 (C). Scale bar represents 50 μ m. Statistically non-significant differences are depicted as n.s., as determined by a two-tailed, equal variance Student's t-test.

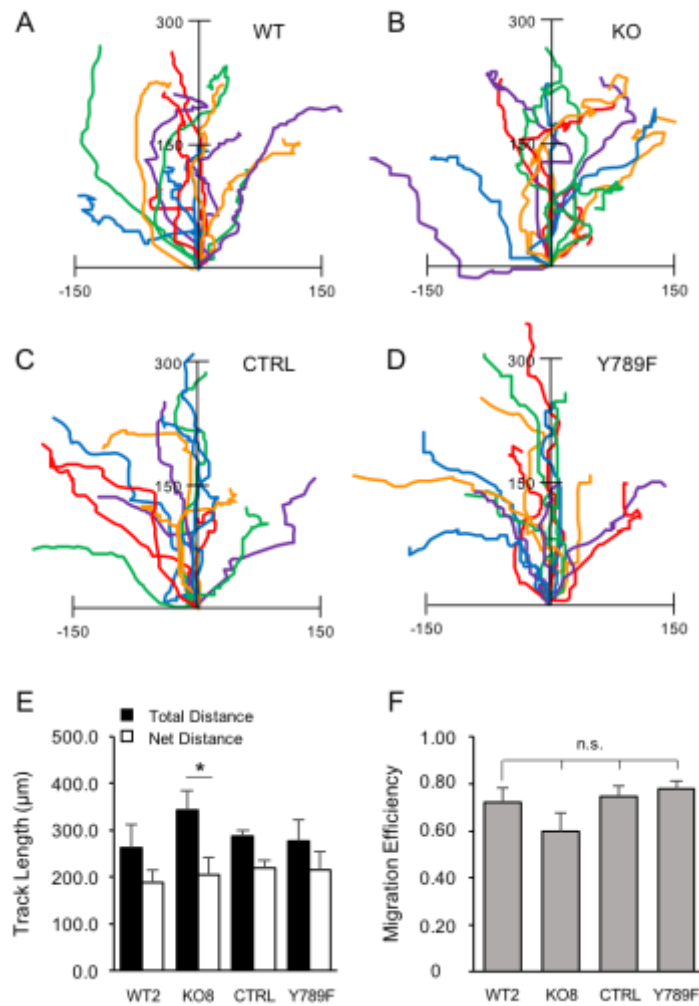


Figure 4.6 Directionality and migration efficiency are unaffected by the absence of PTP α or mutation of PTP α -Tyr789 in MEFs. Directionality and migration efficiency were investigated through a time-lapse wound healing assay. Shortly after reaching confluency, monolayers of WT2, KO8, CTRL, and Y789F MEFs were wounded and placed in serum-depleted media for the duration of the experiment. Wounded monolayers were imaged every 20 min for 24 h. Images were compiled into a time-lapse video and analyzed in ImageJ. Using the MTrackJ plugin, 10 individual cells per cell type per experiment were tracked at each time-point and their coordinates were recorded. **A-D)** Cell track coordinates were graphed to display the migration paths of 15 individual cells (5 per experiment) for WT2, KO8, CTRL, and Y789F MEFs; graph axes units are measured in μm . **E)** Average total track length and net length (distance from start position to finish position) were graphed. **F)** Migration efficiency was calculated by dividing the average net length by the average total length for each cell type. Bars in all graphs show the mean \pm S.D., $n=3$. Statistically non-significant differences are depicted as n.s., asterisks depict $p<0.05$ as determined by a two-way ANOVA followed by Sidak's multiple comparison test (E) or a one-way ANOVA followed by Dunnet's multiple comparison test (F).

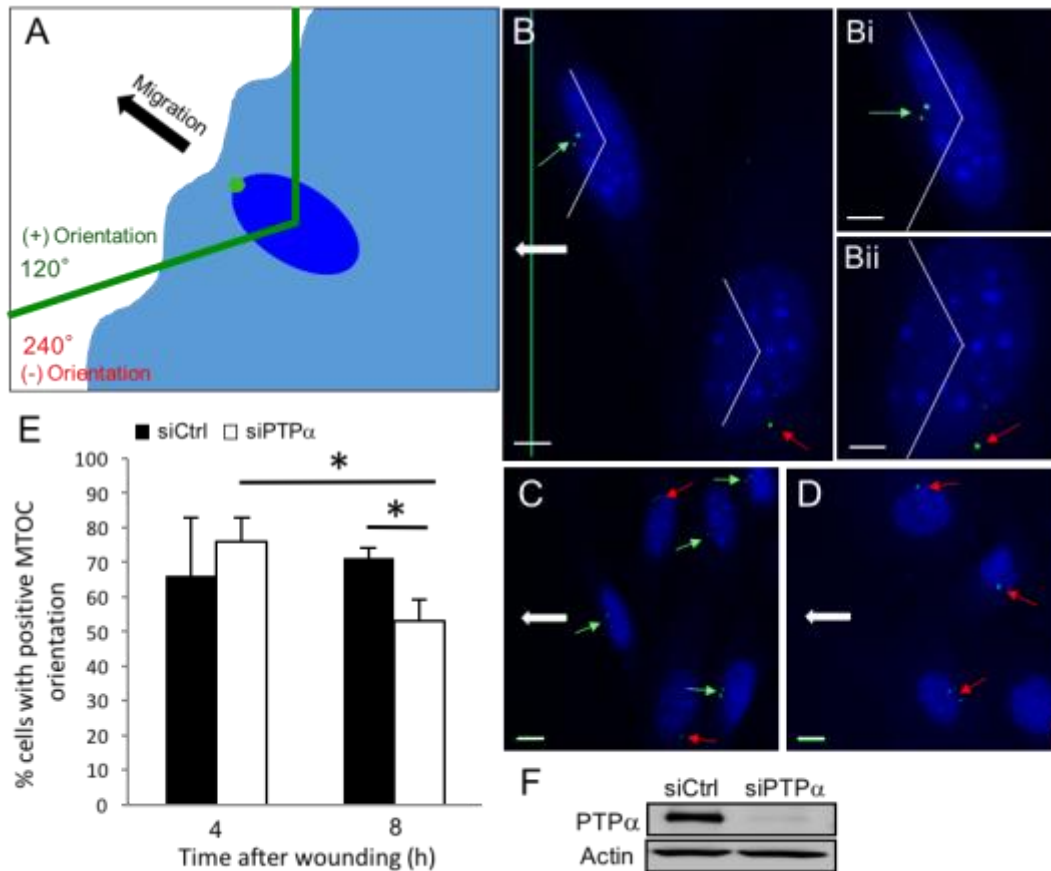


Figure 4.7 Microtubule organizing centers (MTOCs) improperly orient in PTP α -depleted MEFs at the wound edge. To assess cell polarity in PTP α -depleted and control MEFs, the orientation of MTOCs in cells at the wound edge was determined. Cells were transfected with non-targeting control siRNA (siCTRL) or with PTP α -targeting siRNA (siPTP α) and plated on fibronectin-coated (10 μ g/mL) coverslips 48 h prior to wounding. After wounding, cells were incubated in serum-depleted medium, fixed at 4 and 8 h, and stained with fluorescently tagged antibody to γ -tubulin (green) and DAPI (blue). (A) Schematic and (B) representative actual images of orientation scoring. Cells with MTOCs positioned in the leading 120 $^{\circ}$ sector were considered positively oriented and scored as 1 (green arrows). Cells with MTOCs in the trailing 240 $^{\circ}$ sector were not positively oriented and scored as 0 (red arrows). The large arrows indicate the direction of migration and the green line represents the wound edge. (Bi, Bii) larger images of the cells shown in (B). Representative images of (C) siCTRL and (D) siPTP α cells at 8 h. MTOC orientation scoring was quantified using ImageJ. Scale bars represent 10 μ m. (E) The % of cells with a positive MTOC orientation at 4 and 8 h. Bars represent the mean \pm S D., n=3. Asterisks depict p < 0.01, as determined by a two-tailed, equal variance Student's t-test. (F) A representative Western blot showing PTP α and actin expression in lysates of siCTRL and siPTP α cells.

Table 4.1 Focal adhesion characteristics and cell migration properties of MEFs. Summary of the focal adhesion characteristics (Chapter 3) and cell migration properties (Chapter 4) of each MEF cell line. Asterisks depict previously reported values from wound healing assays (Zeng et al., 2003) and Transwell migration assays (Chen et al., 2006b).

Cell Lines	Focal Adhesion Characteristics	Migration (%)		Directionality (μm)		Polarity (%)	
		Wound-Healing	Transwell	Total Length	Net Length	4h	8h
WT601	Thin, elongated, evenly distributed, rapid turnover	100*	100*	---	---	---	---
KO595	Thick, aggregated, impaired turnover	55*	65*	---	---	---	---
WT2	Thin, thick, elongated, aggregated, impaired turnover	100	100	262 \pm 50	188 \pm 26	---	---
KO8	Thin, thick, elongated, aggregated, no impairment in turnover	81 \pm 24	100 \pm 6	342 \pm 42	205 \pm 35	---	---
siCTRL (WT2)	---	100	---	---	---	66 \pm 17	76 \pm 8
siPTPa (WT2 KD)	---	115 \pm 12	---	---	---	72 \pm 3	53 \pm 6
CRISPR CTRL	Thin, small, linear, proper turnover	100	---	287 \pm 12	218 \pm 18	---	---
CRISPR Y789F	Thick, aggregated, no impairment in turnover	127 \pm 20	---	277 \pm 45	214 \pm 40	---	---

Chapter 5: General Discussion

5.1 PTP α in integrin-mediated focal adhesion dynamics and SFK phosphorylation

My findings from this study indicate that the newly generated MEFs do not demonstrate the PTP α -dependent differences in focal adhesion dynamics and integrin signaling that are characteristic of previously established wild-type and PTP α -null MEF lines. The ability of the WT2 and KO8 MEFs to spread on fibronectin was not dependent on the expression of PTP α . Moreover, no significant reduction in focal adhesion formation or turnover at the peripheral edges of spreading cells was observed in the KO8 MEFs. CRISPR-edited Y798F MEFs did not show a significant reduction in cell spreading, but did display larger, aggregated focal adhesions that were more randomly distributed at the cell periphery, a feature characteristic of the KO595 MEFs.

The absence of PTP α -mediated differences in cell spreading and focal adhesion formation was unexpected as previous studies found that PTP α expression is required for fibronectin-induced cell spreading in MEFs (Chen et al., 2006b; Herrera Abreu et al., 2008; Su et al., 1999; von Wichert et al., 2003; Zeng et al., 2003). Formerly, the reduction in cell spreading was concomitant with decreased actin stress fiber assembly, and reduced focal adhesion formation around the cell periphery (Chen et al., 2006b; Herrera Abreu et al., 2008; Su et al., 1999; von Wichert et al., 2003; Zeng et al., 2003). Reintroduction of PTP α but not mutated PTP α -Y789F, to PTP α -null MEFs was sufficient to remediate the defects in cell spreading, actin assembly, and focal adhesion formation elucidating PTP α expression, and more specifically

PTP α phosphorylation, as a key event in these processes (Chen et al., 2006b; Herrera Abreu et al., 2008; Su et al., 1999).

PTP α dephosphorylates SFKs at Tyr527 upon integrin engagement, which activates Src (Chen et al., 2006b; Harder et al., 1998; Ponniah et al., 1999; Su et al., 1999; von Wichert et al., 2003; Zeng et al., 2003). Upon PTP α -mediated Src activation, Src and FAK interact in a complex, leading to maximal FAK phosphorylation (Ruest et al., 2000; Schlaepfer et al., 2004; Sieg et al., 2000; Toutant et al., 2002). My investigation of the molecular response of WT2 and KO8 MEFs to integrin stimulation demonstrated that the C-terminal phosphorylation of Src (pSrc527) was substantially dephosphorylated in the WT601, and surprisingly, also in the KO8 MEFs. In addition, the KO8 MEFs did not show a decrease in FAK-Tyr397 phosphorylation in contrast to WT2 MEFs.

Many studies have previously demonstrated an extensive reduction in Src-Tyr527 phosphorylation in WT MEFs compared to PTP α -null MEFs, in response to integrin stimulation (Chen et al., 2006b; Harder et al., 1998; Ponniah et al., 1999; Su et al., 1999; von Wichert et al., 2003; Zeng et al., 2003). Su et al (1999) demonstrated that pTyr, FAK-pTyr, and Cas-pTyr expression was reduced proportional to decreasing levels of PTP α expression, in response to integrin stimulation, with the lowest expression observed in the PTP α -null MEFs (Su et al., 1999). Thus, the inability of the WT2 and KO8 cell lines to recapitulate these well-established PTP α -dependent signaling responses verified that these cells are functionally distinct from those previously reported. Further investigation of the phenotypes of WT2 and KO8 MEFs was necessary to determine if the new cells possess additional abnormalities. Migration is another

fundamental process that has previously been shown to be dependent on PTP α activity and phosphorylation. Therefore, I studied the migration abilities of the newly generated cells next.

5.2 PTP α -dependence in migration ability, directionality, and cell polarity

My investigations revealed that there was no reduction in migration ability of the KO8 MEFs. The KO8 MEFs and WT2 MEFs depleted of PTP α using siRNA both showed migration abilities that were comparable to their respective controls. I investigated PTP α -dependent migration in another cell line to determine whether or not the depletion of PTP α would affect their migration ability. Breast adenocarcinoma cells (MDA-MB-231) depleted of PTP α did not display a significant change in migration compared to the siRNA-treated control, indicating that PTP α does not regulate migration in these cells. The requirement for phosphorylation of PTP α -Tyr789 in migration was assessed using CRISPR-edited CTRL and Y798F MEFs. Wound healing assays showed there was no difference in migration ability between the two cell lines.

The analogous migration abilities of the WT2 and KO8 MEFs provided more evidence to suggest that they were phenotypically distinct from previously studied WT and PTP α KO cell lines in the literature. Previously, KO595 MEFs displayed significantly reduced migration in wound healing and Transwell assays (Chen et al., 2006b; Zeng et al., 2003). In these other studies, re-introduction of mutant PTP α -Y789F to KO595 MEFs did not rescue the migration defects, revealing phosphorylation of Tyr789 to be a critical regulator of migration in MEFs (Chen et al., 2006b). As there were no significant differences in the migration ability of the WT2 and KO8 MEFs, or CTRL and Y789F MEFs, I investigated other factors that contribute to

migration ability, such as cell polarity and directionality, to see if there were other PTP α -dependent effects on migration.

Examination of the directionality of the WT2, KO8, CTRL, and Y789F MEFs in a wound healing assay found a significant difference between the total distance the net distance travelled by the KO8 MEFs, suggesting that these MEFs exhibit impaired directional migration. Analysis of cell polarity in migrating WT2 MEFs depleted of PTP α indicated a significant reduction in polarity after 4 h of migration in comparison to the control. Taken together, these results suggest that PTP α is important for cell polarity and directional movement in the newly generated MEFs, but that other migratory mechanisms in these cells may alter their dependence on PTP α expression for proper migration to occur, as the WT2 and KO8 MEFs display comparable migration irrespective of PTP α expression.

5.3 Potential reasons for discrepancy in results

Although it is clear from my findings that the newly generated WT2/KO8 MEFs are molecularly distinct from the WT601/KO595 MEF cell lines, the reasons for these differences remain uncertain. The WT2 MEFs demonstrate defects in focal adhesion turnover and Src dephosphorylation. In contrast, the KO8 MEFs demonstrate focal adhesion turnover, increased FAK phosphorylation and Src dephosphorylation, and enhanced cell migration compared to that of reported PTP α -null MEFs in the literature. Therefore, the abnormal characteristics of the WT2 and KO8 MEFs do not appear to be specific to one cell type or the other, but may involve irregularities in both cell lines where the WT2 MEFs are not as efficient in promoting PTP α -mediated events, and the KO8 MEFs are not significantly affected by the absence of PTP α .

Here, I discuss some potential reasons for the abnormal characteristics of the WT2 and KO8 MEFs that I have observed.

5.3.1 Spontaneous immortalization of MEFs

The observation that cells have a finite number of divisions before they cease to proliferate, or senesce, was first made by Hayflick (Hayflick, 1965). Cellular senescence can also be induced using chemical agents, by overexpressing tumor suppressors, or manipulating oncogenes (Drayton and Peters, 2002). Fibroblasts cultured *in vitro* show that the decrease in DNA synthesis exhibited by aging cells is concomitant with the shortening of telomeres (Harley et al., 1990). Extended telomere shortening is an important event in the induction of cell senescence and a proliferative crisis that is associated with cellular senescence (Cong et al., 2002). The cells that evade this crisis and persist in culture demonstrate stabilized telomere length, which is usually accompanied by activation of telomerase (Cong et al., 2002). These cells have acquired the ability to proliferate indefinitely, and are referred to as “immortalized”. Additional mechanisms by which cells can evade senescence have since been elucidated and include genomic instability, epigenetic-regulated gene-silencing, DNA damage due to oxidative stress, expression of oncogenes through viruses, inactivation of critical cell cycle regulatory genes such as p53, and overexpression of oncogenic proteins such as c-myc (Fridman and Tainsky, 2008).

The wide use of genetically modified mice to identify the physiological functions of specific genes has propelled the generation of primary and immortalized lines of different cell types, including MEFs, from these mice. Such cell lines are widely accepted experimental tools for the elucidation of the cellular function and molecular mechanism of action of the protein encoded by a specific modified or ablated gene. The gene of interest can be studied by

investigating various characteristics of the mutant MEFs in contrast to wild-type MEFs (Puigserver et al., 1999; Wu et al., 2004a; Xu, 2005). MEFs express integrins that bind components of the extracellular matrix to initiate intracellular signaling (Hynes, 2002; von Wichert et al., 2003; Zaidel-Bar et al., 2004). Thus, MEFs are a standard cell type used to investigate proteins involved in integrin signaling, focal adhesion formation, and cell migration. In fact, MEFs have been instrumental in elucidating the role of FAK, SFKs, paxillin, vinculin, Cas, and many other proteins in focal adhesion assembly, disassembly, and integrin signaling (Carisey and Ballestrem, 2011; Digman et al., 2008; Janostiak et al., 2011; Mitra et al., 2005; Sieg et al., 1999; Webb et al., 2004). MEFs are also commonly used as a feeder layer to support the growth of other cell types, namely embryonic stem cells. Nevertheless, there are limitations to working with these cells. Due to the short lifespan of primary MEFs, they are often immortalized for use in culture. This process requires the introduction of one or several mutations to enable cells to overcome cellular senescence and continue to proliferate.

Immortalization of primary MEFs is achieved by one of two approaches: spontaneously, through serial passaging of cells; or by transformation which involves the expression of an oncogene (Amand et al., 2016). The process of spontaneous immortalization selects cells that develop growth advantages, allowing them to evade the proliferative crisis of primary cells. This subset of primary cells accumulates various genetic mutations that enhance cell proliferation and/or inhibit apoptosis. These cells continue to proliferate following the crisis event, resulting in a genetically heterogeneous population of immortalized MEFs (Fridman and Tainsky, 2008; Xu, 2005). To reduce genetic variability, cell lines can be generated through colonization of a single cell. I did not generate clonal lines of WT or PTP α -null MEFs, but this could be beneficial in future to reduce the inherent variability of a population of spontaneously immortalized cells and

thereby potentially increase experimental reproducibility.

WT and PTP α -null MEFs reported in the literature have been generated using both methods of immortalization. Dr. Sap's laboratory has provided many groups with WT and PTP α -null MEFs (Herrera Abreu et al., 2008; Petrone et al., 2003; Rajshankar et al., 2013; von Wichert et al., 2003). These cells were generated using both spontaneous immortalization and transformation using polyoma large T antigen (Su et al., 1999). Other labs have utilized WT and PTP α -null MEFs transformed using Simian Virus-40 large tumor-antigen (SV40) (Wang et al., 2014). Additionally, the depletion or overexpression of PTP α has been investigated in human colon cancer (SW480) cells, NIH 3T3 fibroblasts, epidermoid carcinoma (A431) cells and human embryonic kidney (293) cells to understand the role of PTP α in migration and integrin signaling (den Hertog et al., 1993; Harder et al., 1998; Herrera Abreu et al., 2008; Krndija et al., 2010; Rajshankar et al., 2013; Wang et al., 2014). In general, experimental findings involving PTP α have been verified in at least two separate cell lines.

Due to the genetic heterogeneity of spontaneously immortalized MEFs, it can be difficult to compare experimental results between wild-type and mutant MEFs, despite simultaneous generation of the cell lines (Xu, 2005). In regard to my findings, mutations and/or alterations in signaling molecules which regulate cell migration may be able to compensate for the absence of PTP α , thereby allowing the KO8 MEFs to migrate 'normally' despite the lack of PTP α . Rac, Rho, and Cdc42 are a few examples of important proteins involved in the cycle of cell protrusion, contraction, and retraction that govern the process of cell migration (Ridley et al., 2003). Thus changes in expression in any of these proteins or in other components of their signaling pathways may result in altered cell migration. In addition, PTP α plays a key role in

mediating the phosphorylation of cortactin, a substrate of Src that is involved in the organization of the actin cytoskeleton (Truffi et al., 2014). Truffi and colleagues showed that a phosphomimetic cortactin mutant can partially recover the defects in F-actin organization observed in PTP α -depleted cells. A mutation in cortactin, or in another protein involved in cortactin regulation or signaling, is an example of a potential compensatory mechanism that could promote the organization of actin and subsequent cell migration in PTP α KO8 MEFs.

Spontaneous mutations in genes encoding one or more focal adhesion signaling proteins could also interfere with the PTP α -dependent characteristics of MEFs. Src and FAK are important mediators of focal adhesion formation and signaling pathways and closely interact with PTP α in integrin-mediated adhesions. Therefore, mutations to these proteins could significantly change the phenotype of a cell. For example, a mutation affecting Src activity in the WT2 MEFs may involve a sustained increase in phosphorylation at Tyr527 despite the activity of PTP α in dephosphorylating this site, which could in turn result in a decrease in focal adhesion formation and/or signaling and cell migration. FAK-null MEFs display larger focal adhesions and decreased cell migration (Ilic et al., 1995; Sieg et al., 1999), thus dysregulation of FAK activity is one possibility that could account for the unexpected migration characteristics of the WT2 or KO8 MEFs.

BCR-ABL is a tyrosine kinase that is constitutively active in chronic and acute leukemias, and has been implicated in mechanisms involving alteration of cell adhesion, such as the Ras-MAPK and PI3K pathways (Wong and Witte, 2004). c-Abl is the proto-oncogene of BCR-ABL, and has been associated with promoting immortalization of MEFs (Zhang et al., 2013). Abl is a tyrosine kinase that is involved in IGF-1-mediated phosphorylation of PTP α at

Tyr789 (Khanna et al., 2015). A mutation in a kinase such as Abl, which is involved in integrin-proximal events that induce cellular migration, has the potential to alter the phosphorylation of other targets involved in cell migration in the absence of PTP α .

While the above are a few examples, there are many possible alterations that could occur during spontaneous immortalization of the WT2 and KO8 MEFs that could affect integrin or other signaling pathways and the migration abilities of these cells.

5.3.2 Dissection and culture of primary MEFs

Many different protocols in the literature describe the culture conditions used to immortalize MEFs. The protocol that was used to generate the WT2 and KO8 MEFs stresses that the primary or immortalized cells must never be maintained at an over-confluent density (Xu, 2005). This guideline is based on observations that confluent MEFs in culture begin to differentiate, and that high density culture of MEFs over the long-term promotes cellular transformation (Aaronson and Todaro, 1968). During the immortalization of WT2 and KO8 MEFs, cells were cultured using caution to never reach over-confluence, which occasionally included passaging cells that were not yet confluent but would be over-confluent by the next morning. However, other immortalization methods recommend passaging the MEFs every 3-4 days, regardless of the confluence of the monolayer. In fact, spontaneously immortalized MEFs from WT and PTP α -null mice were generated by others by passaging the cells every 3 days and plating them at the same density each time until the crisis had been overcome (Su et al., 1999). Perhaps the WT2 and KO8 MEFs were maintained at lower densities than the previously generated WT601/KO595 MEFs, giving rise to variation in cell differentiation, genetic

mutations, or cell-contact inhibition, which may account for the molecular and functional differences between the two cell lines.

The tryptic digestion of the WT2 and KO8 mouse embryos included part of the lower head that was devoid of the brain and eyes, as these latter tissues contain more differentiated cells at E14.5. It is possible, however, that the part of the head included in the dissection nevertheless contained other differentiated cells, possibly resulting in cell populations that did not contain only fibroblasts. This could also lead to differences between the WT2 and KO8 MEFs, as well as between the counterpart WT2 and WT601 and the KO8 and KO595 cell lines.

5.3.3 Epithelial to mesenchymal transition

Epithelial-mesenchymal transition (EMT) is a process by which an epithelial cell can undergo molecular changes to exhibit a more mesenchymal-like cell phenotype (Kalluri and Weinberg, 2009). This process is referred to as a “transition” to represent the plasticity of the process, as cells can also undergo the reverse process of mesenchymal to epithelial transition (MET). A cell undergoing this transition process can be thought of as representing a spectrum of characteristics, rather than as a strictly epithelial or strictly mesenchymal cell. In other words, cells can express markers characteristic of their original type, while at the same time expressing new markers of the cell type they are transitioning into (Kalluri and Weinberg, 2009). Cells in specific stages of embryogenesis and organ development exhibit plasticity, allowing them to move back and forth between epithelial and mesenchymal-like phenotypes via EMT and MET transitions (Kalluri and Weinberg, 2009). The process of EMT has been implicated in tissue repair, responses to inflammation and pathological stresses, and during neoplasia and metastasis.

During these physiological and pathological events, cells that undergo EMT can become more migratory and invasive (Kalluri and Weinberg, 2009).

Although fibroblasts are mesenchymal cells by nature, they are migratory, but not inherently invasive. This means there is potential for the fibroblasts to become more aggressive in their migratory abilities, and this could theoretically occur in cells under stress such as those undergoing immortalization. A transition in the KO8 fibroblasts to any degree on the EMT spectrum could result in increased migratory capability. Conversely, transition of WT2 MEFs to a more epithelial-like phenotype could produce a decrease in migration ability.

An investigation of the role of PTP α in the migration of mammary epithelial (10A.B2) cells has recently determined that PTP α depletion results in increased cell migration in response to ErbB2 activation (Boivin et al., 2013). In these cells, the oncoprotein ErbB2 displayed a prolonged association with Grb7 and an increased interaction with β -integrin-rich complexes in the absence of PTP α that promoted cell motility. In response to ErbB2 activation, PTP α -depleted cells also demonstrated increased phosphorylation of FAK-Tyr407 which recruited vinculin and initiated the formation of a vinculin-FAK complex (Boivin et al., 2013). These findings suggest that mutations or dysregulation of signaling pathways that PTP α may not be directly involved in could potentially effect cell migration irrespective of PTP α expression. Changes in PTP α expression have been shown to alter the integrity of the cell-cell adherens junctions in epithelial cells (Truffi et al., 2014). Dysregulation of cell-cell contact could also lead to changes in the migration abilities of the WT2 or KO8 MEFs. In relation to my unexpected findings, it is possible that a mutation to a critical signaling protein, or a change in

the regulation of a signaling pathway involved in migration, could be compensating for the defective migration that would otherwise be apparent in the KO8 MEFs.

If desired, future studies could investigate epithelial *vs.* mesenchymal marker expression or the integrity of adherens junctions in the newly generated cells. In addition, techniques such as RNA sequencing, mass spectrometry, and protein microarrays could be used to investigate and compare the expression of focal adhesion signaling proteins or proteins involved in cell migration in the WT2 and KO8 MEFs in comparison to the WT601 MEFs. A global analysis of the proteome might enable a rapid, comprehensive understanding of the aberrant characteristics of the WT2 and KO8 MEFs.

5.3.4 MDA-MB-231 cell migration

MDA-MB-231 cells were derived from a human breast adenocarcinoma. Although these cancerous cells display an invasive phenotype, they are derived from epithelial tissue and exhibit an epithelial morphology. As PTP α -dependent migration in MDA-MB-231 cells is a novel area of research, it is possible that as in the 10A.B2 mammary epithelial cells, PTP α depletion could have unexpected effects on migration of these cells. The ErbB2-Grb7 interaction would be an ideal area to investigate in the MDA-MB-231 cells. Furthermore, understanding how PTP α regulates focal adhesion proteins and cellular migration pathways in MDA-MB-231 cells could provide insight into the role of PTP α in migration of these cells and verify or challenge my findings.

A pitfall of my investigation of MDA-MB-231 migration was the decrease in migration shown by the siCTRL MDA-MB-231 cell population. It is thus possible that any reduction in migratory ability resulting from the siRNA-mediated depletion of PTP α was masked by the up to

25% reduction in migration ability of the counterpart siCTRL cells (compared to the Parental cells). Other non-targeting control siRNAs should be tested to identify those that do not affect migration, and at least two of these could be used in future studies.

5.3.5 CRISPR/Cas off-target effects

The CRISPR/Cas9 gene editing system has become a widely-used technique for studying gene function, however there are important limitations to its efficacy due to the high frequency of off-target effects. The target DNA is specified by the first ~20 nucleotides of the single-guide RNA (sgRNA), which are complimentary to the target DNA (Zhang et al., 2015). This is followed by the 3' end of the guide RNA, the PAM sequence, which also provides specificity for the target. Off-target cleavage of the DNA can occur when there are as little as 3-5 base pair mismatches in the PAM sequence (Zhang et al., 2015). Furthermore, various structures of guideRNA can affect on-target and off-target site cleavage (Hsu et al., 2013). Current studies are working on increasing the sgRNA specificity without diminishing the on-target efficacy but have yet to produce consistent results (Zhang et al., 2015). Methods of off-target detection are available, and could be used to investigate off-target sites of the CRISPR-edited MEFs. For example, GUIDE-Seq is a sequencing technique that identifies genome-wide off-target cleavage by nucleases of CRISPR/Cas9 (Tsai et al., 2015). In addition, deep sequencing has also been used to measure off-target mutations that occur at very low frequencies (Cho et al., 2014). Just as the spontaneous immortalization process can introduce mutations that can compensate for or dominate the phenotype of PTP α -null MEFs, mutations in CRISPR gene editing affecting proteins that regulate cell migration pathways or PTP α -interacting proteins could contribute to the unexpected phenotype of the Y789F MEFs.

5.4 Retrospective experimental directions

The results of this study indicate that there are fundamental problems with the newly generated WT2 and KO8 MEFs. Since established lines of PTP α -null MEFs from our lab and others demonstrated robust reductions in focal adhesion formation and cell migration, the majority of this study unfortunately involved verifying that the peculiar findings in these cells were real, and not the result of technical inexperience. Since I have established that there are no significant differences between the WT2 and KO8 MEFs in key integrin signaling pathways and migration parameters, future directions could include a more detailed molecular analysis of these cells. In addition to studying integrin-induced FAK and SFK phosphorylation and activation, one might look at other important focal adhesion proteins such as paxillin, Cas, Crk, vinculin and BCAR3/Grb2 that may display dysregulated expression or phosphorylation in comparison to established WT and PTP α -null cells.

In retrospect, there are some important experimental and practical considerations that would have facilitated this study. The experience that I have acquired in the lab may have allowed me to accept my data earlier and acknowledge that the newly generated MEFs exhibited atypical behaviors. This would have enabled me to switch my focus to interpretation of the results rather than aiming to perfect the experimental techniques. I would now include side-by-side comparisons of the newly generated MEFs with the established WT601/KO595 MEFs as soon as unexpected results with the former cell lines emerged, as this is what ultimately led me to conclude that these cell line pairs were fundamentally distinct. I would also initiate and conduct a more comprehensive investigation of the molecular responses to integrin stimulation in the WT2 and KO8 MEFs as this was an objective way to look at the mechanistic differences

between the new cell lines and others that have been well characterized by our laboratory and others (Chen et al., 2006b; Herrera Abreu et al., 2008; Su et al., 1999; von Wichert et al., 2003; Zeng et al., 2003). In addition, integrin-mediated signaling could be investigated in primary WT and PTP α -null MEFs prior to immortalization. This would allow the detection of abnormal signaling responses that are not due to the immortalization procedure and might eliminate many additional steps later on in the experimental analysis.

New lines of WT and KO MEFs would be generated and characterized if this study were to be continued. Generation of new WT and KO-PTP α MEFs should incorporate different immortalization techniques to ensure the generation of cells that are consistent with the established WT601/KO595 MEFs and similar MEF lines reported in the literature. Immortalization by overexpression of an oncogene has been elucidated as a robust method of immortalization. Transformation using the well-characterized oncogene, SV40, produced MEFs with high viability and faster doubling rates, in comparison to serially passaged MEFs (Amand et al., 2016). However, it should be noted that the SV40 transformed cells also have limitations, as SV40 inactivates tumor suppressor proteins and could lead to changes in phenotype or cellular metabolism that distort certain experimental results (Amand et al., 2016). However, the McCulloch group has studied PTP α -dependent signaling mechanisms in WT and PTP α -null MEFs that were immortalized using a replication-defective, recombinant retrovirus that expressed SV40 (Wang et al., 2014). These SV40 transformed cells demonstrated established PTP α -dependent characteristics, including the presence of “supermature” adhesions in PTP α -null MEFs, suggesting that this immortalization method might be a valuable alternative to spontaneous immortalization and would be appropriate for my study.

As another independent experimental model, I would also work with commercially available, immortalized NIH 3T3 MEFs. PTP α -depleted NIH 3T3 cells exhibit a reduction in focal adhesion number (Rajshankar et al., 2013). In addition, NIH 3T3 cells that were genetically modified to express HA-tagged WT and Y789F PTP α also demonstrated a reduction in FAK, Src, vinculin, and paxillin in focal adhesions of the PTP α -Y789F NIH 3T3 cells when stimulated with IL-1 β (Rajshankar et al., 2013). These findings suggest that NIH 3T3 cells respond to PTP α depletion and Y789F mutation with reductions in focal adhesion formation and signaling, and thus would be a satisfactory cell line to use for my investigations. Cells could be transiently depleted of PTP α using siRNA, or stable PTP α -knockdown NIH 3T3 cell lines could be created using lentiviral-mediated introduction of PTP α -directed shRNAs. The mutant PTP α -Y789F could be transiently expressed in PTP α -knockdown cells using adenoviral infection, or stably expressed using HA-tagged PTP α -Y789F under the control of a doxycycline sensitive repressor (Rajshankar et al., 2013). Using the well-characterized NIH 3T3 cell line would ensure that experimental observations were the result of PTP α -dependent mechanisms and not due to unknown mutations that occurred in the immortalization process or off-target effects of CRISPR gene editing.

5.5 Conclusion

The results of this study have clearly shown that the newly generated WT2 and KO8 MEFs are phenotypically and molecularly distinct from the WT and PTP α KO MEFs that our lab and others have previously characterized. The mechanisms underlying the variation are unknown, but could include heterozygous cell populations arising from the dissection protocol

and/or mutations acquired or arising from culture conditions during spontaneous immortalization. Thus, future studies of the PTP α -dependent regulation of focal adhesion dynamics and turnover, as well as polarity and directionality, should include the generation of new lines of WT and PTP α KO MEFs. Key integrin signaling responses at the molecular and cellular levels should be verified to be consistent with the well-established responses of the WT vs. PTP α KO MEFs prior to further investigations.

Chapter 6: Bibliography

- Aaronson, S.A., and G.J. Todaro. 1968. Development of 3T3-like lines from Balb-c mouse embryo cultures: transformation susceptibility to SV40. *J Cell Physiol.* 72:141-148.
- Abassi, Y.A., M. Rehn, N. Ekman, K. Alitalo, and K. Vuori. 2003. p130Cas Couples the tyrosine kinase Bmx/Etk with regulation of the actin cytoskeleton and cell migration. *J Biol Chem.* 278:35636-35643.
- Alonso, A., J. Sasin, N. Bottini, I. Friedberg, I. Friedberg, A. Osterman, A. Godzik, T. Hunter, J. Dixon, and T. Mustelin. 2004. Protein tyrosine phosphatases in the human genome. *Cell.* 117:699-711.
- Amand, M. M., J.A. Hanover, and J. Shiloach. 2016. A comparison of strategies for immortalizing mouse embryonic fibroblasts. *J Biol Methods.* 3.2:e41
- Andersen, J.N., O.H. Mortensen, G.H. Peters, P.G. Drake, L.F. Iversen, O.H. Olsen, P.G. Jansen, H.S. Andersen, N.K. Tonks, and N.P. Moller. 2001. Structural and evolutionary relationships among protein tyrosine phosphatase domains. *Mol Cell Biol.* 21:7117-7136.
- Ardini, E., R. Agresti, E. Tagliabue, M. Greco, P. Aiello, L.T. Yang, S. Menard, and J. Sap. 2000. Expression of protein tyrosine phosphatase alpha (RPTPalpha) in human breast cancer correlates with low tumor grade, and inhibits tumor cell growth in vitro and in vivo. *Oncogene.* 19:4979-4987.
- Arias-Salgado, E.G., S. Lizano, S.J. Shattil, and M.H. Ginsberg. 2005. Specification of the direction of adhesive signaling by the integrin beta cytoplasmic domain. *J Biol Chem.* 280:29699-29707.
- Arregui, C.O., J. Balsamo, and J. Lilien. 1998. Impaired integrin-mediated adhesion and signaling in fibroblasts expressing a dominant-negative mutant PTP1B. *J Cell Biol.* 143:861-873.
- Balaban, N.Q., U.S. Schwarz, D. Riveline, P. Goichberg, G. Tzur, I. Sabanay, D. Mahalu, S. Safran, A. Bershadsky, L. Addadi, and B. Geiger. 2001. Force and focal adhesion assembly: a close relationship studied using elastic micropatterned substrates. *Nat Cell Biol.* 3:466-472.
- Ballestrem, C., B. Hinz, B.A. Imhof, and B. Wehrle-Haller. 2001. Marching at the front and dragging behind: differential alphaVbeta3-integrin turnover regulates focal adhesion behavior. *J Cell Biol.* 155:1319-1332.
- Bellis, S.L., J.T. Miller, and C.E. Turner. 1995. Characterization of tyrosine phosphorylation of paxillin in vitro by focal adhesion kinase. *J Biol Chem.* 270:17437-17441.

- Berndt, A., X. Luo, F.D. Bohmer, and H. Kosmehl. 1999. Expression of the transmembrane protein tyrosine phosphatase RPTPalpha in human oral squamous cell carcinoma. *Histochem Cell Biol.* 111:399-403.
- Birge, R.B., J.E. Fajardo, C. Reichman, S.E. Shoelson, Z. Songyang, L.C. Cantley, and H. Hanafusa. 1993. Identification and characterization of a high-affinity interaction between v-Crk and tyrosine-phosphorylated paxillin in CT10-transformed fibroblasts. *Mol Cell Biol.* 13:4648-4656.
- Blanchetot, C., L.G. Tertoolen, J. Overvoorde, and J. den Hertog. 2002. Intra- and intermolecular interactions between intracellular domains of receptor protein-tyrosine phosphatases. *J Biol Chem.* 277:47263-47269.
- Bodrikov, V., V. Sytnyk, I. Leshchyn'ska, J. den Hertog, and M. Schachner. 2008. NCAM induces CaMKIIalpha-mediated RPTPalpha phosphorylation to enhance its catalytic activity and neurite outgrowth. *J Cell Biol.* 182:1185-1200.
- Boivin, B., F. Chaudhary, B.C. Dickinson, A. Haque, S.C. Pero, C.J. Chang, and N.K. Tonks. 2013. Receptor protein-tyrosine phosphatase alpha regulates focal adhesion kinase phosphorylation and ErbB2 oncoprotein-mediated mammary epithelial cell motility. *J Biol Chem.* 288:36926-36935.
- Bouton, A.H., R.B. Riggins, and P.J. Bruce-Staskal. 2001. Functions of the adapter protein Cas: signal convergence and the determination of cellular responses. *Oncogene.* 20:6448-6458.
- Brindle, N.P., M.R. Holt, J.E. Davies, C.J. Price, and D.R. Critchley. 1996. The focal-adhesion vasodilator-stimulated phosphoprotein (VASP) binds to the proline-rich domain in vinculin. *Biochem J.* 318 (Pt 3):753-757.
- Brown, M.C., J.A. Perrotta, and C.E. Turner. 1996. Identification of LIM3 as the principal determinant of paxillin focal adhesion localization and characterization of a novel motif on paxillin directing vinculin and focal adhesion kinase binding. *J Cell Biol.* 135:1109-1123.
- Brown, M.C., J.A. Perrotta, and C.E. Turner. 1998. Serine and threonine phosphorylation of the paxillin LIM domains regulates paxillin focal adhesion localization and cell adhesion to fibronectin. *Mol Biol Cell.* 9:1803-1816.
- Brown, M.C., and C.E. Turner. 2002. Roles for the tubulin- and PTP-PEST-binding paxillin LIM domains in cell adhesion and motility. *Int J Biochem Cell Biol.* 34:855-863.
- Brown, M.C., and C.E. Turner. 2004. Paxillin: adapting to change. *Physiol Rev.* 84:1315-1339.
- Brown, M.T., and J.A. Cooper. 1996. Regulation, substrates and functions of src. *Biochim Biophys Acta.* 1287:121-149.

- Buist, A., Y.L. Zhang, Y.F. Keng, L. Wu, Z.Y. Zhang, and J. den Hertog. 1999. Restoration of potent protein-tyrosine phosphatase activity into the membrane-distal domain of receptor protein-tyrosine phosphatase alpha. *Biochemistry*. 38:914-922.
- Burridge, K., C.E. Turner, and L.H. Romer. 1992. Tyrosine phosphorylation of paxillin and pp125FAK accompanies cell adhesion to extracellular matrix: a role in cytoskeletal assembly. *J Cell Biol*. 119:893-903.
- Cabodi, S., M. del Pilar Camacho-Leal, P. Di Stefano, and P. Defilippi. 2010. Integrin signalling adaptors: not only figurants in the cancer story. *Nat Rev Cancer*. 10:858-870.
- Cai, D., L.K. Clayton, A. Smolyar, and A. Lerner. 1999. AND-34, a novel p130Cas-binding thymic stromal cell protein regulated by adhesion and inflammatory cytokines. *J Immunol*. 163:2104-2112.
- Carisey, A., and C. Ballestrem. 2011. Vinculin, an adapter protein in control of cell adhesion signalling. *Eur J Cell Biol*. 90:157-163.
- Carisey, A., R. Tsang, A.M. Greiner, N. Nijenhuis, N. Heath, A. Nazgiewicz, R. Kemkemer, B. Derby, J. Spatz, and C. Ballestrem. 2013. Vinculin regulates the recruitment and release of core focal adhesion proteins in a force-dependent manner. *Curr Biol*. 23:271-281.
- Carragher, N.O., B. Levkau, R. Ross, and E.W. Raines. 1999. Degraded collagen fragments promote rapid disassembly of smooth muscle focal adhesions that correlates with cleavage of pp125(FAK), paxillin, and talin. *J Cell Biol*. 147:619-630.
- Cary, L.A., J.F. Chang, and J.L. Guan. 1996. Stimulation of cell migration by overexpression of focal adhesion kinase and its association with Src and Fyn. *J Cell Sci*. 109 (Pt 7):1787-1794.
- Cary, L.A., D.C. Han, T.R. Polte, S.K. Hanks, and J.L. Guan. 1998. Identification of p130Cas as a mediator of focal adhesion kinase-promoted cell migration. *J Cell Biol*. 140:211-221.
- Case, L.B., M.A. Baird, G. Shtengel, S.L. Campbell, H.F. Hess, M.W. Davidson, and C.M. Waterman. 2015. Molecular mechanism of vinculin activation and nanoscale spatial organization in focal adhesions. *Nat Cell Biol*. 17:880-892.
- Chen, M. 2007. Functional Interactions of Protein Tyrosine Phosphatase Alpha (PTP α) and Src in Mouse Development and Integrin Signaling: Investigation of Double PTP α / Src-Deficient Mice and Cells (Doctoral Dissertation). Retrieved from ScholarBank@NUS
- Chen, H., D.M. Choudhury, and S.W. Craig. 2006a. Coincidence of actin filaments and talin is required to activate vinculin. *J Biol Chem*. 281:40389-40398.
- Chen, H., D.M. Cohen, D.M. Choudhury, N. Kioka, and S.W. Craig. 2005. Spatial distribution and functional significance of activated vinculin in living cells. *J Cell Biol*. 169:459-470.

Chen, M., S.C. Chen, and C.J. Pallen. 2006b. Integrin-induced tyrosine phosphorylation of protein-tyrosine phosphatase- α is required for cytoskeletal reorganization and cell migration. *J Biol Chem.* 281:11972-11980.

Cheng, S.Y., G. Sun, D.D. Schlaepfer, and C.J. Pallen. 2014. Grb2 promotes integrin-induced focal adhesion kinase (FAK) autophosphorylation and directs the phosphorylation of protein tyrosine phosphatase α by the Src-FAK kinase complex. *Mol Cell Biol.* 34:348-361.

Cho, S.W., S. Kim, Y. Kim, J. Kweon, H.S. Kim, S. Bae, and J.S. Kim. 2014. Analysis of off-target effects of CRISPR/Cas-derived RNA-guided endonucleases and nickases. *Genome Res.* 24:132-141.

Chodniewicz, D., and R.L. Klemke. 2004. Regulation of integrin-mediated cellular responses through assembly of a CAS/Crk scaffold. *Biochim Biophys Acta.* 1692:63-76.

Choi, C.K., M. Vicente-Manzanares, J. Zareno, L.A. Whitmore, A. Mogilner, and A.R. Horwitz. 2008. Actin and alpha-actinin orchestrate the assembly and maturation of nascent adhesions in a myosin II motor-independent manner. *Nat Cell Biol.* 10:1039-1050.

Cobb, B.S., M.D. Schaller, T.H. Leu, and J.T. Parsons. 1994. Stable association of pp60src and pp59fyn with the focal adhesion-associated protein tyrosine kinase, pp125FAK. *Mol Cell Biol.* 14:147-155.

Cohen, D.M., H. Chen, R.P. Johnson, B. Choudhury, and S.W. Craig. 2005. Two distinct head-tail interfaces cooperate to suppress activation of vinculin by talin. *J Biol Chem.* 280:17109-17117.

Cohen, D.M., B. Kutscher, H. Chen, D.B. Murphy, and S.W. Craig. 2006. A conformational switch in vinculin drives formation and dynamics of a talin-vinculin complex at focal adhesions. *J Biol Chem.* 281:16006-16015.

Coll, J.L., A. Ben-Ze'ev, R.M. Ezzell, J.L. Rodriguez Fernandez, H. Baribault, R.G. Oshima, and E.D. Adamson. 1995. Targeted disruption of vinculin genes in F9 and embryonic stem cells changes cell morphology, adhesion, and locomotion. *Proc Natl Acad Sci U S A.* 92:9161-9165.

Cong, Y.S., W.E. Wright, and J.W. Shay. 2002. Human telomerase and its regulation. *Microbiol Mol Biol Rev.* 66:407-425, table of contents.

Cote, J.F., C.E. Turner, and M.L. Tremblay. 1999. Intact LIM 3 and LIM 4 domains of paxillin are required for the association to a novel polyproline region (Pro 2) of protein-tyrosine phosphatase-PEST. *J Biol Chem.* 274:20550-20560.

de Virgilio, M., W.B. Kiosses, and S.J. Shattil. 2004. Proximal, selective, and dynamic interactions between integrin α IIb β 3 and protein tyrosine kinases in living cells. *J Cell Biol.* 165:305-311.

Deakin, N.O., and C.E. Turner. 2008. Paxillin comes of age. *J Cell Sci.* 121:2435-2444.

- DeMali, K.A., C.A. Barlow, and K. Burridge. 2002. Recruitment of the Arp2/3 complex to vinculin: coupling membrane protrusion to matrix adhesion. *J Cell Biol.* 159:881-891.
- den Hertog, J., S. Tracy, and T. Hunter. 1994. Phosphorylation of receptor protein-tyrosine phosphatase alpha on Tyr789, a binding site for the SH3-SH2-SH3 adaptor protein GRB-2 in vivo. *EMBO J.* 13:3020-3032.
- den Hertog, J., and T. Hunter. 1996. Tight association of GRB2 with receptor protein-tyrosine phosphatase alpha is mediated by the SH2 and c-terminal SH3 domains. *EMBO J.* 15:3016-3027.
- den Hertog, J., C.E.G.M. Pals, M.P. Peppelenbosch, L.G.J. Tertoolen, S.W. Delaat, and W. Kruijer. 1993. Receptor Protein-Tyrosine Phosphatase-Alpha Activates Pp60(C-Src) and Is Involved in Neuronal Differentiation. *EMBO J.* 12:3789-3798.
- Denu, J.M., D.L. Lohse, J. Vijayalakshmi, M.A. Saper, and J.E. Dixon. 1996. Visualization of intermediate and transition-state structures in protein-tyrosine phosphatase catalysis. *Proc Natl Acad Sci U S A.* 93:2493-2498.
- Digman, M.A., C.M. Brown, A.R. Horwitz, W.W. Mantulin, and E. Gratton. 2008. Paxillin dynamics measured during adhesion assembly and disassembly by correlation spectroscopy. *Biophys J.* 94:2819-2831.
- Donato, D.M., L.M. Ryzhova, L.M. Meenderink, I. Kaverina, and S.K. Hanks. 2010. Dynamics and mechanism of p130Cas localization to focal adhesions. *J Biol Chem.* 285:20769-20779.
- Drayton, S., and G. Peters. 2002. Immortalisation and transformation revisited. *Curr Opin Genet Dev.* 12:98-104.
- Efimov, A., N. Schiefermeier, I. Grigoriev, R. Ohi, M.C. Brown, C.E. Turner, J.V. Small, and I. Kaverina. 2008. Paxillin-dependent stimulation of microtubule catastrophes at focal adhesion sites. *J Cell Sci.* 121:196-204.
- Eimer, W., M. Niermann, M.A. Eppe, and B.M. Jockusch. 1993. Molecular shape of vinculin in aqueous solution. *J Mol Biol.* 229:146-152.
- Felberg, J., and P. Johnson. 1998. Characterization of recombinant CD45 cytoplasmic domain proteins. Evidence for intramolecular and intermolecular interactions. *J Biol Chem.* 273:17839-17845.
- Feller, S.M., G. Posern, J. Voss, C. Kardinal, D. Sakkab, J. Zheng, and B.S. Knudsen. 1998. Physiological signals and oncogenesis mediated through Crk family adapter proteins. *J Cell Physiol.* 177:535-552.
- Fincham, V.J., and M.C. Frame. 1998. The catalytic activity of Src is dispensable for translocation to focal adhesions but controls the turnover of these structures during cell motility. *EMBO J.* 17:81-92.

- Fish, K.N. 2009. Total internal reflection fluorescence (TIRF) microscopy. *Curr Protoc Cytom.* Chapter 12:Unit12 18.
- Fonseca, P.M., N.Y. Shin, J. Brabek, L. Ryzhova, J. Wu, and S.K. Hanks. 2004. Regulation and localization of CAS substrate domain tyrosine phosphorylation. *Cell Signal.* 16:621-629.
- Francis, R., X. Xu, H. Park, C.J. Wei, S. Chang, B. Chatterjee, and C. Lo. 2011. Connexin43 modulates cell polarity and directional cell migration by regulating microtubule dynamics. *PLoS One.* 6:e26379.
- Franco, S.J., and A. Huttenlocher. 2005. Regulating cell migration: calpains make the cut. *J Cell Sci.* 118:3829-3838.
- Fridman, A.L., and M.A. Tainsky. 2008. Critical pathways in cellular senescence and immortalization revealed by gene expression profiling. *Oncogene.* 27:5975-5987.
- Garcia-Guzman, M., F. Dolfi, M. Russello, and K. Vuori. 1999. Cell adhesion regulates the interaction between the docking protein p130(Cas) and the 14-3-3 proteins. *J Biol Chem.* 274:5762-5768.
- Garton, A.J., M.R. Burnham, A.H. Bouton, and N.K. Tonks. 1997. Association of PTP-PEST with the SH3 domain of p130cas; a novel mechanism of protein tyrosine phosphatase substrate recognition. *Oncogene.* 15:877-885.
- Garvalov, B.K., T.E. Higgins, J.D. Sutherland, M. Zettl, N. Scaplehorn, T. Kocher, E. Piddini, G. Griffiths, and M. Way. 2003. The conformational state of Tes regulates its zyxin-dependent recruitment to focal adhesions. *J Cell Biol.* 161:33-39.
- Gasparotto, D., R. Maestro, S. Piccinin, T. Vukosavljevic, L. Barzan, S. Sulfaro, and M. Boiocchi. 1997. Overexpression of CDC25A and CDC25B in head and neck cancers. *Cancer Res.* 57:2366-2368.
- Ginsberg, M.H., X. Du, and E.F. Plow. 1992. Inside-out integrin signalling. *Current opinion in cell biology.* 4:766-771.
- Gotoh, T., D. Cai, X. Tian, L.A. Feig, and A. Lerner. 2000. p130Cas regulates the activity of AND-34, a novel Ral, Rap1, and R-Ras guanine nucleotide exchange factor. *J Biol Chem.* 275:30118-30123.
- Hamadi, A., M. Bouali, M. Dontenwill, H. Stoeckel, K. Takeda, and P. Ronde. 2005. Regulation of focal adhesion dynamics and disassembly by phosphorylation of FAK at tyrosine 397. *J Cell Sci.* 118:4415-4425.
- Hamasaki, K., T. Mimura, N. Morino, H. Furuya, T. Nakamoto, S. Aizawa, C. Morimoto, Y. Yazaki, H. Hirai, and Y. Nojima. 1996. Src kinase plays an essential role in integrin-mediated tyrosine phosphorylation of Crk-associated substrate p130Cas. *Biochem Biophys Res Commun.* 222:338-343.

- Hanks, S.K., L. Ryzhova, N.Y. Shin, and J. Brabek. 2003. Focal adhesion kinase signaling activities and their implications in the control of cell survival and motility. *Front Biosci.* 8:d982-996.
- Harburger, D.S., and D.A. Calderwood. 2009. Integrin signalling at a glance. *J Cell Sci.* 122:159-163.
- Harder, K.W., N.P. Moller, J.W. Peacock, and F.R. Jirik. 1998. Protein-tyrosine phosphatase alpha regulates Src family kinases and alters cell-substratum adhesion. *J Biol Chem.* 273:31890-31900.
- Harley, C.B., A.B. Futcher, and C.W. Greider. 1990. Telomeres shorten during ageing of human fibroblasts. *Nature.* 345:458-460.
- Hayflick, L. 1965. The Limited in Vitro Lifetime of Human Diploid Cell Strains. *Exp Cell Res.* 37:614-636.
- Helfman, D.M., E.T. Levy, C. Berthier, M. Shtutman, D. Rivelino, I. Grosheva, A. Lachish-Zalait, M. Elbaum, and A.D. Bershadsky. 1999. Caldesmon inhibits nonmuscle cell contractility and interferes with the formation of focal adhesions. *Mol Biol Cell.* 10:3097-3112.
- Herrera Abreu, M.T., P.C. Penton, V. Kwok, E. Vachon, D. Shalloway, L. Vidali, W. Lee, C.A. McCulloch, and G.P. Downey. 2008. Tyrosine phosphatase PTPalpha regulates focal adhesion remodeling through Rac1 activation. *Am J Physiol Cell Physiol.* 294:C931-944.
- Honda, H., T. Nakamoto, R. Sakai, and H. Hirai. 1999. p130(Cas), an assembling molecule of actin filaments, promotes cell movement, cell migration, and cell spreading in fibroblasts. *Biochem Biophys Res Commun.* 262:25-30.
- Hotulainen, P., and P. Lappalainen. 2006. Stress fibers are generated by two distinct actin assembly mechanisms in motile cells. *J Cell Biol.* 173:383-394.
- Hsu, P.D., D.A. Scott, J.A. Weinstein, F.A. Ran, S. Konermann, V. Agarwala, Y. Li, E.J. Fine, X. Wu, O. Shalem, T.J. Cradick, L.A. Marraffini, G. Bao, and F. Zhang. 2013. DNA targeting specificity of RNA-guided Cas9 nucleases. *Nat Biotechnol.* 31:827-832.
- Hu, K., L. Ji, K.T. Applegate, G. Danuser, and C.M. Waterman-Storer. 2007. Differential transmission of actin motion within focal adhesions. *Science.* 315:111-115.
- Humphries, J.D., A. Byron, M.D. Bass, S.E. Craig, J.W. Pinney, D. Knight, and M.J. Humphries. 2009. Proteomic analysis of integrin-associated complexes identifies RCC2 as a dual regulator of Rac1 and Arf6. *Sci Signal.* 2:ra51.
- Humphries, J.D., A. Byron, and M.J. Humphries. 2006. Integrin ligands at a glance. *J Cell Sci.* 119:3901-3903.

- Humphries, J.D., P. Wang, C. Streuli, B. Geiger, M.J. Humphries, and C. Ballestrem. 2007. Vinculin controls focal adhesion formation by direct interactions with talin and actin. *J Cell Biol.* 179:1043-1057.
- Humphries, M.J. 1990. The molecular basis and specificity of integrin-ligand interactions. *J Cell Sci.* 97 (Pt 4):585-592.
- Huttelmaier, S., P. Bubeck, M. Rudiger, and B.M. Jockusch. 1997. Characterization of two F-actin-binding and oligomerization sites in the cell-contact protein vinculin. *Eur J Biochem.* 247:1136-1142.
- Huttenlocher, A., and A.R. Horwitz. 2011. Integrins in cell migration. *Cold Spring Harb Perspect Biol.* 3:a005074.
- Hynes, R.O. 2002. Integrins: bidirectional, allosteric signaling machines. *Cell.* 110:673-687.
- Ilic, D., Y. Furuta, S. Kanazawa, N. Takeda, K. Sobue, N. Nakatsuji, S. Nomura, J. Fujimoto, M. Okada, and T. Yamamoto. 1995. Reduced cell motility and enhanced focal adhesion contact formation in cells from FAK-deficient mice. *Nature.* 377:539-544.
- Janostiak, R., J. Brabek, V. Auernheimer, Z. Tatarova, L.A. Lautscham, T. Dey, J. Gemperle, R. Merkel, W.H. Goldmann, B. Fabry, and D. Rosel. 2014a. CAS directly interacts with vinculin to control mechanosensing and focal adhesion dynamics. *Cellular and molecular life sciences : CMLS.* 71:727-744.
- Janostiak, R., A.C. Pataki, J. Brabek, and D. Rosel. 2014b. Mechanosensors in integrin signaling: the emerging role of p130Cas. *Eur J Cell Biol.* 93:445-454.
- Janostiak, R., O. Tolde, Z. Bruhova, M. Novotny, S.K. Hanks, D. Rosel, and J. Brabek. 2011. Tyrosine phosphorylation within the SH3 domain regulates CAS subcellular localization, cell migration, and invasiveness. *Mol Biol Cell.* 22:4256-4267.
- Janssen, M.E., E. Kim, H. Liu, L.M. Fujimoto, A. Bobkov, N. Volkmann, and D. Hanein. 2006. Three-dimensional structure of vinculin bound to actin filaments. *Mol Cell.* 21:271-281.
- Jemc, J., and I. Rebay. 2007. The eyes absent family of phosphotyrosine phosphatases: properties and roles in developmental regulation of transcription. *Annu Rev Biochem.* 76:513-538.
- Jia, Z., D. Barford, A.J. Flint, and N.K. Tonks. 1995. Structural basis for phosphotyrosine peptide recognition by protein tyrosine phosphatase 1B. *Science.* 268:1754-1758.
- Jiang, G., J. den Hertog, and T. Hunter. 2000. Receptor-like protein tyrosine phosphatase alpha homodimerizes on the cell surface. *Mol Cell Biol.* 20:5917-5929.
- Jockusch, B.M., and G. Isenberg. 1981. Interaction of alpha-actinin and vinculin with actin: opposite effects on filament network formation. *Proc Natl Acad Sci U S A.* 78:3005-3009.

- Johnson, R.P., and S.W. Craig. 1994. An intramolecular association between the head and tail domains of vinculin modulates talin binding. *J Biol Chem.* 269:12611-12619.
- Johnson, R.P., and S.W. Craig. 1995. F-actin binding site masked by the intramolecular association of vinculin head and tail domains. *Nature.* 373:261-264.
- Johnson, R.P., and S.W. Craig. 2000. Actin activates a cryptic dimerization potential of the vinculin tail domain. *J Biol Chem.* 275:95-105.
- Kalluri, R., and R.A. Weinberg. 2009. The basics of epithelial-mesenchymal transition. *J Clin Invest.* 119:1420-1428.
- Kanchanawong, P., G. Shtengel, A.M. Pasapera, E.B. Ramko, M.W. Davidson, H.F. Hess, and C.M. Waterman. 2010. Nanoscale architecture of integrin-based cell adhesions. *Nature.* 468:580-584.
- Khanna, R.S., H.T. Le, J. Wang, T.C. Fung, and C.J. Pallen. 2015. The interaction of protein-tyrosine phosphatase alpha (PTPalpha) and RACK1 protein enables insulin-like growth factor 1 (IGF-1)-stimulated Abl-dependent and -independent tyrosine phosphorylation of PTPalpha. *J Biol Chem.* 290:9886-9895.
- Kim, M., C.V. Carman, W. Yang, A. Salas, and T.A. Springer. 2004. The primacy of affinity over clustering in regulation of adhesiveness of the integrin $\{\alpha\}L\{\beta\}_2$. *J Cell Biol.* 167:1241-1253.
- Kim, S.J., and S.E. Ryu. 2012. Structure and catalytic mechanism of human protein tyrosine phosphatase. *BMB Rep.* 45:693-699.
- Kioka, N., K. Ueda, and T. Amachi. 2002. Vinexin, CAP/ponsin, ArgBP2: a novel adaptor protein family regulating cytoskeletal organization and signal transduction. *Cell Struct Funct.* 27:1-7.
- Kiyokawa, E., Y. Hashimoto, T. Kurata, H. Sugimura, and M. Matsuda. 1998. Evidence that DOCK180 up-regulates signals from the CrkII-p130(Cas) complex. *J Biol Chem.* 273:24479-24484.
- Klemke, R.L., J. Leng, R. Molander, P.C. Brooks, K. Vuori, and D.A. Cheresh. 1998. CAS/Crk coupling serves as a "molecular switch" for induction of cell migration. *J Cell Biol.* 140:961-972.
- Klinghoffer, R.A., C. Sachsenmaier, J.A. Cooper, and P. Soriano. 1999. Src family kinases are required for integrin but not PDGFR signal transduction. *EMBO J.* 18:2459-2471.
- Kostic, A., and M.P. Sheetz. 2006. Fibronectin rigidity response through Fyn and p130Cas recruitment to the leading edge. *Mol Biol Cell.* 17:2684-2695.
- Kristjansdottir, K., and J. Rudolph. 2004. Cdc25 phosphatases and cancer. *Chem Biol.* 11:1043-1051.

Krndija, D., H. Schmid, J.L. Eismann, U. Lothar, G. Adler, F. Oswald, T. Seufferlein, and G. von Wichert. 2010. Substrate stiffness and the receptor-type tyrosine-protein phosphatase alpha regulate spreading of colon cancer cells through cytoskeletal contractility. *Oncogene*. 29:2724-2738.

Kuo, J.C. 2013. Mechanotransduction at focal adhesions: integrating cytoskeletal mechanics in migrating cells. *J Cell Mol Med*. 17:704-712.

Kuo, J.C., X. Han, C.T. Hsiao, J.R. Yates, 3rd, and C.M. Waterman. 2011. Analysis of the myosin-II-responsive focal adhesion proteome reveals a role for beta-Pix in negative regulation of focal adhesion maturation. *Nat Cell Biol*. 13:383-393.

Kupfer, A., D. Louvard, and S.J. Singer. 1982. Polarization of the Golgi apparatus and the microtubule-organizing center in cultured fibroblasts at the edge of an experimental wound. *Proc Natl Acad Sci U S A*. 79:2603-2607.

Lammers, R., M.M. Lerch, and A. Ullrich. 2000. The carboxyl-terminal tyrosine residue of protein-tyrosine phosphatase alpha mediates association with focal adhesion plaques. *J Biol Chem*. 275:3391-3396.

Le, H.T., L. Maksumova, J. Wang, and C.J. Pallen. 2006. Reduced NMDA receptor tyrosine phosphorylation in PTPalpha-deficient mouse synaptosomes is accompanied by inhibition of four src family kinases and Pyk2: an upstream role for PTPalpha in NMDA receptor regulation. *J Neurochem*. 98:1798-1809.

Lee, C.F., C. Haase, S. Deguchi, and R. Kaunas. 2010. Cyclic stretch-induced stress fiber dynamics - dependence on strain rate, Rho-kinase and MLCK. *Biochem Biophys Res Commun*. 401:344-349.

Lei, G., Xue, S., Chéry, N., Liu, Q., Xu, J., Kwan, C. L., Fu, Y.-P., Lu, Y.-M., Liu, M., Harder, K.W., and Yu, X.-M. 2002. Gain control of N-methyl-d-aspartate receptor activity by receptor-like protein tyrosine phosphatase α . *The EMBO Journal*. 21.12: 2977-2989.

Leung, T., X.Q. Chen, E. Manser, and L. Lim. 1996. The p160 RhoA-binding kinase ROK alpha is a member of a kinase family and is involved in the reorganization of the cytoskeleton. *Mol Cell Biol*. 16:5313-5327.

Ley, K., J. Rivera-Nieves, W.J. Sandborn, and S. Shattil. 2016. Integrin-based therapeutics: biological basis, clinical use and new drugs. *Nat Rev Drug Discov*. 15:173-183.

Li, E., D.G. Stupack, S.L. Brown, R. Klemke, D.D. Schlaepfer, and G.R. Nemerow. 2000. Association of p130CAS with phosphatidylinositol-3-OH kinase mediates adenovirus cell entry. *J Biol Chem*. 275:14729-14735.

- Li, X., and H.S. Earp. 1997. Paxillin is tyrosine-phosphorylated by and preferentially associates with the calcium-dependent tyrosine kinase in rat liver epithelial cells. *J Biol Chem.* 272:14341-14348.
- Liang, F., S.Y. Lee, J. Liang, D.S. Lawrence, and Z.Y. Zhang. 2005. The role of protein-tyrosine phosphatase 1B in integrin signaling. *J Biol Chem.* 280:24857-24863.
- Lietha, D., X. Cai, D.F. Ceccarelli, Y. Li, M.D. Schaller, and M.J. Eck. 2007. Structural basis for the autoinhibition of focal adhesion kinase. *Cell.* 129:1177-1187.
- Lim, K.L., P.R. Kolatkar, K.P. Ng, C.H. Ng, and C.J. Pallen. 1998. Interconversion of the kinetic identities of the tandem catalytic domains of receptor-like protein-tyrosine phosphatase PTPalpha by two point mutations is synergistic and substrate-dependent. *J Biol Chem.* 273:28986-28993.
- Liu, F., D.E. Hill, and J. Chernoff. 1996. Direct binding of the proline-rich region of protein tyrosine phosphatase 1B to the Src homology 3 domain of p130(Cas). *J Biol Chem.* 271:31290-31295.
- Lu, C., F. Wu, W. Qiu, and R. Liu. 2013. P130Cas substrate domain is intrinsically disordered as characterized by single-molecule force measurements. *Biophys Chem.* 180-181:37-43.
- Madhurantakam, C., E. Rajakumara, P.A. Mazumdar, B. Saha, D. Mitra, H.G. Wiker, R. Sankaranarayanan, and A.K. Das. 2005. Crystal structure of low-molecular-weight protein tyrosine phosphatase from Mycobacterium tuberculosis at 1.9-A resolution. *J Bacteriol.* 187:2175-2181.
- Maekawa, M., T. Ishizaki, S. Boku, N. Watanabe, A. Fujita, A. Iwamatsu, T. Obinata, K. Ohashi, K. Mizuno, and S. Narumiya. 1999. Signaling from Rho to the actin cytoskeleton through protein kinases ROCK and LIM-kinase. *Science.* 285:895-898.
- Magdalena, J., T.H. Millard, and L.M. Machesky. 2003. Microtubule involvement in NIH 3T3 Golgi and MTOC polarity establishment. *J Cell Sci.* 116:743-756.
- Maksumova, L., Y. Wang, N.K. Wong, H.T. Le, C.J. Pallen, and P. Johnson. 2007. Differential function of PTPalpha and PTPalpha Y789F in T cells and regulation of PTPalpha phosphorylation at Tyr-789 by CD45. *J Biol Chem.* 282:20925-20932.
- Michaelis, U.R. 2014. Mechanisms of endothelial cell migration. *Cellular and molecular life sciences : CMLS.* 71:4131-4148.
- Mitra, S.K., D.A. Hanson, and D.D. Schlaepfer. 2005. Focal adhesion kinase: in command and control of cell motility. *Nat Rev Mol Cell Biol.* 6:56-68.
- Mitra, S.K., and D.D. Schlaepfer. 2006. Integrin-regulated FAK-Src signaling in normal and cancer cells. *Current opinion in cell biology.* 18:516-523.

- Nakamoto, T., R. Sakai, H. Honda, S. Ogawa, H. Ueno, T. Suzuki, S. Aizawa, Y. Yazaki, and H. Hirai. 1997. Requirements for localization of p130cas to focal adhesions. *Mol Cell Biol.* 17:3884-3897.
- Nicholson-Dykstra, S., H.N. Higgs, and E.S. Harris. 2005. Actin dynamics: growth from dendritic branches. *Curr Biol.* 15:R346-357.
- Niediek, V., S. Born, N. Hampe, N. Kirchgessner, R. Merkel, and B. Hoffmann. 2012. Cyclic stretch induces reorientation of cells in a Src family kinase- and p130Cas-dependent manner. *Eur J Cell Biol.* 91:118-128.
- Okabe, Y., T. Sano, and S. Nagata. 2009. Regulation of the innate immune response by threonine-phosphatase of Eyes absent. *Nature.* 460:520-524.
- Okada, M., and H. Nakagawa. 1989. A protein tyrosine kinase involved in regulation of pp60c-src function. *J Biol Chem.* 264:20886-20893.
- Owen, J.D., P.J. Ruest, D.W. Fry, and S.K. Hanks. 1999. Induced focal adhesion kinase (FAK) expression in FAK-null cells enhances cell spreading and migration requiring both auto- and activation loop phosphorylation sites and inhibits adhesion-dependent tyrosine phosphorylation of Pyk2. *Mol Cell Biol.* 19:4806-4818.
- Palecek, S.P., A. Huttenlocher, A.F. Horwitz, and D.A. Lauffenburger. 1998. Physical and biochemical regulation of integrin release during rear detachment of migrating cells. *J Cell Sci.* 111 (Pt 7):929-940.
- Pallen, C.J. 2003. Protein tyrosine phosphatase alpha (PTPalpha): a Src family kinase activator and mediator of multiple biological effects. *Curr Top Med Chem.* 3:821-835.
- Papusheva, E., F. Mello de Queiroz, J. Dalous, Y. Han, A. Esposito, E.A. Jares-Erijmanxa, T.M. Jovin, and G. Bunt. 2009. Dynamic conformational changes in the FERM domain of FAK are involved in focal-adhesion behavior during cell spreading and motility. *J Cell Sci.* 122:656-666.
- Parsons, J.T., A.R. Horwitz, and M.A. Schwartz. 2010. Cell adhesion: integrating cytoskeletal dynamics and cellular tension. *Nat Rev Mol Cell Biol.* 11:633-643.
- Petit, V., B. Boyer, D. Lentz, C.E. Turner, J.P. Thiery, and A.M. Valles. 2000. Phosphorylation of tyrosine residues 31 and 118 on paxillin regulates cell migration through an association with CRK in NBT-II cells. *J Cell Biol.* 148:957-970.
- Petrone, A., F. Battaglia, C. Wang, A. Dusa, J. Su, D. Zagzag, R. Bianchi, P. Casaccia-Bonnel, O. Arancio, and J. Sap. 2003. Receptor protein tyrosine phosphatase alpha is essential for hippocampal neuronal migration and long-term potentiation. *EMBO J.* 22:4121-4131.
- Playford, M.P., and M.D. Schaller. 2004. The interplay between Src and integrins in normal and tumor biology. *Oncogene.* 23:7928-7946.

- Plotnikov, S.V., A.M. Pasapera, B. Sabass, and C.M. Waterman. 2012. Force fluctuations within focal adhesions mediate ECM-rigidity sensing to guide directed cell migration. *Cell*. 151:1513-1527.
- Pollard, T.D., and G.G. Borisy. 2003. Cellular motility driven by assembly and disassembly of actin filaments. *Cell*. 112:453-465.
- Polte, T.R., and S.K. Hanks. 1995. Interaction between focal adhesion kinase and Crk-associated tyrosine kinase substrate p130Cas. *Proc Natl Acad Sci U S A*. 92:10678-10682.
- Ponniah, S., D.Z. Wang, K.L. Lim, and C.J. Pallen. 1999. Targeted disruption of the tyrosine phosphatase PTPalpha leads to constitutive downregulation of the kinases Src and Fyn. *Curr Biol*. 9:535-538.
- Ponti, A., M. Machacek, S.L. Gupton, C.M. Waterman-Storer, and G. Danuser. 2004. Two distinct actin networks drive the protrusion of migrating cells. *Science*. 305:1782-1786.
- Pratt, S.J., H. Epple, M. Ward, Y. Feng, V.M. Braga, and G.D. Longmore. 2005. The LIM protein Ajuba influences p130Cas localization and Rac1 activity during cell migration. *J Cell Biol*. 168:813-824.
- Puigserver, P., G. Adelmant, Z. Wu, M. Fan, J. Xu, B. O'Malley, and B.M. Spiegelman. 1999. Activation of PPARgamma coactivator-1 through transcription factor docking. *Science*. 286:1368-1371.
- Rajshankar, D., C. Sima, Q. Wang, S.R. Goldberg, M. Kazembe, Y. Wang, M. Glogauer, G.P. Downey, and C.A. McCulloch. 2013. Role of PTPalpha in the destruction of periodontal connective tissues. *PLoS One*. 8:e70659.
- Reinhard, M., M. Rudiger, B.M. Jockusch, and U. Walter. 1996. VASP interaction with vinculin: a recurring theme of interactions with proline-rich motifs. *FEBS Lett*. 399:103-107.
- Ren, X.D., W.B. Kiosses, D.J. Sieg, C.A. Otey, D.D. Schlaepfer, and M.A. Schwartz. 2000. Focal adhesion kinase suppresses Rho activity to promote focal adhesion turnover. *J Cell Sci*. 113 (Pt 20):3673-3678.
- Richardson, A., R.K. Malik, J.D. Hildebrand, and J.T. Parsons. 1997. Inhibition of cell spreading by expression of the C-terminal domain of focal adhesion kinase (FAK) is rescued by coexpression of Src or catalytically inactive FAK: a role for paxillin tyrosine phosphorylation. *Mol Cell Biol*. 17:6906-6914.
- Ridley, A.J., M.A. Schwartz, K. Burridge, R.A. Firtel, M.H. Ginsberg, G. Borisy, J.T. Parsons, and A.R. Horwitz. 2003. Cell migration: integrating signals from front to back. *Science*. 302:1704-1709.
- Riggins, R.B., L.A. Quilliam, and A.H. Bouton. 2003. Synergistic promotion of c-Src activation and cell migration by Cas and AND-34/BCAR3. *J Biol Chem*. 278:28264-28273.

- Roskoski, R., Jr. 2004. Src protein-tyrosine kinase structure and regulation. *Biochem Biophys Res Commun.* 324:1155-1164.
- Roskoski, R., Jr. 2005. Src kinase regulation by phosphorylation and dephosphorylation. *Biochem Biophys Res Commun.* 331:1-14.
- Rottner, K., A. Hall, and J.V. Small. 1999. Interplay between Rac and Rho in the control of substrate contact dynamics. *Curr Biol.* 9:640-648.
- Ruest, P.J., S. Roy, E. Shi, R.L. Mernaugh, and S.K. Hanks. 2000. Phosphospecific antibodies reveal focal adhesion kinase activation loop phosphorylation in nascent and mature focal adhesions and requirement for the autophosphorylation site. *Cell Growth Differ.* 11:41-48.
- Ruest, P.J., N.Y. Shin, T.R. Polte, X. Zhang, and S.K. Hanks. 2001. Mechanisms of CAS substrate domain tyrosine phosphorylation by FAK and Src. *Mol Cell Biol.* 21:7641-7652.
- Ruoslahti, E., and M.D. Pierschbacher. 1987. New perspectives in cell adhesion: RGD and integrins. *Science.* 238:491-497.
- Sakai, R., A. Iwamatsu, N. Hirano, S. Ogawa, T. Tanaka, H. Mano, Y. Yazaki, and H. Hirai. 1994. A Novel Signaling Molecule, P130, Forms Stable Complexes in-Vivo with V-Crk and V-Src in a Tyrosine Phosphorylation-Dependent Manner. *Embo Journal.* 13:3748-3756.
- Samayawardhena, L.A., and C.J. Pallen. 2008. Protein-tyrosine phosphatase alpha regulates stem cell factor-dependent c-Kit activation and migration of mast cells. *J Biol Chem.* 283:29175-29185.
- Samayawardhena, L.A., and C.J. Pallen. 2010. PTPalpha activates Lyn and Fyn and suppresses Hck to negatively regulate FcepsilonRI-dependent mast cell activation and allergic responses. *J Immunol.* 185:5993-6002.
- Sap, J., P. D'Eustachio, D. Givol, and J. Schlessinger. 1990. Cloning and expression of a widely expressed receptor tyrosine phosphatase. *Proc Natl Acad Sci U S A.* 87:6112-6116.
- Sastry, S.K., P.D. Lyons, M.D. Schaller, and K. Burridge. 2002. PTP-PEST controls motility through regulation of Rac1. *J Cell Sci.* 115:4305-4316.
- Saunders, R.M., M.R. Holt, L. Jennings, D.H. Sutton, I.L. Barsukov, A. Bobkov, R.C. Liddington, E.A. Adamson, G.A. Dunn, and D.R. Critchley. 2006. Role of vinculin in regulating focal adhesion turnover. *Eur J Cell Biol.* 85:487-500.
- Sawada, Y., M. Tamada, B.J. Dubin-Thaler, O. Cherniavskaya, R. Sakai, S. Tanaka, and M.P. Sheetz. 2006. Force sensing by mechanical extension of the Src family kinase substrate p130Cas. *Cell.* 127:1015-1026.

Schaller, M.D., J.D. Hildebrand, J.D. Shannon, J.W. Fox, R.R. Vines, and J.T. Parsons. 1994. Autophosphorylation of the focal adhesion kinase, pp125FAK, directs SH2-dependent binding of pp60src. *Mol Cell Biol.* 14:1680-1688.

Schaller, M.D., and J.T. Parsons. 1995. pp125FAK-dependent tyrosine phosphorylation of paxillin creates a high-affinity binding site for Crk. *Mol Cell Biol.* 15:2635-2645.

Schiller, H.B., C.C. Friedel, C. Boulegue, and R. Fassler. 2011. Quantitative proteomics of the integrin adhesome show a myosin II-dependent recruitment of LIM domain proteins. *EMBO Rep.* 12:259-266.

Schlaepfer, D.D., M.A. Broome, and T. Hunter. 1997. Fibronectin-stimulated signaling from a focal adhesion kinase-c-Src complex: involvement of the Grb2, p130cas, and Nck adaptor proteins. *Mol Cell Biol.* 17:1702-1713.

Schlaepfer, D.D., S.K. Hanks, T. Hunter, and P. van der Geer. 1994. Integrin-mediated signal transduction linked to Ras pathway by GRB2 binding to focal adhesion kinase. *Nature.* 372:786-791.

Schlaepfer, D.D., K.C. Jones, and T. Hunter. 1998. Multiple Grb2-mediated integrin-stimulated signaling pathways to ERK2/mitogen-activated protein kinase: summation of both c-Src- and focal adhesion kinase-initiated tyrosine phosphorylation events. *Mol Cell Biol.* 18:2571-2585.

Schlaepfer, D.D., S.K. Mitra, and D. Ilic. 2004. Control of motile and invasive cell phenotypes by focal adhesion kinase. *Biochim Biophys Acta.* 1692:77-102.

Shemesh, T., A.B. Verkhovskiy, T.M. Svitkina, A.D. Bershadsky, and M.M. Kozlov. 2009. Role of focal adhesions and mechanical stresses in the formation and progression of the lamellipodium-lamellum interface [corrected]. *Biophys J.* 97:1254-1264.

Shen, Y., P. Lyons, M. Cooley, D. Davidson, A. Veillette, R. Salgia, J.D. Griffin, and M.D. Schaller. 2000. The noncatalytic domain of protein-tyrosine phosphatase-PEST targets paxillin for dephosphorylation in vivo. *J Biol Chem.* 275:1405-1413.

Shen, Y., G. Schneider, J.F. Cloutier, A. Veillette, and M.D. Schaller. 1998. Direct association of protein-tyrosine phosphatase PTP-PEST with paxillin. *J Biol Chem.* 273:6474-6481.

Sieg, D.J., C.R. Hauck, D. Ilic, C.K. Klingbeil, E. Schaefer, C.H. Damsky, and D.D. Schlaepfer. 2000. FAK integrates growth-factor and integrin signals to promote cell migration. *Nat Cell Biol.* 2:249-256.

Sieg, D.J., C.R. Hauck, and D.D. Schlaepfer. 1999. Required role of focal adhesion kinase (FAK) for integrin-stimulated cell migration. *J Cell Sci.* 112 (Pt 16):2677-2691.

Skelton, M.R., S. Ponniah, D.Z. Wang, T. Doetschman, C.V. Vorhees, and C.J. Pallen. 2003. Protein tyrosine phosphatase alpha (PTP alpha) knockout mice show deficits in Morris water maze learning, decreased locomotor activity, and decreases in anxiety. *Brain Res.* 984:1-10.

- Sonnenburg, E.D., A. Bilwes, T. Hunter, and J.P. Noel. 2003. The structure of the membrane distal phosphatase domain of RPTPalpha reveals interdomain flexibility and an SH2 domain interaction region. *Biochemistry*. 42:7904-7914.
- Streuli, M., N.X. Krueger, T. Thai, M. Tang, and H. Saito. 1990. Distinct functional roles of the two intracellular phosphatase like domains of the receptor-linked protein tyrosine phosphatases LCA and LAR. *EMBO J*. 9:2399-2407.
- Su, J., A. Batzer, and J. Sap. 1994. Receptor tyrosine phosphatase R-PTP-alpha is tyrosine-phosphorylated and associated with the adaptor protein Grb2. *J Biol Chem*. 269:18731-18734.
- Su, J., M. Muranjan, and J. Sap. 1999. Receptor protein tyrosine phosphatase alpha activates Src-family kinases and controls integrin-mediated responses in fibroblasts. *Curr Biol*. 9:505-511.
- Su, J., L.T. Yang, and J. Sap. 1996. Association between receptor protein-tyrosine phosphatase RPTP alpha and the Grb2 adaptor - Dual Src homology (SH)2/SH3 domain requirement and functional consequences. *Journal of Biological Chemistry*. 271:28086-28096.
- Sun, G., S.Y. Cheng, M. Chen, C.J. Lim, and C.J. Pallen. 2012. Protein tyrosine phosphatase alpha phosphotyrosyl-789 binds BCAR3 to position Cas for activation at integrin-mediated focal adhesions. *Mol Cell Biol*. 32:3776-3789.
- Tabiti, K., D.R. Smith, H.S. Goh, and C.J. Pallen. 1995. Increased mRNA expression of the receptor-like protein tyrosine phosphatase alpha in late stage colon carcinomas. *Cancer Lett*. 93:239-248.
- Takahashi, H., M. Mitsushima, N. Okada, T. Ito, S. Aizawa, R. Akahane, T. Umemoto, K. Ueda, and N. Kioka. 2005. Role of interaction with vinculin in recruitment of vinexins to focal adhesions. *Biochem Biophys Res Commun*. 336:239-246.
- Tamada, M., M.P. Sheetz, and Y. Sawada. 2004. Activation of a signaling cascade by cytoskeleton stretch. *Dev Cell*. 7:709-718.
- Thomas, S.M., and J.S. Brugge. 1997. Cellular functions regulated by Src family kinases. *Annu Rev Cell Dev Biol*. 13:513-609.
- Tikhmyanova, N., J.L. Little, and E.A. Golemis. 2010. CAS proteins in normal and pathological cell growth control. *Cellular and molecular life sciences : CMLS*. 67:1025-1048.
- Tilghman, R.W., J.K. Slack-Davis, N. Sergina, K.H. Martin, M. Iwanicki, E.D. Hershey, H.E. Beggs, L.F. Reichardt, and J.T. Parsons. 2005. Focal adhesion kinase is required for the spatial organization of the leading edge in migrating cells. *J Cell Sci*. 118:2613-2623.
- Tiran, Z., A. Peretz, T. Sines, V. Shinder, J. Sap, B. Attali, and A. Elson. 2006. Tyrosine phosphatases epsilon and alpha perform specific and overlapping functions in regulation of voltage-gated potassium channels in Schwann cells. *Mol Cell Biol*. 17:4330-42.

- Tonks, N.K. 2006. Protein tyrosine phosphatases: from genes, to function, to disease. *Nat Rev Mol Cell Biol.* 7:833-846.
- Toutant, M., A. Costa, J.M. Studler, G. Kadare, M. Carnaud, and J.A. Girault. 2002. Alternative splicing controls the mechanisms of FAK autophosphorylation. *Mol Cell Biol.* 22:7731-7743.
- Truffi, M., V. Dubreuil, X. Liang, N. Vacaresse, F. Nigon, S.P. Han, A.S. Yap, G.A. Gomez, and J. Sap. 2014. RPTPalpha controls epithelial adherens junctions, linking E-cadherin engagement to c-Src-mediated phosphorylation of cortactin. *J Cell Sci.* 127:2420-2432.
- Tsai, S.Q., Z. Zheng, N.T. Nguyen, M. Liebers, V.V. Topkar, V. Thapar, N. Wyvekens, C. Khayter, A.J. Iafrate, L.P. Le, M.J. Aryee, and J.K. Joung. 2015. GUIDE-seq enables genome-wide profiling of off-target cleavage by CRISPR-Cas nucleases. *Nat Biotechnol.* 33:187-197.
- Tsubouchi, A., J. Sakakura, R. Yagi, Y. Mazaki, E. Schaefer, H. Yano, and H. Sabe. 2002. Localized suppression of RhoA activity by Tyr31/118-phosphorylated paxillin in cell adhesion and migration. *J Cell Biol.* 159:673-683.
- Tumbarello, D.A., M.C. Brown, and C.E. Turner. 2002. The paxillin LD motifs. *FEBS Lett.* 513:114-118.
- Turner, C.E. 1998. Paxillin. *Int J Biochem Cell Biol.* 30:955-959.
- Turner, C.E. 2000. Paxillin and focal adhesion signalling. *Nat Cell Biol.* 2:E231-236.
- Turner, C.E., M.C. Brown, J.A. Perrotta, M.C. Riedy, S.N. Nikolopoulos, A.R. McDonald, S. Bagrodia, S. Thomas, and P.S. Leventhal. 1999. Paxillin LD4 motif binds PAK and PIX through a novel 95-kD ankyrin repeat, ARF-GAP protein: A role in cytoskeletal remodeling. *J Cell Biol.* 145:851-863.
- Turner, C.E., J.R. Glenney, Jr., and K. Burridge. 1990. Paxillin: a new vinculin-binding protein present in focal adhesions. *J Cell Biol.* 111:1059-1068.
- van Agthoven, T., T.L. van Agthoven, A. Dekker, P.J. van der Spek, L. Vreede, and L.C. Dorssers. 1998. Identification of BCAR3 by a random search for genes involved in antiestrogen resistance of human breast cancer cells. *EMBO J.* 17:2799-2808.
- Vanden Borre, P., R.I. Near, A. Makkinje, G. Mostoslavsky, and A. Lerner. 2011. BCAR3/AND-34 can signal independent of complex formation with CAS family members or the presence of p130Cas. *Cell Signal.* 23:1030-1040.
- Vicente-Manzanares, M., C.K. Choi, and A.R. Horwitz. 2009. Integrins in cell migration--the actin connection. *J Cell Sci.* 122:199-206.
- Volberg, T., B. Geiger, Z. Kam, R. Pankov, I. Simcha, H. Sabanay, J.L. Coll, E. Adamson, and A. Ben-Ze'ev. 1995. Focal adhesion formation by F9 embryonal carcinoma cells after vinculin gene disruption. *J Cell Sci.* 108 (Pt 6):2253-2260.

- von Wichert, G., G.Y. Jiang, A. Kostic, K. De Vos, J. Sap, and M.P. Sheetz. 2003. RPTP-alpha acts as a transducer of mechanical force on alpha(v)/beta(3)-integrin-cytoskeleton linkages. *Journal of Cell Biology*. 161:143-153.
- Vuori, K., H. Hirai, S. Aizawa, and E. Ruoslahti. 1996. Introduction of p130cas signaling complex formation upon integrin-mediated cell adhesion: a role for Src family kinases. *Mol Cell Biol*. 16:2606-2613.
- Wang, P.S., J. Wang, Z.C. Xiao, and C.J. Pallen. 2009. Protein-tyrosine phosphatase alpha acts as an upstream regulator of Fyn signaling to promote oligodendrocyte differentiation and myelination. *J Biol Chem*. 284:33692-33702.
- Wang, Q., Y. Wang, D. Fritz, D. Rajshankar, G.P. Downey, and C.A. McCulloch. 2014. Interactions of the protein-tyrosine phosphatase-alpha with the focal adhesion targeting domain of focal adhesion kinase are involved in interleukin-1 signaling in fibroblasts. *J Biol Chem*. 289:18427-18441.
- Wang, Y., and C.J. Pallen. 1991. The receptor-like protein tyrosine phosphatase HPTP alpha has two active catalytic domains with distinct substrate specificities. *EMBO J*. 10:3231-3237.
- Webb, D.J., K. Donais, L.A. Whitmore, S.M. Thomas, C.E. Turner, J.T. Parsons, and A.F. Horwitz. 2004. FAK-Src signalling through paxillin, ERK and MLCK regulates adhesion disassembly. *Nat Cell Biol*. 6:154-161.
- Wehrle-Haller, B. 2012. Assembly and disassembly of cell matrix adhesions. *Current opinion in cell biology*. 24:569-581.
- Wen, K.K., P.A. Rubenstein, and K.A. DeMali. 2009. Vinculin nucleates actin polymerization and modifies actin filament structure. *J Biol Chem*. 284:30463-30473.
- Weng, Z., J.A. Taylor, C.E. Turner, J.S. Brugge, and C. Seidel-Dugan. 1993. Detection of Src homology 3-binding proteins, including paxillin, in normal and v-Src-transformed Balb/c 3T3 cells. *J Biol Chem*. 268:14956-14963.
- West, K.A., H. Zhang, M.C. Brown, S.N. Nikolopoulos, M.C. Riedy, A.F. Horwitz, and C.E. Turner. 2001. The LD4 motif of paxillin regulates cell spreading and motility through an interaction with paxillin kinase linker (PKL). *J Cell Biol*. 154:161-176.
- Winkler, J., H. Lunsdorf, and B.M. Jockusch. 1996. The ultrastructure of chicken gizzard vinculin as visualized by high-resolution electron microscopy. *J Struct Biol*. 116:270-277.
- Winograd-Katz, S.E., R. Fassler, B. Geiger, and K.R. Legate. 2014. The integrin adhesome: from genes and proteins to human disease. *Nat Rev Mol Cell Biol*. 15:273-288.
- Wong, S., and O.N. Witte. 2004. The BCR-ABL story: bench to bedside and back. *Annu Rev Immunol*. 22:247-306.

- Wu, C.W., H.L. Kao, A.F. Li, C.W. Chi, and W.C. Lin. 2006. Protein tyrosine-phosphatase expression profiling in gastric cancer tissues. *Cancer Lett.* 242:95-103.
- Wu, R.C., J. Qin, P. Yi, J. Wong, S.Y. Tsai, M.J. Tsai, and B.W. O'Malley. 2004a. Selective phosphorylations of the SRC-3/AIB1 coactivator integrate genomic responses to multiple cellular signaling pathways. *Mol Cell.* 15:937-949.
- Wu, X., S. Suetsugu, L.A. Cooper, T. Takenawa, and J.L. Guan. 2004b. Focal adhesion kinase regulation of N-WASP subcellular localization and function. *J Biol Chem.* 279:9565-9576.
- Xing, Z., H.C. Chen, J.K. Nowlen, S.J. Taylor, D. Shalloway, and J.L. Guan. 1994. Direct interaction of v-Src with the focal adhesion kinase mediated by the Src SH2 domain. *Mol Biol Cell.* 5:413-421.
- Xu, J. 2005. Preparation, culture, and immortalization of mouse embryonic fibroblasts. *Curr Protoc Mol Biol.* Chapter 28:Unit 28 21.
- Xu, W., H. Baribault, and E.D. Adamson. 1998. Vinculin knockout results in heart and brain defects during embryonic development. *Development.* 125:327-337.
- Yamaguchi, H., J. Wyckoff, and J. Condeelis. 2005. Cell migration in tumors. *Current opinion in cell biology.* 17:559-564.
- Zaidel-Bar, R., M. Cohen, L. Addadi, and B. Geiger. 2004. Hierarchical assembly of cell-matrix adhesion complexes. *Biochem Soc Trans.* 32:416-420.
- Zaidel-Bar, R., and B. Geiger. 2010. The switchable integrin adhesome. *J Cell Sci.* 123:1385-1388.
- Zaidel-Bar, R., S. Itzkovitz, A. Ma'ayan, R. Iyengar, and B. Geiger. 2007. Functional atlas of the integrin adhesome. *Nat Cell Biol.* 9:858-867.
- Zeng, L., L. D'Alessandri, M.B. Kalousek, L. Vaughan, and C.J. Pallen. 1999. Protein tyrosine phosphatase alpha (PTPalpha) and contactin form a novel neuronal receptor complex linked to the intracellular tyrosine kinase fyn. *J Cell Biol.* 147:707-714.
- Zeng, L., X. Si, W.P. Yu, H.T. Le, K.P. Ng, R.M. Teng, K. Ryan, D.Z. Wang, S. Ponniah, and C.J. Pallen. 2003. PTP alpha regulates integrin-stimulated FAK autophosphorylation and cytoskeletal rearrangement in cell spreading and migration. *J Cell Biol.* 160:137-146.
- Zhai, J., H. Lin, Z. Nie, J. Wu, R. Canete-Soler, W.W. Schlaepfer, and D.D. Schlaepfer. 2003. Direct interaction of focal adhesion kinase with p190RhoGEF. *J Biol Chem.* 278:24865-24873.
- Zhang, M., L. Li, Z. Wang, H. Liu, J. Hou, M. Zhang, A. Hao, Y. Liu, G. He, Y. Shi, L. He, X. Wang, Y. Wan, and B. Li. 2013. A role for c-Abl in cell senescence and spontaneous immortalization. *Age (Dordr).* 35:1251-1262.

Zhang, M., J. Liu, A. Cheng, S.M. Deyoung, X. Chen, L.H. Dold, and A.R. Saltiel. 2006. CAP interacts with cytoskeletal proteins and regulates adhesion-mediated ERK activation and motility. *EMBO J.* 25:5284-5293.

Zhang, X.H., L.Y. Tee, X.G. Wang, Q.S. Huang, and S.H. Yang. 2015. Off-target Effects in CRISPR/Cas9-mediated Genome Engineering. *Mol Ther Nucleic Acids.* 4:e264.

Zhang, Z.Y., and J.E. Dixon. 1994. Protein tyrosine phosphatases: mechanism of catalysis and substrate specificity. *Adv Enzymol Relat Areas Mol Biol.* 68:1-36.

Zhao, Z.S., E. Manser, T.H. Loo, and L. Lim. 2000. Coupling of PAK-interacting exchange factor PIX to GIT1 promotes focal complex disassembly. *Mol Cell Biol.* 20:6354-6363.

Zheng, X.M., R.J. Resnick, and D. Shalloway. 2000. A phosphotyrosine displacement mechanism for activation of Src by PTPalpha. *EMBO J.* 19:964-978.

Zheng, X.M., and D. Shalloway. 2001. Two mechanisms activate PTPalpha during mitosis. *EMBO J.* 20:6037-6049.

Zheng, X.M., Y. Wang, and C.J. Pallen. 1992. Cell transformation and activation of pp60c-src by overexpression of a protein tyrosine phosphatase. *Nature.* 359:336-339.

Zimmerman, B., T. Volberg, and B. Geiger. 2004. Early molecular events in the assembly of the focal adhesion-stress fiber complex during fibroblast spreading. *Cell Motil Cytoskeleton.* 58:143-159.